The Role of The Type III Transforming Growth Factor–β Receptor in Epicardial Cell Behavior and Coronary Vessel Development

By

Nora Sylvia Sánchez

Dissertation

Submitted to the Faculty of the

Graduate School of Vanderbilt University

in partial fulfillment of the requirements

for the degree of

DOCTOR OF PHILOSOPHY

In

Pharmacology

December 2011

Nashville, TN

Approved:

Joey V. Barnett, Ph.D.

Christopher B. Brown, Ph.D.

Florent Elefteriou, Ph.D.

Harold L. Moses, M.D.

For my mom, dad and husband

ACKNOWLEDGEMENTS

First and foremost I would like to thank the generous support from the National Institutes of Health which has made a first tier graduate education accessible to me. In particular NIH Grant HL085708, GM007628, American Heart Association AHA0655129.

I am forever indebted to my thesis advisor, Joey Barnett, PhD, for not only recruiting me to Vanderbilt but accepting me into his laboratory even when he was trying very hard not to take any more graduate students. He taught me to think like a scientist, but more than anything he taught me that learning is a never ending task that is not confined to reading the scientific literature.

To my committee members Hal Moses, M.D., Christopher B. Brown, Ph.D., Florent Elefteriou, Ph.D., thank you for your exceptional guidance and for your willingness to meet with me so often this last year. A special thanks to Gregory Mundy, M.D. † who unfortunately was not able to make it through completion of my thesis. I had a limited amount of time to interact with him, but his dedication to science and attention to detail really amazed and inspired me.

I will be eternally grateful to my parents Arnulfo and Concepción for believing that education was the best gift they could give us. To my oldest sister Norma, for defying the norm and being the first one in my family to pursue a higher

education and in doing so inspired the rest of us, all 6 siblings, to follow in her footsteps. To my older brother Arnulfo, Jr., for getting me to Nashville despite my parents' reluctance to let me go. To my older sister, Claudia, for always being the mother figure during the rough times in our family. To my younger sister, Lorena, for being my confidant and understanding my non-traditional beliefs. To my younger sister, Faviola for all the trust and faith she holds in me. To my youngest brother Daniel, for trying at least, to teach me how to just kick back, relax and enjoy life as it comes. Last but certainly not least, to my husband Luis for his unconditional love and support through ALL phases of my education. He has been my best friend and life coach…I would be lost without him.

TABLE OF CONTENTS

Page

LIST OF TABLES

Table Page

LIST OF FIGURES

LIST OF ABBREVIATIONS

ºC	Degrees Celsius
β-arr2	β-arrestin2
β-gal	Beta-galactosidase
µM	micromolar
µL	microliter
ActRII	Activin Receptor Type II
Akt	Protein Kinase B
ALK	Activin Receptor-like Kinase
AV	Atrioventricular
BSA	Bovine Serum Albumin
ca	constitutively active
cdc42	cell division cycle 42
cDNA	complementary Deoxyribonucleic Acid
CO_2	Carbon dioxide
Cre	Cre Recombinase
Cx	Connexin
cy3	cyanine 3
DAPI	4',6-diamidino-2-phenylindole
DNA	Deoxyribonucleic Acid
DNase	deoxyribonuclease
DORV	Double Outlet Right Ventricle
E	Embryonic
ED	Embryonic Day
EMT	Epithelial-Mesenchymal Transformation
ES	Embryonic stem
FBS	Fetal Bovine Serum
FGF	Fibroblast Growth Factor
FGFR	Fibroblast Growth Factor Receptor
Fig	Figure
FOG-2	Friend of GATA - 2
GATA4	guanosine, adenine, thymidine, adenosine - 4
GFP	Green Fluorescent Protein
GIPC	GTPase activated protein for Gαi subunits interacting protein C-terminus
HSVtk	Harvey Sarcoma Virus Thymidine Kinase
kDa	Kilodalton
LAP	Latency Associated Peptide
LLC	Large Latency Complex
LTBP	Latent TGFβ Binding Protein
M	Molar
MAP	Mitogen Activated Protein

min	minute
ml	milliliter
mRNA	messenger Ribonucleic Acid
neo	Neomycin
NFκB	Nuclear Factor - kappa B
ng	nanograms
oligo	oligonucleotide
PAI-1	Plasminogen Activator Inhibitor - 1
PAR	Partitioning Defective
PBS	Phosphate Buffered Saline
PCR	Polymerase Chain Reaction
PDGF	Platelet-Derived Growth Factor
PDGFR	Platelet-Derived Growth Factor Receptor
PE	Proepicardium
PECAM	Platelet Endothelial Cell Adhesion Molecule
PFA	Paraformaldehyde
PFU	Plaque Forming Unit
PI3K	Phosphoinositol 3 Kinase
pM	picomolar
R-	Receptor
RhoA	ras homologue A
RNA	Ribonucleic Acid
RT	Room Temperature
qRT- PCR	Quantitative Reverse Transcriptase Polymerase Chain Reaction
SARA	Smad Anchor for Receptor Activation
SDS	Sodium Dodecyl Sulfate
SEM	Standard Error of the Mean
SM22α	Smooth Muscle 22 kDa actin-binding protein
SMαA	Smooth Muscle Alpha Actin
Smurf	Smad Ubiquitination Regulatory Factor
SRF	Serum Response Factor
TAE	Tris Acetate Ethylenediaminetetracetic Acid
TBRI	Transforming Growth Factor -Beta Receptor I
TBRII	Transforming Growth Factor -Beta Receptor II
TBRIII	Transforming Growth Factor -Beta Receptor III
TGFβ	Transforming Growth Factor -Beta
TUNEL	Terminal deoxynucleotidyl transferase-mediated dUridine Triphosphate Nick End Labeling
VCAM-1	Vascular cell adhesion molecule
VEGF	Vascular Endothelial Growth Factor
VEGFR	Vascular Endothelial Growth Factor Receptor
VSD	Ventricular Septal Defect
Wnt-1	wingless type-1
WT-1	Wilm's Tumor - 1
ZO-1	Zonula Occludins - 1

CHAPTER I

INTRODUCTION

Coronary artery disease

Coronary heart disease (CHD) continues to be the leading cause of death in developed countries (Lloyd-Jones, Adams et al. 2010). According to the latest Heart Disease and Stroke Statistics report by the American Heart Association, it is estimated that 785,000 Americans will have a new coronary attack and 470,000 will have a recurrent attack this year. This translates into one coronary event every 25 seconds, and approximately one death every minute (Lloyd-Jones, Adams et al. 2010). For patients fortunate enough to survive the event , the limited or non-regenerative capacity of the heart to replace the injured area and the development of non-contractile scar tissue in place of the myocardial tissue, significantly inhibits recovery and increases the risk for a second myocardial event (Hellermann, Jacobsen et al. 2005).

Recent studies in zebrafish models have uncovered a unique ability for cardiac regeneration. This ability relies on contributions from two cardiac cell populations, cardiac myocytes and epicardial cells (Poss, Wilson et al. 2002; Lepilina, Coon et al. 2006). The ability of cardiac myocytes to contribute to cardiac regeneration is significant considering that these cells were previously

thought either to have little or no regenerative capacity (Heallen, Zhang et al. 2011). The contribution of epicardial cells, the precursors of coronary vessels, is particularly interesting as this layer had been formerly known as simply a protective barrier for the myocardium. What is more, the contribution of the epicardium to cardiac regeneration is mediated by re-activation of molecular pathways now known to be involved in embryonic coronary vessel development (Lepilina, Coon et al. 2006). Although mammals possess significantly less regenerative capacity than zebrafish, analysis of the response of the epicardium to injury reveals striking similarities (Smart, Risebro et al. 2007; Cai, Martin et al. 2008; Zhou, Ma et al. 2008; Bock-Marquette, Shrivastava et al. 2009; Christoffels, Grieskamp et al. 2009; Rentschler and Epstein 2011). Therefore, understanding coronary vessel development during embryonic development may provide an opportunity to target the epicardium to modulate the response to injury.

Origin of Coronary Vessels

The field of developmental biology has entertained various hypotheses as to the origin coronary vessels. One hypothesis suggested coronary vessels arose as a result of endocardial cell migration to the subepicardial space where they were encased by the ventricle during trabeculation to form sinusoids that then penetrated to the myocardium and formed the subepicardial plexus (Grant 1926; Viragh and Challice 1981). A second hypothesis proposed that coronary vessels

formed through the process of angiogenesis as an outgrowth of the proximal aorta (Bennett 1936; Goldsmith and Butler 1973). Our current understanding is that coronary vessels arise from the proepicardium (PE) and the epicardium through a multistep process involving *de novo* synthesis of blood vessels (Mikawa and Fischman 1992; Poelmann, Gittenberger-de Groot et al. 1993).

The PE arises from a group a mesothelial cells that lies adjacent to the sinus venosus (SV) and opposite the atrio-ventricular (AV) groove (Figure 1A) of the developing heart tube by embryonic day (ED) 9.0 in mice (Ho and Shimada 1978). These cells migrate as an epithelial sheet to the heart via the pericardial fluid in mammals (Komiyama, Ito et al. 1987; Kuhn and Liebherr 1988; Nahirney, Mikawa et al. 2003). The actual mechanism by which the proepicardium covers the surface of the heart to form the epicardium has been an area of debate. The initial hypothesis proposed that free-floating clusters of PE cells attached to the primitive myocardium forming multiple islands of cells that then converged across the myocardial surface to form the epicardium (Komiyama et al., 1987; Kuhn and Liebherr, 1988). However, this hypothesis failed to consider how these free floating clusters could be directed towards the heart. Studies by Rodgers et al., address this issue and propose a model in which the PE sheet extends multiple villi towards the beating heart establishing multiple points of contact. As the heart contracts and relaxes, the distance between the villi and the heart extends and retracts until eventually the tips are sheared off from the PE and transferred to the surface of the heart forming multiple islands of cells as well as free-floating

cysts as the original hypothesis suggested (Rodgers, Lalani et al. 2008). PE-derived cells migrate and proliferate as an epithelial sheet across the surface of the myocardium to form the epicardium, that extends from the AV groove to the ventricles and atria and finally the inflow and outflow tracts (Figure 1B). Some of these cells then undergo epithelial to mesenchymal transformation (EMT) and invade the subepicardial space (Figure 1C) (Viragh and Challice 1981; Mikawa and Fischman 1992; Manner 1993; Poelmann, Gittenberger-de Groot et al. 1993; Olivey, Compton et al. 2004; Tomanek 2005). The subepicardial space is an extracellular matrix that forms between the epicardium and myocardium and is particularly thick along the AV groove. A subset of these cells further migrates into the compact zone of the myocardium and give rise to vascular smooth muscle cells and cardiac fibroblasts. The actual formation of the coronary plexus begins as angioblasts coalesce in the subepicardial space and myocardium along the heart, which then join to form larger vessels and link to the ascending aorta (Mikawa and Fischman 1992) (Figure 1D). Once linked to the right atrium, a functional coronary system is formed. Additional PE-derived smooth muscle cells and fibroblasts, are subsequently recruited to complete the vascular network (Munoz-Chapuli, Gonzalez-Iriarte et al. 2002) (Figure 1E).

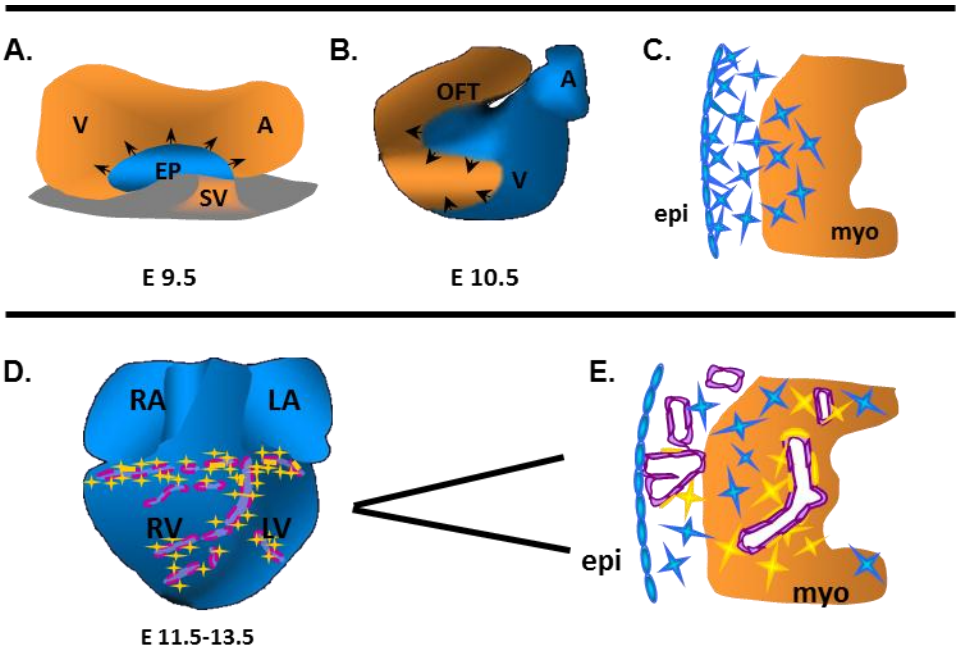

Figure 1 Key stages in coronary vasculogenesis. (A.) The initial migration of the epicardium from the AV groove at E9.5 is depicted in a left lateral view. (B.) Progression of epicardial migration at E10.5 is depicted in a ventral view. Migration is complete by E11.0. (C.) Epicardial EMT begins soon after contact with the myocardium. In cross section, epicardially-derived mesenchymal cells are depicted invading the supepicardial space and the myocardium. (D.) Endothelial vesicles coalesce to form nascent coronary vessels (purple) beginning at E11.5. Coronary vessels attach to the systemic circulation by E13.5. After attachment to the aorta, smooth muscle progenitors derived from the epicardium are recruited to the artery walls in a proximal to distal fashion with respect to the aorta. Nascent vessels are concentrated along the AV and IV surface of the heart as depicted in the ventral view. (E.) In cross section, endothelial tubule (purple) formation and smooth muscle (yellow) recruitment in the subepicardial and intramyocardial spaces are depicted. . AV: atrioventricular; IV: interventricular; SV: sinus venosus; V: ventricle; Aaatrium; epi: epicardium; myo: myocardium; RA: right atrium; LA: left atrium; RV: right ventricle; LV: left ventricle. From *Olivey, H.E., et al, Trends Cardiovac Med 2004*

Whether the PE gives rise to all vascular cells types: smooth muscle, cardiac fibroblasts and endothelial cells, has been a topic that has been widely debated. Early lineage tracing experiments using chick and quail chimeric epicardial explants suggested that the PE contributes to all cell lineages (Dettman, Denetclaw et al. 1998). Recent lineage tracing experiments in mice, argue that while the PE can give rise to myocardial and vascular smooth muscle lineages, it only minimally contributes to the endothelial cell lineage (Merki, Zamora et al. 2005; Cai, Martin et al. 2008; Zhou, Ma et al. 2008). Using histological and clonal analysis in mice, Red-Horse, et al., provide evidence to suggest that coronary arteries derive from endothelial sprouts of the sinus venosus and a small portion from the endocardium lining the cardiac chambers, and not the PE (Red-Horse, Ueno et al. 2010). Together these cells, contributed by the epicaridium and sinus venosus, are coordinately regulated to form the coronary vasculature.

Signaling Pathways Involved in Coronary Vessel Formation

The formation of the coronary vasculature depends on the ability of the epicardium to communicate with the myocardium and vice versa (Olivey and Svensson 2010). Signals that mediate this communication are not limited to soluble factors that can be secreted from one compartment to another but extends to include transcription factors, adhesion molecules, growth factor ligands and receptors that act in autocrine and paracrine fashion to direct vessel formation. Disruption of any of these signals can delay or abolish coronary vessel formation all together at any of the steps of this complex process.

Establishment of a functional PE is a requirement for subsequent epicardial-myocardial communication and coronary vessel formation. Conditional deletion of the zinc finger transcription factor, GATA4, in mice abolishes the formation of a functional PE (Watt, Battle et al. 2004). Similarly, physically inhibiting the PE from interacting with the myocardium results in failed delivery of the PE and subsequent formation of a functional epicardium (Gittenberger-de Groot, Vrancken Peeters et al. 2000).

Failure to form an intact epicardium and its contribution to failed coronary vessel formation are supported by multiple knockout mouse models (Table 1). Together these studies support the mutual requirement for communication between the epicardium and myocardium, as deletions affecting the epicardium often result in

a thin, myocardium, and deletions in the myocardium alter the integrity of the epicardium. For example, deletion of the reciprocal adhesion molecules, vascular endothelial adhesion molecule 1 (VCAM1), expressed throughout the myocardium (Kwee, Baldwin et al. 1995) and its counter receptor, α4β integrin, expressed in the PE and epicardium (Yang, Rayburn et al. 1995) results in an inability to form or maintain an intact epicardium, leading to failed coronary vessel development. Both *Vcam1*$^{-/-}$ and *Itga4*$^{-/-}$ embryos die in utero between E12.5 and E15.5, and both fail to form or maintain a ventricular epicardial sheath (Kwee, Baldwin et al. 1995; Yang, Rayburn et al. 1995). The overlapping phenotype, time of death and respective expression in myocardium and epicardium, provide evidence for the need to establish communication between these two compartments as early as formation of the epicardium. Deletion of the zinc finger transcription factor, Wilm's tumor 1 (WT1) in mice also results in formation of an incomplete epicardium (Moore, McInnes et al. 1999). *WT1*$^{-/-}$ and *Itga4*$^{-/-}$ embryos have a similar phenotype since WT1 transcriptionally regulates α4β integrin and shares similar expression pattern (Kirschner, Wagner et al. 2006). Other gene knockouts resulting in compromised epicardial integrity or complete epicardial ablation include the gap junction protein Connexin43 (Li, Waldo et al. 2002), the mucin-like transmembrane glycoprotein Podoplanin (Mahtab, Wijffels et al. 2008), epicardial specific deletion of the TGFβ Type I Receptor, ALK5 (Sridurongrit, Larsson et al. 2008) or Retinoid x Receptor α (Merki, Zamora et al. 2005). While some of these mice are able to form an epicardium, it is partially detached and coronary vessel development is

compromised. This suggests that the proximity of the epicardium to the myocardium is important for proper communication.

Many genes involved in coronary vessel formation play a role at several stages of development. WT1, in addition to participating in the formation of the epicardium, also regulates epicardial EMT (Moore, McInnes et al. 1999; Perez-Pomares, Phelps et al. 2002), thus *WT1*$^{-/-}$ embryos also have deficits in epicardial EMT. EMT is regulated by both epicardial and myocardial-derrived signals. FOG-2 is a transcriptional co-factor for GATA4 expressed in cardiomyocytes, together this complex regulates epicardial EMT (Lu, McKinsey et al. 1999; Svensson, Tufts et al. 1999). Disrupting the interaction between FOG-2 and GATA4, either by deleting FOG-2 or by inactivating the site required for FOG-2/GATA-4 interaction on GATA-4 leads to the formation of an intact epicardium that fails to undergo EMT (Svensson, Tufts et al. 1999). Overexpression of FOG-2 in the myocardium rescues epicardial EMT, supporting a role for the myocardium in mediating epicardial EMT (Tevosian, Deconinck et al. 2000; Crispino, Lodish et al. 2001). Other transcription factors involved in coronary vessel development at the level of EMT include, Brahma-related gene-1 associated factor 180 (BAF180)(Huang, Gao et al. 2008), p300(Shikama, Lutz et al. 2003) and avian erythroblastosis virus oncogene-1 (Ets-1)(Lie-Venema, Gittenberger-de Groot et al. 2003). The impact of these factors is in part due to the variety of genes they regulate. For example, animals in which BAF180 has been deleted have reduced expression levels of the epicardially expressed

growth factors, FGF, PDGF and TGFβ(Huang, Gao et al. 2008). Collectively, these data suggests that epicardial EMT is regulated in part by transcription factors acting in the myocardium and the epicardium.

Growth factors play a particularly important role in regulating epicardial EMT, differentiation, and invasion into the subepicardial space and myocardium. FGF, PDGF and TGFβ are known regulators of epicardial EMT (Tomanek, Zheng et al. 2001). Deletion of *Fgfr1* and *Fgfr2* in the myocardium delays, but does not completely abrogate coronary vascular plexus formation (Lavine, Yu et al. 2005). However, FGFR-1 expression is not restricted to the myocardium. Indeed, FGFR-1 expression increases in epicardial cells after EMT as revealed by experiments using quail explants (Pennisi and Mikawa 2009). In this system, overexpression of FGFR-1 resulted in increased epicardial EMT, however, knockdown of FGFR-1 did not inhibit EMT, but decreased epicardial migration into the myocardium (Pennisi and Mikawa 2009). Thus, the role of FGF's in coronary vessel development is cell context specific, but not mutually exclusive between the epicardium and myocardium; increased FGF production in the myocardium is accompanied by increased in FGFR expression in the epicardium (Pennisi and Mikawa 2005).

Deletion of the Platelet Derived Growth factor Receptor β (PDGFRβ) in mice also results in deficits in epicardial EMT, migration into the myocardium and an inability to differentiate into vascular smooth muscle cells, culminating in failure to

form dominant coronary vessels on the ventral surface of the heart (Mellgren, Smith et al. 2008). Altered epicardial EMT and smooth muscle differentiation is also evident when the TGFβ Type I Receptor, ALK5, is specifically deleted in the epicardium (Sridurongrit, Larsson et al. 2008). Conditional deletion of β-catenin, a member of the Wnt signaling family of proteins, also leads to decreased EMT and smooth muscle differentiation (Zamora, Manner et al. 2007). Although the coronary venus system remodels appropriately in these animals, the coronary arterial vessels fail to form (Zamora, Manner et al. 2007).

Successful integration of all these signaling components depends not only spatial, but temporal regulation of all these molecules as the time window within which coronary vessels must develop is strictly regulated by the growing demands of the myocardium. This is exemplified by mouse models in which premature or delayed differentiation of the epicardium into the various lineages gives rise to, leads to failed coronary vessel development. Knockdown of Thymosin β4, a factor identified to be secreted from the myocardium, results in premature epicardial differentiation into smooth muscle cells (Smart, Risebro et al. 2007). On the other hand, mis-expression of angiopoietin-1 in the myocardium, leads to the formation of an irregular or completely absent epicardium, along with premature expression of endothelial cell markers while still in the epicardium (Ward, Van Slyke et al. 2004).

In summary, many signaling pathways stemming from both the epicardium and myocardium direct coronary vessel development. Understanding how each of these pathways integrates to coordinate coronary vessel development is an area that continues to be investigated for its potential to offer therapeutic targets only during development but to modulate response to injury following a myocardial infarction.

Table 1: Animal Models with Coronary Vascular Defects

Gene	Animal Model	Coronary Phenotype
α4 integrin	Itga4$^{-/-}$	Does not maintain epicardium
VCAM-1	Vcam1$^{-/-}$	Does not form epicardium
WT-1	Wt1$^{-/-}$	Does not form complete epicardium
Angiopoietin1	MHC-Ang 1 Transgenic	Failure to maintain an intact epicardium
Podoplanin	Podo$^{-/-}$	Delayed epicardial formation; partially detached epicardium
TGFβ Receptor III	Tgfbr3$^{-/-}$	Excessive epicardial EMT; capillary plexus formation reduced
RXRα	RXRα$^{f/f}$; GATA5-Cre	Partially detached epicardium; thin subepicardial mesenchymal layer; reduced coronary branching
EpoR	EpoR$^{-/-}$	Partially detached epicardium; PECAM-positive cells unable to form subepicardial vascular plexus
BAF180	Pbrm1$^{-/-}$	Attenuated epicardial EMT; PECAM-positive subepicardial modules
Thymosin β4	Tb4shrna^{f}; Nkx2.5-Cre	Partially detached epicardium; Tie2-positive cells unable to form plexus; failed recruitment of coronary smooth muscle
Connexin 43	Cx43$^{-/-}$	Partially detached epicardium; decreased epicardial EMT and migration; perturbed capillary plexus remodeling
FOG-2	Zfpm2$^{-/-}$	Epicardium intact; does not form capillary plexus
GATA4	GATA4$^{ki/ki}$	Epicardium intact; does not form capillary plexus
p300	p300$^{+/\Delta S}$	Delayed epicardial and capillary plexus formation
FGF9	FGF9$^{-/-}$	Delayed formation of the capillary plexus
FGFRs	FGFR1$^{f/-}$;FGFR2$^{f/}$; Mlc2v-Cre	Delayed formation of the capillary plexus
Hedgehog signaling	Smo$^{f/-}$;Mlc2v-Cre	Absent subepicardial mesenchyme; failure to form coronary veins (EphB4- positive subepicardial vessels)
	Smo$^{f/-}$;Dermo1-Cre	Reduced intramyocardial arterial vessels (Ephrin B2-positive vessels)
PDGF Receptor	Pdgfrb$^{-/-}$	Decreased epicardial migration; no coronary vascular smooth muscle
β-Catenin	Ctnnb1$^{f/f}$;Gata5-Cre	Thin subepicarial mesenchymal layer; decreased migration of subepicardial mesenchymal cells; impaired differentiation of coronary arterial smooth muscle cells
ALK5	Alk5$^{f/-}$; Gata5-Cre	Partially detached epicardium; increased capillary density; failed recruitment of coronary smooth muscle
Vangl2	Lp/Lp	Reduced smooth muscle cell recruitment; aberrant subepicardial vessels
Smad6	Smad6$^{-/-}$	Dilated coronary vessels with reduced smooth muscle
Tbx-1	Tbx-1$^{-/-}$	Abnormal patterning of proximal coronary arteries

From Olivey and Svensson, Circulation Research 2010

Transforming Growth Factor β (TGFβ) Signaling

The TGFβ superfamily of signaling proteins is involved in a variety of physiological processes, including development, wound healing, proliferation, apoptosis, differentiation and migration (Roberts 1988; Derynck and Zhang 2003; Siegel and Massague 2003). Given its widespread participation in regulating cell behavior, members of the TGFβ family have been implicated in a variety of pathological processes including atherosclerosis, tumorigenesis, fibrosis and inflammation (Siegel and Massague ; Derynck and Zhang 2003; Bierie and Moses 2006).

Members of the TGFβ superfamily

The prototypical ligands of the TGFβ superfamily are TGFβ1, TGFβ2, and TGFβ3 (Attisano, Wrana et al. 1994), however the superfamily is actually composed of three subgroups: TGFβ's, activins and bone morphogenic proteins (BMP's) (Attisano, Wrana et al. 1994). TGFβ1, TGFβ2, and TGFβ3 are synthesized as precursor polypeptides, and are associated with latency associated protein (LAP) at the N-terminus and latent TGFβ binding protein (LTBP) prior to secretion from the cell (Rifkin 2005). Once secreted ligands can be stored in their inactive form in the extracellular matrix; alternatively, ligands can be activated via proteolytic cleavage, changes in pH or reactive oxygen species into the active 25 kDa peptide (Miyazono, Ichijo et al. 1993). TGFβ1 and

TGFβ3 have identical receptor binding profiles (Cheifetz, Hernandez et al. 1990), that is distinct from TGFβ2, thus TGFβ2 has unique biological activities.

TGFβ receptors can be divided into two classes (Figure 2): the first class contains the serine/threonine receptors, TGFβR1 and TGFβR2 (Lin, Wang et al. 1992; Ebner, Chen et al. 1993; Bassing, Yingling et al. 1994). To date, seven isoforms of TGFβR1, collectively termed the ALKs (activin-like kinases, ALK 1-7) have been identified (Bassing, Yingling et al. 1994). TGFβR2 can bind TGFβ1 and TGFβ3 with high affinity, but has a lower affinity for TGFβ2 (Lin and Moustakas 1994). Upon ligand binding, TGFβR2's constitutively active kinase domain recruits TGFβR1, and phosphorylates it, leading to its activation (Wrana, Attisano et al. 1994; Shi and Massagué 2003) (Figure 2). ALK5 is the prototypic TGFβ Type I Receptor, upon binding, TGFβ induces plasminogen activator inhibitor-1 (PAI-1) gene expression (Overall, Wrana et al. 1989; Overall, Wrana et al. 1989) and cell-cycle arrest (Massague and Weis-Garcia 1996; Wu, Buckley et al. 1996). ALK2 and 3 are activated by BMP's. Nonetheless, recent studies have demonstrated that TGFβ ligands can activate the BMP receptors, ALK2 and 3, and BMP ligands can activate the TGFβ receptor, ALK5, adding another layer of complexity to TGFβ signaling (Townsend, Wrana et al. 2008; Townsend, Robinson et al. 2011). Differential ALK activation will be discussed shortly.

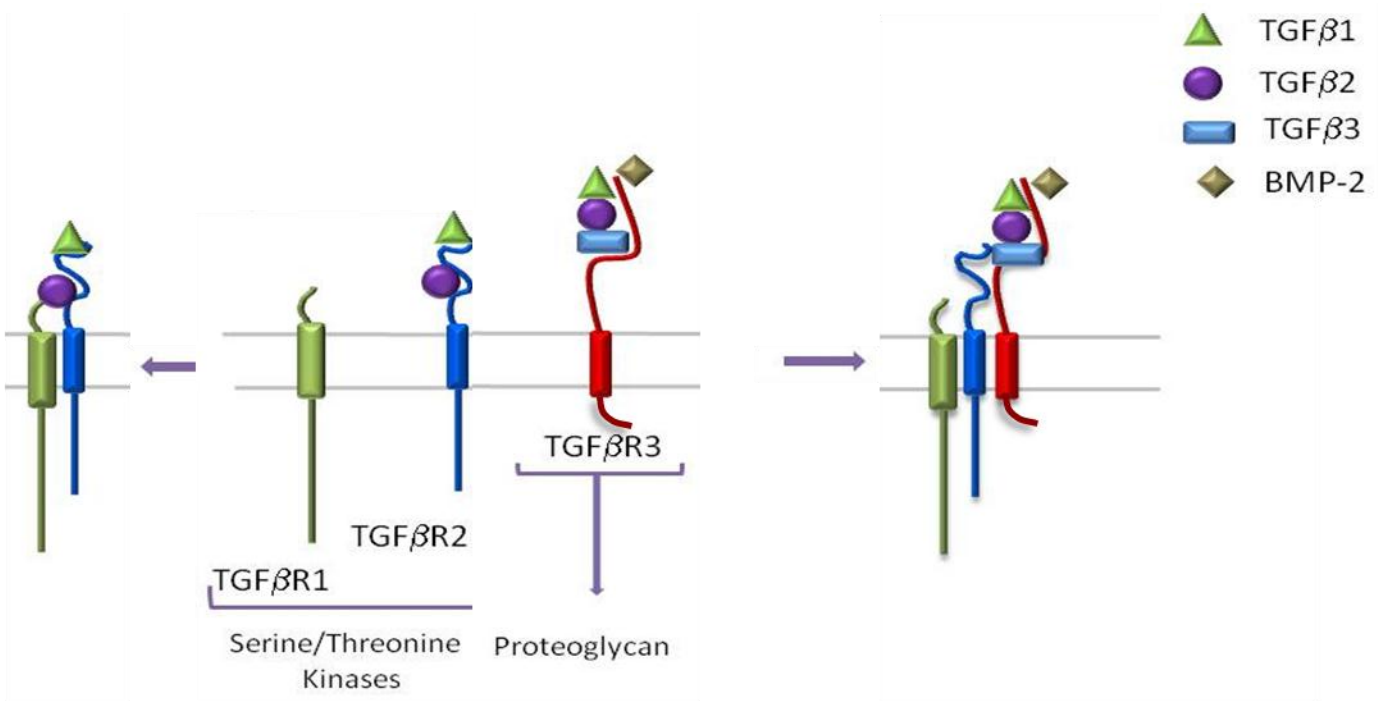

Figure 2 Members of the TGFβ Signaling Family Two classes of receptors make up the TGFβ family. Class I consists of TGFβR1 and TGFβR2, and are serine/threonine kinases. Class II includes the proteoglycan, TGFβR3. TGFβR1 and TGFβR2 can bind TGFβ1 and TGFβ3 with high affinity but require TGFβR3 to bind TGFβ2. TGFβR3 can bind all ligands and members of the BMP2 family, including BMP2. TGFβR3 can present ligand to the TGFβR1/TGFβR2 complex to augment canonical signaling but can also signal independently.

The second class of receptors includes the TGFβR3, or betaglycan, and endoglin (Figure 2) (Attisano, Wrana et al. 1994), which contain a highly conserved, 43amino acid intracellular domain with no known catalytic activity and a heavy glycosylated extracellular domain (Lopez-Casillas, Cheifetz et al. 1991; Wang, Lin et al. 1991; Cheifetz, Bellon et al. 1992). TGFβR3 can also bind TGFβ1 and TGFβ3 with high affinity but is unique in its ability to bind TGFβ2 (Lin and Moustakas 1994), inhibin (Lewis, Gray et al. 2000) and several BMP ligands including BMP-2, BMP-4, BMP-7 and GDF-5 with similar kinetics and ligand binding domains as previously identified for TGFβ (Kirkbride, Townsend et al. 2008). Upon ligand binding, TGFβR3 can present ligand to the TGFβR1/TGFβR2 complex to augment Smad signaling but can also signal independent of the Smads, through a process requiring the cytoplasmic domain (Blobe, Liu et al. 2001; Blobe, Schiemann et al. 2001). Endoglin and TGFβR3 are highly homologous, however endoglin expression is restricted to endothelial cells and its ligand binding profile is restricted to TGFβ1 and TGFβ3, whereas TGFβR3 is expressed ubiquitously and has a diverse ligand binding profile (Cheifetz, Bellon et al. 1992). Furthermore, endoglin requires TGFβR2 to bind to TGFβ1 and TGFβ3, whereas TGFβR3 can bind each ligand independently (Barbara, Wrana et al. 1999)

Smad-Dependent Signaling Pathways

The canonical TGFβ signaling pathway is mediated by a family of transcription factors known as the Smads (Attisano and Wrana 2002)(Figure 3). There are three classes of Smads: receptor-regulated Smads (R-Smads), the common-mediator Smads (co-Smads), and the antagonistic or inhibitory Smads (I-Smads)(Wrana 2000). Following ligand-induced activation of TGFβ receptors, R-Smads are recruited to the complex by SARA (**S**mad **a**nchor for **r**eceptor **a**ctivation), a FYVE domain protein localized at the cell membrane (Tsukazaki, Chiang et al. 1998). Phosphorylation of R-Smads by TGFβR1 induces dissociation from SARA with concomitant formation of a heterotrimeric complex comprising two receptor-activated Smads (Attisano and Wrana 2002). The receptor Smads 2 and 3 are specifically activated by ALK 4, 5 and 7 whereas Smads 1, 5 and 8 are activated by ALK 1, 2, 3 and 6 (Miyazawa, Shinozaki et al. 2002; Massague and Gomis 2006). Smad6 and 7 are inhibitory Smads, inhibiting BMP and TGFβ signaling, respectively (Nakao, Afrakhte et al. 1997; Bai, Shi et al. 2000; Ishida, Hamamoto et al. 2000). Smad6 acts by competing with Smad4 for binding to Smad 1, 5 and 8, thus inhibiting nuclear translocation (Hata, Lagna et al. 1998). In contrast, Smad7 competes with TGFβR1 for binding to all of the Smads, thus preventing their activation (Nakao, Afrakhte et al. 1997). Smad4 is the common mediator Smad that forms a heterocomplex with the above Smads allowing translocation into the nucleus to regulate gene expression (Wrana and Attisano 2000).

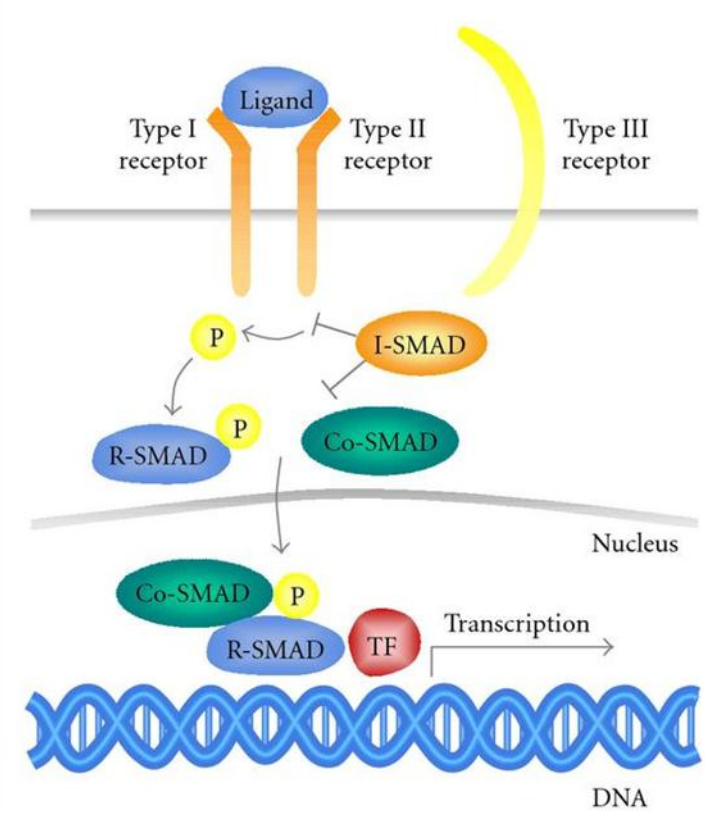

Figure 3 Generalized Smad Signaling Upon ligand binding the constitutively active kinase of the Type II receptor transphosphorylates and activates the Type I receptor. TGFβR3 facilitates ligand binding to the type I and II receptors. Downstream signaling is mediated via R-SMADs which are phosphorylated by the activated Type I receptor and form a complex with CoSMADs. This complex translocates to the nucleus where it induces transcription of downstream signaling. I-SMAD proteins represent important negative feedback structures, since they can block the signaling via competitive binding to the Type I receptors or R-SMADs. R-SMAD: receptor-regulated SMAD; CoSMAD: common mediator SMAD; I-SMAD: inhibitory SMAD; TF: transcription factor. *Adapted from Otten, J., et al, J Oncology 2010*

Our current understanding of the function of Smads has been greatly aided by the generation of transgenic mice. Deletion of Smad2 is embryonic lethal due to defective mesoderm formation (Waldrip, Bikoff et al. 1998; Weinstein, Yang et al. 2000). *Smad3*$^{-/-}$ survive past birth but develop metastatic colorectal cancer (Zhu, Richardson et al. 1998). *In vitro, Smad3*$^{-/-}$ cells also have impaired TGFβ-induced growth arrest which may in part contribute to its tumorgenicity (Datto, Frederick et al. 1999). Although both Smad2 and 3 form heterodimers to mediate signaling downstream of ALK4, 5 and 7, the non-overlapping phenotype between *Smad2*$^{-/-}$ and *Smad3*$^{-/-}$ suggest each has independent roles outside the context of TGFβ. Deletion of the common mediator Smad4 induces embryonic lethality by E7.5 due to the inability to initiate gastrulation (Sirard, de la Pompa et al. 1998). *Smad4*$^{-/-}$ mice display the earliest embryonic lethality probably due to its central role in converging signals from multiple pathways. *Smad5*$^{-/-}$ mice are able to initiate organogenesis but are unable to properly support heart and gut development and consequently die between E9.5 and E11.5 (Chang, Huylebroeck et al. 1999), This is similar to *Bmp2*$^{-/-}$ *and Bmp4*$^{-/-}$ mice, both Smad5-activating ligands. Furthermore, *Smad5*$^{-/-}$ mice also have defects in yolk sac vasculogenesis and amnion-allantois generation, similar to *Tgfb1*$^{-/-}$ (Dickson, Martin et al. 1995) and *Tgfbr2*$^{-/-}$ mice (Oshima, Oshima et al. 1996) This overlap in phenotypes not only validate Smad5 as a downstream target of BMP-2 and BMP-4 ligands, but support cross-talk between TGFβ and BMP signaling pathways.

Smad-Independent Signaling Pathways

Studies using mutant type I receptors that cannot interact with Smads (Yu, Hebert et al. 2002) as well as studies using Smad deficient cell lines provided the first indication that TGFβ signaling can occur independent of Smads (Kretzschmar and Massague 1998) (Figure 4). Some of these pathways include PI3K/Akt (Bakin, Tomlinson et al. 2000), MAP kinases (Bakin, Rinehart et al. 2002; Deaton, Su et al. 2005), Ras (Ward, Gadbut et al. 2002) NFκB (Criswell and Arteaga 2007; You, How et al. 2009) and the small GTPases, cdc42 and RhoA (Yamaguchi, Shirakabe et al. 1995; Kimura, Matsuo et al. 2000; Mulder 2000; Takatsu, Nakamura et al. 2000; Bhowmick, Ghiassi et al. 2001; Edlund, Landstrom et al. 2002; Ward, Gadbut et al. 2002; You, How et al. 2009). Whereas Smad signaling tends to have slower kinetics given its role in regulating gene expression, activation of many of these pathways is rapid, occurring within minutes following TGFβ stimulation (Engel, McDonnell et al. 1999) Together these pathways regulate many aspects of cell behavior from cell survival to EMT and invasion each occurring in a cell-context specific manner (Massague and Gomis 2006).

The link between each of these pathways and TGFβ receptors is an area of active investigation. One link that has been established, however, is that of TGFβ activation of the Par6/Smurf1/RhoA. In mammary epithelial cells, where this pathway was initially described, ALK5 is localized with Par6, a protein that

regulates epithelial cell polarity to tight junctions by the occludins (Ozdamar, Bose et al. 2005). Upon TGFβ stimulation, TGFβR2 is recruited to the complex where it phosphorylates and activates ALK5. ALK5 in turn activates Par6 which facilitates the subsequent interaction with the E3 ubiquitin ligase, Smurf1. This in turn targets RhoA for degradation leading to tight junction dissolution and EMT (Ozdamar, Bose et al. 2005). In contrast to other TGFβ activated pathways whose activities are cell type dependent, the Par6/Smurf1/RhoA pathways seems to be conserved across many types of epithelial cells and across species from *C.elegans* to mammals (Gao and Macara 2004).

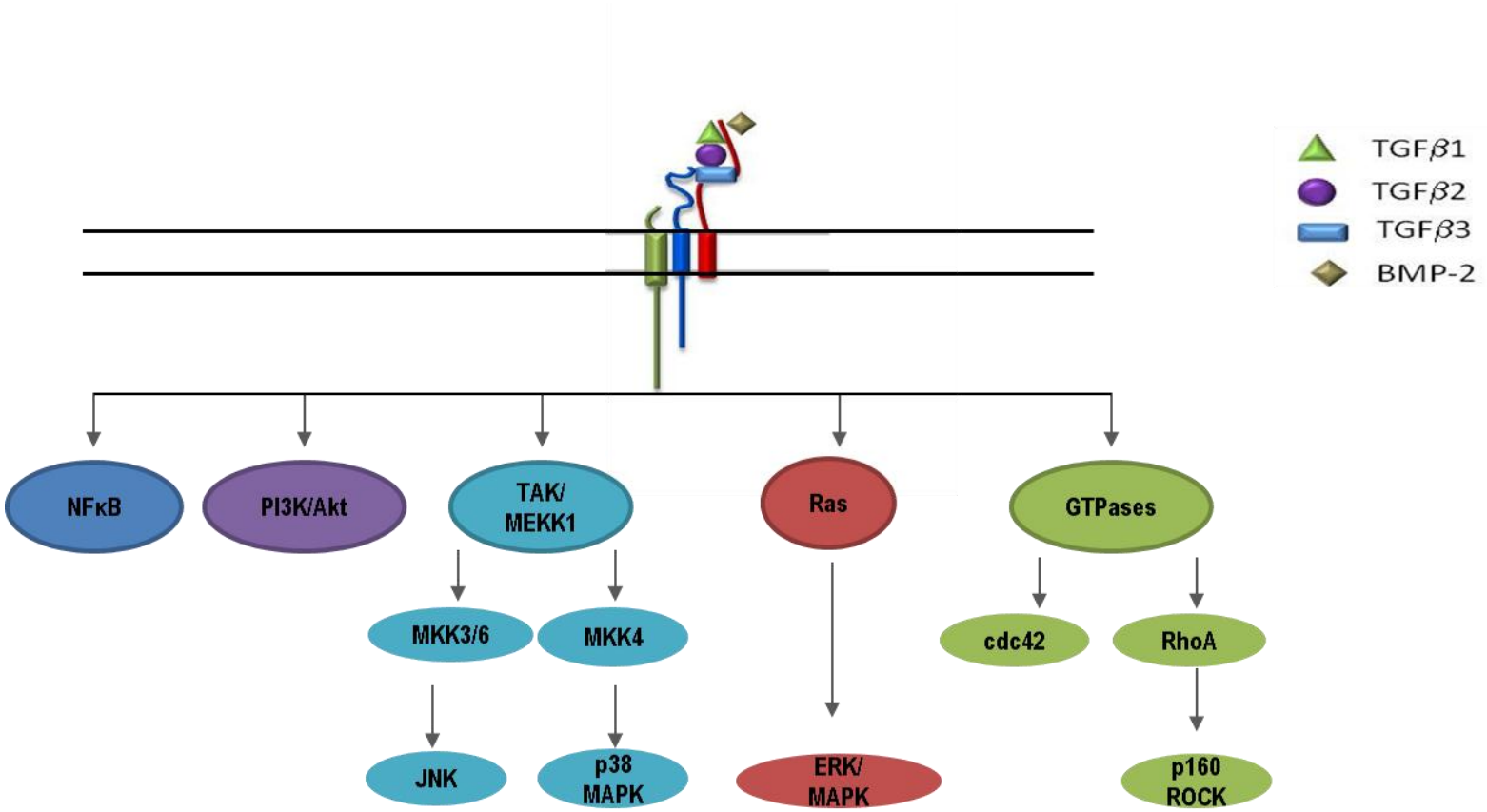

Figure 4 Smad Independent Signaling TGFβ can signal in a Smad-independent manner through pathways such as MAPK, RAS, RHOA, and PP2A. Moified from *Derynck, R. and Zhang, Y.E. Nature 2003*

Differential ALK Activation and TGFβ Signaling

Smad dependent and independent pathways are not mutually exclusive. In fact, these pathways act concurrently to mediate the effects of TGFβ (Derynck and Zhang). Whether Smad-dependent or Smad-independent pathways, or TGFβ-or BMP-responsive-Smads are activated depends greatly on which Type I TGFβ Receptors are present and activated. Differential ALK activation has been hypothesized to be partially responsible for the plethora of effects ascribed to TGFβ (Roberts 1988; Derynck and Zhang 2003; Siegel and Massague 2003). Studies of TGFβR3's counterpart in endothelial cells, endoglin, have provided great insight into differential ALK regulation.

In endothelial cells, TGFβ can both inhibit and stimulate endothelial cell proliferation, migration and angiogenesis (Pepper 1997). Both TGFβ and BMP responsive ALK's and Smads are expressed in these cell types (Goumans, Valdimarsdottir et al. 2002; Goumans, Valdimarsdottir et al. 2003), however, depending on the dose of TGFβ, ALK1 or ALK5-dependent pathways can be activated to either stimulate or inhibit angiogenesis (Figure 5). Low doses of TGFβ activate ALK1 signaling leading to Smad1/5/8 activation, *Id1* expression and stimulates endothelial cell proliferation and migration; higher doses of TGFβ activate ALK5, Smad2/3, PAI-1 expression and inhibits endothelial cell proliferation and migration (Goumans, Valdimarsdottir et al. 2002; Goumans, Valdimarsdottir et al. 2003).Although the exact underlying mechanism of

differential ALK activation continues to be investigated, several lines of evidence have emerged supporting a novel role for endoglin's 47 amino acid cytoplasmic domain. Following ligand addition, ALK5 phosphorylates endoglin at Serines 646 and 649 located on its cytoplasmic domain (Ray, Lee et al. 2010). This modification facilitates endoglin interaction with ALK1 and is hypothesized to lead to the formation of a single complex that activates either Smad2/3 or Smads1/5/8 (Ray, Lee et al. 2010). In addition to Smad activation, these phosphorylation events also facilitate the interaction with the scaffolding proteins, GIPC (Lee, Ray et al. 2008) and β-arrestin2(Lee and Blobe 2007). The interaction of endoglin with β-arrestin2 leads to receptor internalization and ERK activation and migration (Lee and Blobe 2007). The interaction of endoglin with GIPC adds another layer of complexity to TGFβ signaling, as this interaction, although it promotes TGFβ-mediated Smad1/5/8 signaling as previously stated, also inhibits endothelial cell migration, in contrast to the previous study (Lee, Ray et al. 2008), and suggests the activation of Smad-independent pathways. This additional level of complexity brings us back to the notion that Smad dependent and independent pathways are not mutually exclusive, but function side by side to yield one final event.

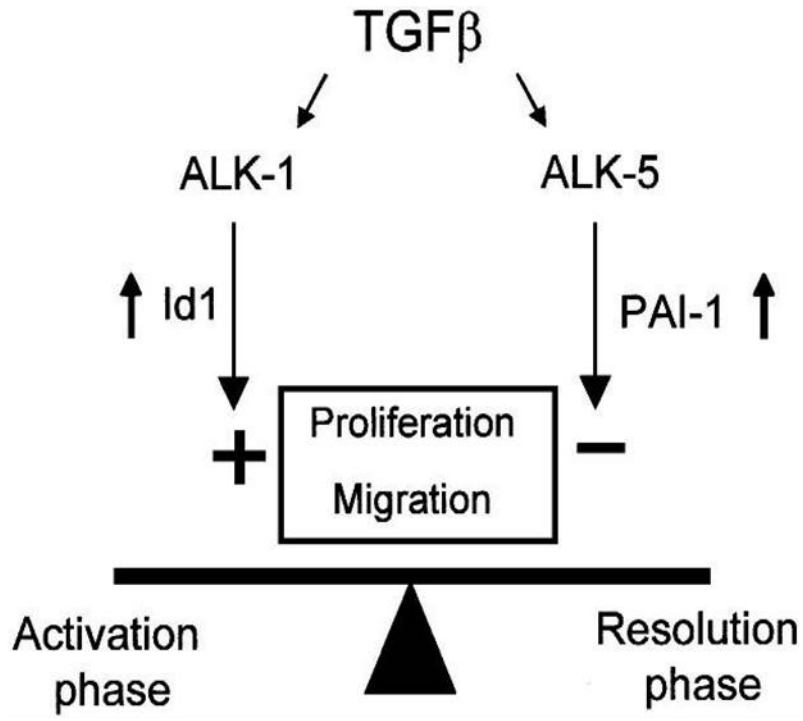

Figure 5 Differential ALK activation in endothelial cells Schematic figure of the functional role of ALK1 and ALK5 in ECs. TGF-β regulates the state of the endothelium via a fine balance between ALK5 and ALK1 signaling. Activation of ALK5 by TGF-β induces PAI-1 expression and inhibits migration and proliferation, whereas TGF-β-induced ALK1 activation induces Id1 expression and stimulates migration and proliferation. The ratio of TGF-β signals via ALK1 versus ALK5 will determine whether TGF-β will have a pro- or anti-angiogenic effect. *From Goumans, M.J., et al, Embo J 2002*

TGFβR3's Unique Signaling Ability

TGFβR3 can present ligand to TGFβR2/TGFβR1 and augment Smad signaling; however several lines of evidence support a role for TGFβR3 other than simply ligand presentation: First, TGFβR3 is required for the high affinity binding of TGFβ2 ligand (Lopez-Casillas, Cheifetz et al. 1991). Second, TGFβR3 is required for endocardial cell transformation *in vitro* (Brown, Boyer et al. 1999) Third, *Tgfbr3*$^{-/-}$ mice are embryonic lethal (Compton, Potash et al. 2007), and have a unique phenotype that does not overlap with other TGFβ ligand and receptor null mice (Azhar, Schultz Jel et al. 2003; Barnett and Desgrosellier 2003).

Deletion of the cytoplasmic domain does not inhibit the ability of TGFβR3 to present ligand to TGFβR1 and TGFβR2 and its subsequent ability to augment the canonical signaling pathway (Blobe, Schiemann et al. 2001) which suggests a unique role for the 43 amino acid cytoplasmic domain. Two proteins have been reported to bind the cytoplasmic domain. Phosphorylation by TGFβR2 at Threonine 841 on TGFβR3's cytoplasmic domain generates a binding site for β-arrestin2 (β-arr2), which subsequently leads to receptor internalization and down-regulation of TGFβ signaling (Blobe, Schiemann et al. 2001; Chen, Kirkbride et al. 2003). Studies of its counterpart in endothelial cells, endoglin, as described in preceding sections have shed light on our understanding of this receptor's unique function, but the role of its interacting proteins with other receptors has also aided

in deciphering their role with TGFβR3. β-arr2 interactions with G protein coupled receptors have been well established to facilitate receptor internalization and serve as scaffolds for mitogen activated protein kinase (MAPK) cascades (Gurevich and Gurevich 2003). In comparison, β-arr2-mediated internalization of TGFβR3 has also recently been shown to produce such signaling scaffolds. One of the proteins recruited to this signaling hub, is cdc42, which leads to migration inhibition in both cancer and normal epithelial cells (Mythreye and Blobe 2009) (Figure 6). NFκB, also recruited by β-arr2 following TGFβR3 internalization, has been reported in several cancer cell lines, and plays a role in promoting epithelial cell homeostasis (You, How et al. 2009) (Figure 6).

The second cytoplasmic protein that binds TGFβR3 is the PDZ domain containing protein, GIPC (**G**AIP-**i**nteracting **p**rotein, **C** terminus). GIPC binds the last three C-terminal amino acids, STA, and stabilizes TGFβR3 at the plasma membrane (Blobe, Liu et al. 2001). The role of GIPC in TGFβR3 signaling is currently under study, and current knowledge stems from understanding its role with other receptors. In endothelial cells, the interaction of GIPC1 with syndecan-4 activates Rac1 localizing it to the leading edge to promote migration (Tkachenko, Elfenbein et al. 2006). In contrast, interaction of GIPC with endoglin, inhibits endothelial cell migration (Lee, Ray et al. 2008). GIPC1 also regulates the stability of the IGF-I receptor, a major regulator of cell survival and proliferation in breast and pancreatic cancer cell lines (Muders, Vohra et al. 2009; Wang, Lau et al. 2010). Although less is known about the role of GIPC's

interaction with TGFβR3, it has been established that this interaction can inhibit migration and invasion *in vitro,* and breast cancer cell progression *in vivo* (Lee, Hempel et al.). Less is known about the downstream targets of this interaction (Figure 6).

In summary, TGFβR3, with its short, non-enzymatic cytoplasmic domain plays an important role in regulating TGFβ signaling and must be considered when trying to understand the role of TGFβ in any system, from development to pathological state.

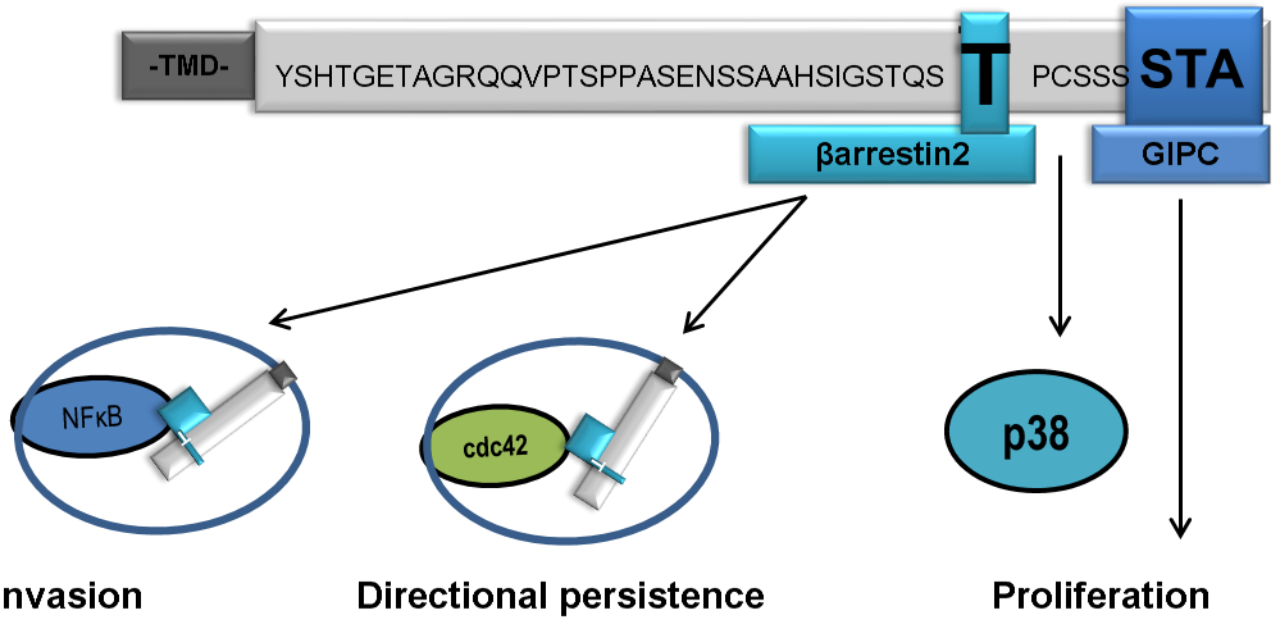

Figure 6 TGFβR3's Unique Signaling TGFβR3 can signal independent of TGFβR1 and TGFβR2 or the Smads. After ligand binding, TGFβR2 phosphorylates TGFβR3's cytoplasmic domain at Threonine 841, allowing binding of β-arrestin2, that leads to receptor internalization. The internalized receptor and β-arrestin2 (Blobe, Schiemann et al., 2001) serve as a scaffolding protein for NFκB (You, How et al., 2009) and cdc42 (Mythreye and Blobe, 2009), that can then regulate invasion and directional persistence, respectively. GIPC binding at the three C terminal amino acids, retains receptor at the cellular surface but can activate downstream mediators to regulate proliferation (Blobe, et al., 2001). Although the exact residues on TGFβR3's cytoplasmic domain have not been established, TGFβR3 has been shown to regulate p38 activity leading to regulation of proliferation (You, et al., 2007).

TGFβ Signaling During Cardiovascular Development

Studies *in vitro* and *in vivo* have demonstrated that TGFβ signaling plays a unique role during cardiovascular development. Given our interest in coronary vessel development, this section will focus on the unique contributions of members of the TGFβ family to overall cardiovascular development, with a focus on coronary vessel development.

TGFβ ligands have unique and overlapping patterns of expression. Here I focus on the expression pattern and phenotype of null mice of these ligands. *Tgfb1* is expressed throughout the epicardium at E12.5 and is localized to the outflow tract later during development (Molin, Bartram et al. 2003). Half of *Tgfb1*$^{-/-}$ mice die *in utero* due to defects in yolk sac vasculogenesis, and the remaining die about 20 days after birth due to multifocal inflammatory disease and tissue necrosis that results in organ failure (Shull, Ormsby et al. 1992). *Tgfb2* is expressed in the PE and epicardium beginning at E9.5 and continuing until E10.5. By E12.5, its expression is limited to the compact zone myocardium (Molin, Bartram et al. 2003). *Tgfb2*$^{-/-}$ mice display multiple cardiac defects including double-outlet right ventricle (DORV), dual inlet left ventricle (DILV) and ventricular septal defect (VSD) (Sanford, Ormsby et al. 1997). Despite this, no coronary vessel defects have been ascribed to *Tgfb2*$^{-/-}$ mice. TGFβ3 expression is restricted to the epicardium beginning at E11.5 and persisting through E15. 5 (Molin, Bartram et al. 2003). *Tgfb3*$^{-/-}$ mice die at P1 with severe delays in lung

development and defects in maxillary palate fusion (Kaartinen, Voncken et al. 1995). *In vitro,* TGFβ1, TGFβ2, or TGFβ3 have been shown to induce EMT in proepicardial explants and epicardial cells demonstrating a role for these growth factors in coronary vessel development (Morabito, Dettman et al. 2001; Compton, Potash et al. 2006; Olivey, Mundell et al. 2006; Austin, Compton et al. 2008). Thus, the absence of coronary vessel phenotypes in mice where either of these ligands has been knocked out suggests redundancy in some of the physiological roles these ligands play during coronary vessel development.

The first insights into the role of the TGFβ receptors during cardiovascular development come from *in vitro* studies using proepicardial (Brown, Boyer et al. 1996; Jiao, Langworthy et al. 2006). and epicardial explants (Compton, Potash et al. 2006) Through the use of epicardial explants and cells, ALK5 has been demonstrated to be required for TGFβ-induced EMT and smooth muscle differentiation (Compton, Potash et al. 2006; Olivey, Mundell et al. 2006; Austin, Compton et al. 2008). Conditional deletion of ALK5 in the endocardium, myocardium or epicardium has further uncovered the role of ALK5 during cardiovascular development (Sridurongrit, Larsson et al. 2008). While ALK5 appears to be redundant in cardiomyocyte development, it is important for endocardial EMT *in vitro* and *in vivo*, and cushion development (Sridurongrit, Larsson et al. 2008). In the epicardium, ALK5 is required and sufficient for EMT *in vitro* and epicardial attachment *in vivo.* Failure of the epicardium to attach results in deficits in coronary vessel formation resulting from defective

differentiation into the smooth muscle lineage and increased capillary vessels in the myocardium. Furthermore, myocardial growth is significantly attenuated in mice where ALK5 is specifically deleted from the epicardium. *ALK2*$^{-/-}$ and *ALK3*$^{-/-}$ mice die before E9.5 due to deficits in gastrulation, thus contributions to cardiac morphogenesis have been difficult to uncover (Gu, Reynolds et al. 1999; Mishina, Crombie et al. 1999). However, *in vitro*, ALK2 signaling is required for BMP-2-induced EMT in the proepicardium and endocardial cells, suggesting a role for ALK2 during cardiac development (Desgrosellier, Mundell et al. 2005; Olivey, Mundell et al. 2006). Conditional deletion of ALK2 in endocardial cells leads to AV valve defects as a consequence of decreased proliferation and differentiation of the cushion mesenchyme(Wang, Sridurongrit et al. 2005). Neural crest deletion of ALK2 results in multiple cardiac deficits, including persistent truncus arteriosus and abnormal maturation of aortic arch(Kaartinen, Dudas et al. 2004). In the proepicardium, overexpression of ALK2 like ALK5 induces EMT *in vitro* (Olivey, Mundell et al. 2006). The role of ALK2 in the epicardium remains to be elucidated

Deletion of TGFβR2 is also embryonic lethal due to defects in yolk sac hematopoiesis and vasculogenesis (Oshima, Oshima et al. 1996). Conditional deletion of TGFβR2 in the myocardium reveals no disruption in cardiogenesis (Jiao, Langworthy et al. 2006). Eventhough TGFβR2 is ALK5's prototypical binding partner, deletion of TGFβR2 does not inhibit endocardial EMT as does deletion of ALK5 in the endocardium (Jiao, Langworthy et al. 2006). Deletion of

TGFβR2 in the endothelium does affect atrioventricular canal and cardiac looping remodeling and results in double-inlet left ventricle (DILV) (Jiao, Langworthy et al. 2006). Inactivation of TGFβR2 under the control of the smooth muscle cell-specific protein, SM22α, which is expressed in vascular smooth muscle cells, epicardium and myocardium results in embryo lethality during the last week of gestation due to vascular abnormalities, ventricular myocardial hypoplasia, and septal defects (Langlois, Hneino et al. 2010). TGFβR2, like ALK5, is required for vascular smooth muscle differentiation during coronary vessel formation, thus inactivation of TGFβR2 in the epicardium results in overlapping phenotypes with conditional inactivation of ALK5 in the epicardium (Sridurongrit, Larsson et al. 2008). Vascular abnormalities resulting from inactivation of TGFβR2 under the control of SM22α were particularly profound in the descending thoracic aorta where defective elastogenesis led to rupture of thoracic aorta and embryonic lethality.

TGFβR3 knockout mice

The targeted deletion of TGFβR3 revealed the role of this receptor in cardiovascular development (Compton, Potash et al. 2007). TGFβR3 is expressed in both the epicardium and myocardium during development (Barnett, Moustakas et al. 1994), unpublished). Deletion of *Tgfbr3* in mice is embryonic lethal due to failed coronary vessel development but the molecular mechanisms remain to be elucidated (Compton, Potash et al. 2007). Gross analysis of

Tgfbr3$^{-/-}$ embryonic hearts reveals the formation of a primitive vascular plexus on both the ventral and dorsal surfaces of the heart as demonstrated by decreased immunoreactivity to the vascular endothelial cell marker, Platelet Endothelial Cell Adhesion Molecule (PECAM) at E14.0 (Figure 7). In contrast to *Tgfbr3*$^{+/+}$ and *Tgfbr3*$^{+/-}$, embryonic hearts whose epicardium is tightly opposed to the myocardium, and have a thin subepicardial layer (Figure 8 A and C), *Tgfbr3*$^{-/-}$ embryonic hearts display a discontinuous epicardium that is detached from the myocardium, an expanded subepicardial space with multiple blood islands and an abundance of mesenchymal cells (Figure 8 B and D). *Tgfbr3*$^{-/-}$ hearts also display a thin compact zone myocardium, that could be secondary to deficits in the epicardium. In contrast to the coronary system, vascular beds outside the heart in *Tgfbr3*$^{-/-}$ mice appear to form and pattern normally (Figure 9), suggesting that TGFβR3 has a unique role in coronary vessel development. Collectively, these data suggest that the failure of coronary vessel formation in *Tgfbr3*$^{-/-}$ embryos may be explained by altered epicardial cell behavior.

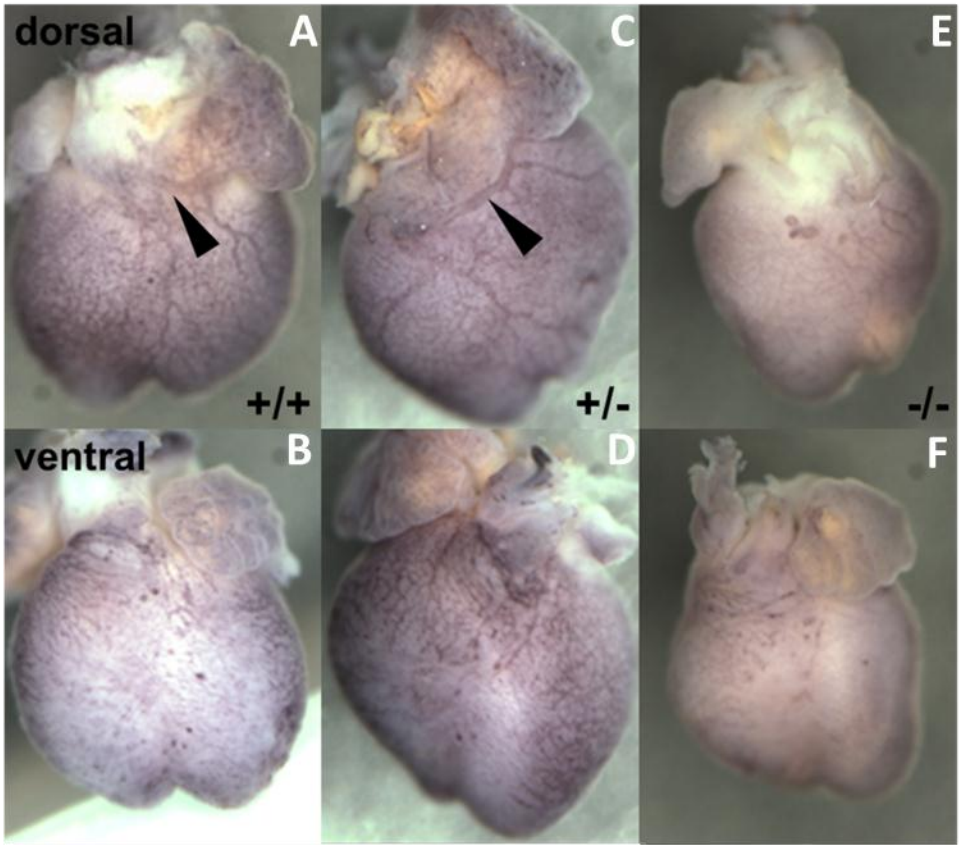

Figure 7 Reduced coronary vessels in *tgfbr3* null mice (A-F) PECAM immunostaining of whole hearts at E14.0. Wild-type (A,B) and heterozygous null (C,D) hearts display an elaborate primary vascular plexus on the ventral (B,D) and dorsal (A,C) surfaces of the heart. Numerous large, remodeled vessels were also present on the dorsal surface. Homozygous null hearts (E,F) display a marked reduction in the primary vascular plexus on both the ventral (F) and dorsal (E) surfaces of the heart and few to no large remodeled vessels were observed on the dorsal surface. From *Compton, et. al. Circ Res 2007*

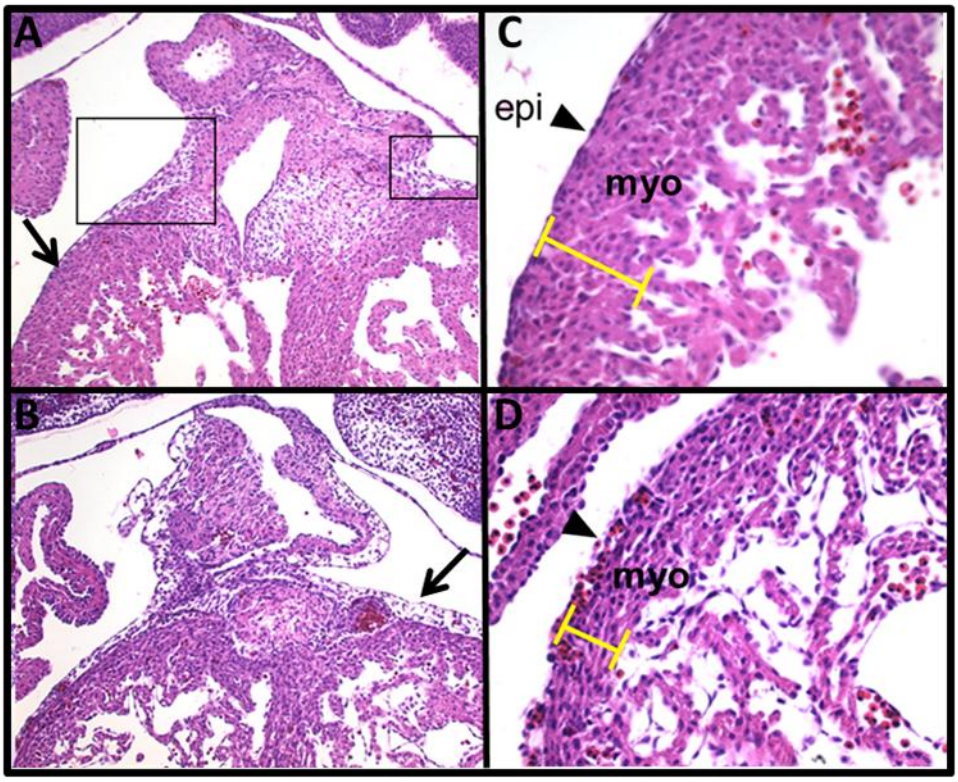

Figure 8 Thickened epicardium and blood islands in *Tgfbr3*$^{-/-}$ mice Photomicrographs of sections through E13.5 hearts at the level of the atrial root (A and B). (A) In *Tgfbr3*$^{+/-}$ mice the epicardium is tightly apposed to the myocardium along the ventricles (arrow, A) and atrial root. Subepicardial mesenchyme is only evident along the AV groove (boxed area, A). (B) In *Tgfbr3*$^{-/-}$ mice, subepicardial mesenchyme is present along the surface of the ventricles (arrow, B) and atrial root (not shown). (C and D) Photomicrographs depicting subepicardial vessels in the AV groove and epicardium along the ventricular myocardium at E13.5 at 40X magnification. (C) *Tgfbr3*$^{+/-}$ mice have an epicardium that is closely apposed to the ventricular myocardium (D) In*Tgfbr3*$^{-/-}$ mice, blood cells are evident in the epicardium along the ventricles. The myocardium is thickened in*Tgfbr3*$^{-/-}$ mice compared to *Tgfbr3*$^{+/-}$ All sections stained with hemotoxylin and eosin (A,B 20X; C,D 40X) *From Compton, et. al. Circ Res 2007*

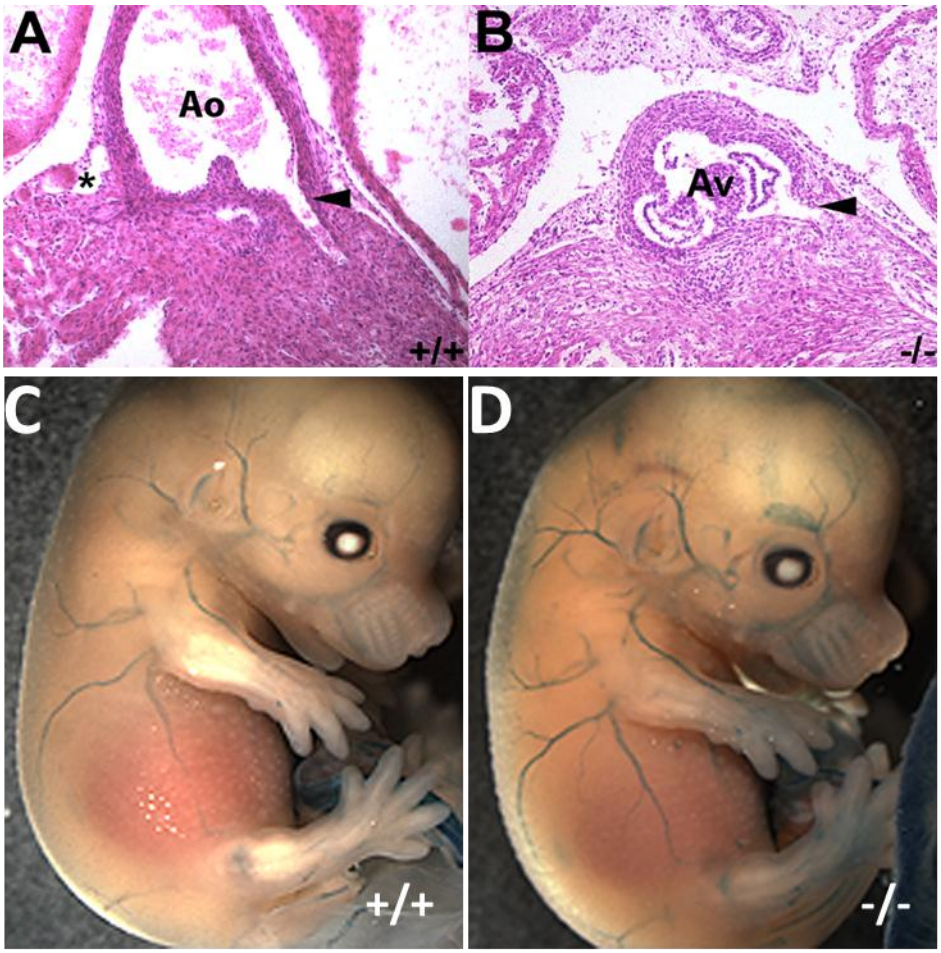

Figure 9 Presence of coronary ostia in E15.5 embryos and indistinguishable vessel patterning outside the heart. Sections through the aortic valve region. (A) Wildtype embryo depicting the left coronary ostia and direct communication between the aorta and the coronary vessel. Coronary vessels in close apposition to the aorta is also shown (asterisk). (B) Similar section of a null embryo demonstrating the presence of communication between the aorta and coronary vessel. All sections stained with hemotoxylin and eosin. All photomicrographs at 40X. Ao, aorta; Av, aortic valve. (C,D) *Tgfbr3*$^{+/+}$ and *Tgfbr3*$^{-/-}$ embryos expressing LacZ under the control of SM22αpromoter show no patterning defects in vessels outside the heart. *From Compton, et. al. Circ Res 2007*

Although embryonic lethality results from an inability to form coronary vessels, *Tgfbr3*$^{-/-}$ embryos display other cardiovascular defects, including double outlet right ventricle, ventricular septal defect, and hyperplastic cushions (Compton, Potash et al. 2007), unpublished). Some of these phenotypes (DORV, VSD) are shared with *Tgfb2*$^{-/-}$ mice (Sanford et al., 1997), consistent with TGFβ2 and TGFβR3 functioning as receptor ligand pair in the formation of these structures. None of the other ligand knockouts have been reported to have cardiovascular defects. This demonstrates that TGFβR3 has a unique and non-redundant role in coronary vessel formation. The molecular mechanisms by which the loss of TGFβR3 disrupts epicardial cell behavior and consequently coronary vessel formation, will be addressed here.

.

Summary

Understanding the pathways that regulate embryonic coronary vessel development has direct implications to cardiovascular development but more recently has expanded as a potential therapeutic target to direct repair of myocardial and vascular structures in adult hearts. We have shown that TGFβR3 is required for coronary vessel development. Here, I uncover the molecular mechanism for failed coronary vessel development in *Tgfb3*$^{-/-}$ mice and provide data supporting a unique and non-redundant role in for TGFβR3 in TGFβ signaling. My observations suggest TGFβR3 as a potential therapeutic target to consider in coronary vessel development and disease.

CHAPTER II

THE CYTOPLASMIC DOMAIN OF TGFβR3 THROUGH ITS INTERACTION WITH THE SCAFFOLDING PROTEIN, GIPC, DIRECTS EPICARDIAL CELL BEHAVIOR

Introduction

Coronary vessel development begins when a group of mesothelial cells known as the proepicardium are transferred from the liver promordium to the surface of the heart where they form an epithelial sheet termed as the epicardium (Viragh and Challice 1981; Manner 1993; Olivey, Compton et al. 2004; Tomanek 2005). A subset of these cells undergoes epithelial to mesenchymal transformation (EMT) and invades the subepicardial space with some of these cells continuing into the myocardium. Cells then differentiate into several cell lineages including vascular smooth muscle cells and cardiac fibroblasts (Mikawa and Fischman 1992; Poelmann, Gittenberger-de Groot et al. 1993). The origin of endothelial cells is controversial (Tomanek, Ishii et al. 2006; Lavine, Long et al. 2008; Xiong 2008), but recent work (Red-Horse, Ueno et al. 2010) demonstrates that these cells arise from the sinus venosus. Together these cells contributed by the epicardium and sinus venosus are coordinately regulated to form the coronary vasculature.

Deletion of the gene encoding the Type III Transforming Growth Factor β Receptor (TGFβR3) in mice is embryonic lethal due to failed coronary vessel development (Compton, Potash et al. 2007). TGFβR3 contains a heavily glycosylated extracellular domain and a highly conserved, 43 amino acid intracellular domain with no known catalytic activity (Lopez-Casillas, Cheifetz et al. 1991; Wang, Lin et al. 1991). TGFβR3 is required for the high affinity binding of TGFβ2 but also binds TGFβ1 and TGFβ3 (Lopez-Casillas, Wrana et al. 1993). In addition, TGFβR3 can bind and signal in response to BMP-2 (Kirkbride, Townsend et al. 2008) and function as an inhibin receptor (Wiater, Harrison et al. 2006). Upon binding TGFβ, TGFβR3 presents ligand to the Type I (TGFβR1) and Type II (TGFβR2) TGFβ Receptors to augment signaling via the canonical signaling pathway that is dependent on the phosphorylation and nuclear translocation of the Smads (Torlopp, Schlueter et al. 2010). Deletion of the cytoplasmic domain does not inhibit the ability of TGFβR3 to present ligand to TGFβR1 and TGFβR2 and subsequently augment the canonical signaling pathway (Blobe, Schiemann et al. 2001). The results of targeting TGFβR3 in mice (Compton, Potash et al. 2007) and cardiac cushion explants (Brown, Boyer et al. 1999) demonstrate a unique and non-redundant role for TGFβR3 in addition to ligand presentation. Regulation of the migration and invasion of several cancer cell lines has been shown to require the cytoplasmic domain of TGFβR3 (Lee, Hempel et al. 2009; Mythreye and Blobe 2009) suggesting the presence of a noncannonical signaling pathway activated by TGFβR3.

Efforts to understand this noncanonical pathway downstream of TGFβR3 have focused on the identification of proteins that interact with the cytoplasmic domain of the receptor. Phosphorylation of Thr841 by TGFβR2 has been shown to be required for βarrestin2 binding and leads to TGFβR3 internalization and down-regulation of TGFβ signaling (Chen, Kirkbride et al. 2003). The 3 C-terminal amino acids of TGFβR3, STA, serve as a Class I PDZ binding motif and bind the scaffolding protein, GIPC (GAIP-interacting protein, C terminus) (Blobe, Liu et al. 2001). Interaction with GIPC stabilizes TGFβR3 at the surface and enhances TGFβ signaling (Blobe, Liu et al. 2001). The interaction between TGFβR3 and either βarrestin2 (Mythreye and Blobe 2009; You, How et al. 2009) or GIPC (Lee, Hempel et al. 2009) have been reported to regulate cell behavior, specifically proliferation, invasion and cell migration in breast and ovarian cancer cell lines.

Here we demonstrate that the loss of TGFβR3 results in decreased proliferation and invasion in intact embryos and cultured epicardial cells. The decreased invasion of epicardial cells *in vitro* is seen in response to not only TGFβ1 and TGFβ2 but also FGF2 and HMW-HA suggesting a dysregulation of key regulators of epicardial cell behavior following the loss of TGFβR3. The restoration of the invasive response to all these ligands in null cells was shown to be dependent on the cytoplasmic domain of TGFβR3, specifically the 3 terminal amino acids, and interaction with GIPC. Based on our observations we propose that failed coronary vessel development in *Tgfbr3*$^{-/-}$ mice is due to decreased

epicardial cell proliferation and mesenchymal cell invasion into the myocardium where these cells are required to participate in coronary vessel development.

Experimental Methods

Generation of Embryos

Tgfbr3$^{+/-}$ mice were generated as described (Compton, Potash et al. 2007) and maintained on a C57BL/6 SV129 mixed background. *Tgfbr3*$^{+/-}$ littermates were crossed to generate *Tgfbr3*$^{+/+}$ and *Tgfbr3*$^{-/-}$ embryos.

Cell Culture

Immortalized epicardial cell lines were obtained as previously described (Austin, Compton et al. 2008). To maintain the immortalized state, cells were grown in immorto media: DMEM containing 10% FBS (fetal bovine serum), 100 U/ml Penicillin/Streptomycin (P/S), 1X Insulin-Transferrin-Selenium (ITS;1 µg/ml insulin, 5.5 x 10^{-4}µg/ml transferrin, 0.677 µg /ml selenium), and 10U/ml (interferon γ) INFγ at 33°C. For experiments, the T antigen was silenced by culturing at 37˚C in the absence of ITS or I INFγ. Multiple *Tgfbr3*$^{+/+}$ and *Tgfbr3*$^{-/-}$ littermate pairs were used where available. E11.5 epicardial cells were used in all experiments unless otherwise specified.

Growth Factors

TGFβ1, TGFβ2, and high molecular weight hyaluronic acid (HMW-HA) (~980 kDa) were purchased from R&D Systems. FGF-2, PDGF-AA, PDGF-BB, EGF, and VEGF were purchased from (Pepprotech).

Immunohistochemistry

Tgfbr3$^{+/+}$ and *Tgfbr3*$^{-/-}$ cells were plated at a density of 25,000 cells per well in one well of a 4-well collagen coated chamber slide and allowed to adhere overnight at 37˚C. The following day the media was replaced with DMEM containing 5% FBS and incubated with vehicle (4mM HCl/0.01% BSA), 250 pM TGFβ1 or TGFβ2. After a 72 hour incubation period at 37˚C, cells were fixed. For ZO-1 staining, cells were fixed in 70% methanol on ice for 10 minutes; for SM22α, 2% paraformaldehyde (PFA) for 30 min and permeabilized with PBS and 0.2% Triton X-100 for 5 min at room temperature. Cells immunostained for ZO-1 were blocked with 2% bovine serum albumin (BSA) in PBS for 1 hr and incubated with dilute primary antibody (ZO-1, 2μg/ml, Zymed) overnight at 4˚C. For SM22α (Abcam) cells were blocked with 5% horse serum, and incubated with primary antibody (SM22α, 1:200) overnight at 4˚C. Primary antibody detection was with goat anti-rabbit cy3 (ZO-1) or donkey anti-goat cy3 (SM22α) secondary antibody (1:800; Jackson ImmunoResearch). Cells infected with adenovirus co-expressing GFP and TGFβR3 were fixed in 2%PFA and stained for TGFβR3 (5μg/ml, AF-242-PB,R&D) for 1 hour at RT, and detected with Alexa555 conjugated donkey anti-goat antibody (Invitrogen) for 1 hour at RT. Nuclei were stained with 4',6-diamidino-2-phenylinodole (DAPI; Sigma). Photomicrographs were captured with Nikon Eclipse TE2000-E microscope and QED imagining software.

qRT-PCR

Tgfbr3$^{+/+}$ and *Tgfbr3*$^{-/-}$ cells were seeded at 200,000 cells per well of a 6 well tissue culture plate and allowed to adhere overnight at 37˚C. The following day the media was replaced with DMEM containing 5% FBS and incubated with vehicle, 250 pM TGFβ1 or TGFβ2. After a 72 hour incubation period at 37˚C, total RNA was isolated using the TRIzol reagent (Invitrogen) according to the manufacturer's protocol. cDNA was generated from 1ug total RNA using oligo-dT primers and Superscript III polymerase (Invitrogen). Real-time PCR analysis was done with iQ SYBR Green Supermix (Bio-Rad) in the Bio-Rad iCycler for 40 cycles. The expression levels are calculated using the $\Delta\Delta C_T$ method. The threshold cycle (C_T) represents the PCR cycle at which an increase of the reporter fluorescence above the baseline is first detected. The fold change in expression levels, R, is calculated as follows:

$R=2^{-\Delta\Delta CT}$ (where $R = 2^{(\Delta CT\ treated-\Delta CT\ control)}$).This method normalizes the abundance of all transcripts to the constitutive expression level of *GAPDH* RNA. Primer pairs for the smooth muscle markers, Sm22α, SMαA, and calponin are as follows:

Gene	**Sense primer (5'→3')**	**Anti-sense primer (5'→3')**
Sm-22α	AGCCAGTGAAGGTGCCTGAGAAC	TGCCCAAAGCCATTAGAGTCCTC
SmαA	GAGAAGCCCAGCCAGTCG	CTCTTGCTCTGGGCTTCA
Calponin	GAAGGCAGGAACATCATTGGACTG	CTCAAAGATCTGCCGCTTGGTGCC
GAPDH	ATGACAATGAATACGGCTACAG	TCTCTTGCTCAGTGTCCTTG

Wound Healing Assay

Cells were seeded in a 35-mm culture plate coated with collagen at a density of $3x10^6$ cells/plate in immorto media and incubated at 33°C. Cells were allowed to form a confluent monolayer within 2 days. Upon reaching confluency, cells were starved with DMEM containing 0.5% FBS and 100U/ml P/S and incubated overnight at 37°C. Eight-1mm circular cell free areas were created with a stabilized rotating silicone tip, and immediately photographed. Wound closure was monitored by for 72 hours. The denuded area was measured using ImageJ software. Percent wound closure relative to the initial wound area was calculated. Experiments were repeated three times.

Time Lapse, Two Dimensional Motility Assay

Cells were seeded in 35 mm culture plates, either coated with collagen or containing 1 ml collagen gel, prepared at a density of 1.75 mg/ml as described (Runyan and Markwald 1983). Two or four sister cultures, containing cells derived from littermate embryos, were recorded with an automated inverted microscope system (Leica DMIRE2, Leica Microsystems, Germany) equipped with a stage-attached incubator (Perryn, Czirok et al. 2008). Images (608×512 pixels spatial and 12 bit intensity resolution) were obtained with a 10X objective (0.30 N.A.) and a cooled Retiga 1300 camera (QImaging, Burnaby, British Columbia). The control software recorded multiple microscopic fields within each culture dish. The time lag between consecutive image frames was 10 minutes.

Cell movements were obtained from the recorded image sequences by two independent procedures. Manual cell tracking (Perryn, Czirok et al. 2008) results in cell trajectories over long time periods, but the number of cells tracked is limited to 20-30 per field, around 10% of the cells present. An automated flow field estimator (Particle Image Velocimetry (PIV) algorithm (Zamir, Czirok et al. 2005), combined with a cell/background segmenter (Wu, Gauthier et al. 1995) yields unbiased velocity fields over the entire cell covered area, without distinguishing individual cells.

Cell displacements can be characterized by the mean magnitudes of displacements during various time intervals as $d(\tau) = \{|x_i(t + \tau) - x_i(t)|\}_{i,t}$ where $x_i(t)$ denotes the position of cell i at various time points t, and the average $\{\}_{i,t}$ is calculated for all possible choices of i and t (Rupp, Visconti et al. 2008). Speed values are defined as $d(\tau = 1\ \text{h})$, i.e., mean cell displacements during a one hour long time period (6 frames). The PIV method directly yields speed values (albeit not for each cell but rather per unit area) when the compared images were recorded 1 hour apart. For statistical purposes, we compared mean speed values obtained from independent time lapse recordings (n≥3).

Proliferation

BrdU Incorporation in vitro

Cells were plated in 4-well collagen coated chamber slides at a density of 25,000 cells/ well and were allowed to attach overnight at 37˚C in DMEM containing

10%FBS and 100U/ml Penn/Strep. To synchronize at G_0, 24h post-plating, cells were serum starved in DMEM containing 0.5% FBS and 100U/ml Penn/Strep overnight, followed by replacement of DMEM containing 10% FBS and 100U/ml P/S. Cells were fixed in ethanol at 24, 48 and 72h after replacing growth medium. BrdU (bromodeoxyuridine) incorporation assay was carried out as instructed by manufacturer (Roche: BRDU Labeling and Detection Kit II). Random fields were selected and photographed for each well using Nikon Eclipse TE2000-E microscope and QED imaging software. Percent proliferation was calculated by counting the number of BrdU positive cells in a total of 500 cells per genotype at each time point. Experiments were repeated three times on cells from one littermate pair.

MTS Assay

This method relies on the *in vivo* reduction of MTS tetrazolium to a colored formazan product by NADPH in metabolically active cells. The product formed is read at 490nm and is directly proportional to the number of living cells in culture. Cells were plated in triplicate in a 96-well plate at a density of 5,000 cells/well in 100 µl of DMEM containing 10% FBS and 100U/ml P/S overnight at 37˚C. At 24, 48, and 72h post-plating, 20 µl of substrate (Promega: Cell Titer 96 Aqueous Solution) was added to each well. Colorimetric reaction was allowed to proceed for 30 minutes at 37˚C, followed by reading at 490nm. Experiments were repeated three times in triplicate per littermate pair. At least 3 different littermate pairs were analyzed.

BrdU incorporation in vivo

Pregnant mice at E12.5 and E13.5 were injected with BrdU 100μg/kg at 6 hours, 4 hours, and 2 hours before sacrifice. The embryos were genotyped and embedded and *Tgfbr3*$^{+/+}$ and *Tgfbr3*$^{-/-}$ littermate embryos were sectioned. Sections (7μm) through the heart were blocked with 5% Normal Donkey Serum/ 1% BSA and immunostained with a rat Anti-BrdU antibody (Accurate Chemical & Scientific Corp; 1:200) and an AlexaFluor 594 Donkey Anti-Rat secondary antibody (Invitrogen, 1:200). DAPI was used to stain nuclei. Photographs of each section were acquired using Nikon Eclipse TE2000-E microscope at 20x magnification and QED imaging software. The total number of nuclei and the number of BrdU positive nuclei were determined in representative sections of the epicardium using Image J software. The percentage of BrdU positive nuclei were calculated as a measure of cell proliferation. Three animals per genotype, per stage were analyzed.

Apoptosis Assays

Caspase 3/7 Homogenous Assay

Cells were plated in triplicate in a 96-well plate at a density of 10,000 cells/well in 100 μl of DMEM containing 10% FBS and 100U/ml P/S overnight at 37˚C. At each time point, 24, 48, and 72h post-plating, 100 μl of substrate (ApoONE Homogenous Caspase 3/7 Assay; Promega) was added to each well. Colorimetric reaction was allowed to proceed for 2 hours at room temperature. Caspase 3/7 activity was then detected by reading the fluorescence of each well

(Ex: 499nm, Em: 521nm). Experiments were repeated three times in triplicate per littermate pair. At least 3 different littermate pairs were analyzed.

Trypan Blue Exclusion

Cells were plated in duplicate in 12-well collagen coated plates a density of 100,000 cells/ well and were allowed to attach overnight at 37˚C in DMEM containing 10%FBS and 100U/ml Penn/Strep. At 24, 48 and 72 hours post-plating, cell were trypsinized and re-suspended in 500 µl media. Trypan blue was added to cells at a 1:1 ratio and allowed to sit at room temperature for 1 minute. Five hundred cells per genotype were counted at each time point, and the proportion of trypan blue positive cells to total cells was calculated Experiments were repeated three times in triplicate per littermate pair.

TUNEL in vivo

E12.5 and E13.5 embryos were genotyped, embedded, and *Tgfbr3*$^{+/+}$ and *Tgfbr3*$^{-/-}$ littermate embryos were sectioned. TUNEL staining was performed using DeadEnd Fluoremetric TUNEL System (Promega) on 7µm sections through the heart and the nuclei stained with DAPI. Photographs of each section were acquired using Nikon Eclipse TE2000-E microscope and QED imaging software. The total number of nuclei and the number of TUNEL positive nuclei were determined in representative sections of the epicardium to determine the percentage of apoptotic cells present. Three animals per genotype, per stage were analyzed.

Invasion Assays

Calcein Labeled/Plate Reader

To determine the invasive potential of immortalized epicardial cells in response to growth factor stimulation, a modified Boyden chamber assay was employed. Collagen gels were prepared as described (Craig, Parker et al. 2010). Briefly, cells were fluorescently labeled with CalceinAM (BD Biosciences) and then plated at 12,000 cells per well in DMEM containing 0.5% FBS (fetal bovine serum) in the top chamber. Cells were then allowed to settle overnight at 37˚C. The following day, DMEM containing 20% FBS +/- vehicle (4mM HCl/0.1% BSA), 250 pM TGFβ1 or TGFβ2 (R&D Systems) or 10ng/ml FGF-2, PDGF-AA, PDGF-BB, EGF, or VEGF was added to the bottom chamber and incubated for an additional 24 hours at 37˚C. Cells receiving HMW-HA treatment were pre-treated with 300 µg/ml HMW-HA (unless otherwise specified) in DMEM containing 0.5% FBS in the top well for 30 minutes. Media was then removed and replaced with fresh DMEM containing 0.5% FBS. 300 µg/ml HMW-HA was then added to the bottom chamber as described for the other ligands. The top insert was then removed and placed in a plate containing 0.25% Trypsin/2.21 mM-EDTA in HBSS (CellGro). Cells were allowed to detach from the membrane into the trypsin containing plate, which was then read using SpectraMax 96-well plate reader (Ex: 485, Em: 538, Cutoff: 530; sensitivity: 30). Relative invasion was calculated by normalizing treatment to vehicle treated groups.

Cyrstal Violet Stain

Cells were plated as described above. Instead of placing wells in trypsin, membranes were fixed in 2.5% Gluteraldehyde (Sigma) for 2 minutes, rinsed once with 1X PBS then stained in 0.4% Crystal Violet (Fisher) for 5 minutes, and mounted. Photographs of each membrane were acquired using Nikon Eclipse TE2000-E microscope and QED imaging software.

WT-1 staining in vivo

E13.5 embryos were genotyped, embedded, and *Tgfbr3*$^{+/+}$ and *Tgfbr3*$^{-/-}$ littermate embryos were sectioned. Sections through the heart were immunostained with a rabbit anti-WT-1 (Santa Cruz, 1:200) and the nuclei stained with DAPI. Photographs of each section were acquired using Nikon Eclipse TE2000-E microscope at 40x magnification and QED imaging software. The total numbers of WT-1 positive cells were determined in representative sections of the heart to determine the percentage of WT-1 positive cells invading the subepicardial space and myocardium.

Expression Analysis

Expression levels of LYVE1, CD44, FGFR1, FGFR2b, FGFR2c, FGFR3 and FGFR4 were analyzed using qRT-PCR as described above. Primer sequences were previously published and purchased from IDT (Quarto and Longaker 2008; Craig, Parker et al. 2010).

Gene	Sense primer (5'→3')	Anti-sense primer (5'→3')
Lyve1	*CAGCATTCAAGAACGAAGCAG*	*GCCTTCACATACCTTTTCACG*
CD44	*TCCTTCTTTATCCGGAGCAC*	*AGCTGCTGCTTCTGCTGTACT*
Fgfr1	*GTGGCCGTGAAGATGTTGAAGTCC*	*GCCGGCCGTTGGTGGTTTT*
Fgfr2b	*CACCCGGGGATAAATAGCTCCAATG*	*GCTGTTTGGGCAGGACAGT*
Fgfr2c	*CACCCCGGTGTTAACACCACGG*	*CTGGCAGAACTGTCAACCATG*
Fgfr3	*TGCCGGCCAACCAGACAGC*	*GCGCAGGCGGCAGAGTATCAC*
Fgfr4	*ATGAGCCGGGGAGCAGCAATGTT*	*GGGGGATGGCAGGGGGTGGTG*

Western Blots

Tgfbr3$^{+/+}$ and *Tgfbr3*$^{-/-}$ littermate epicardial cells were lysed and diluted in TNEN buffer (1 M Tris base, 5 M NaCl, 0.5 M EDTA and NP40) as described (Craig, Parker et al. 2010). Total cellular lysates were then resolved by sodium dodecyl sulfate-polyacrylamide gel electrophoresis (SDS-PAGE) and transferred onto a polyvinylidene difluoride (PVDF) membrane. After blocking in 3% BSA, membranes were probed with Rat anti-CD44 antibody (clone KM201) (Southern Biotech), rabbit anti-LYVE1 (XLKD1) Antibody (C-term) (Abgen). β-actin (Affinity Bio Reagents) was used as a loading control. TGFβR3 expression was confirmed using goat-polyclonal antibody (AF-242-PB) (R&D) and donkey anti-goat-HRP secondary R&D). Detection was performed using Super Signal West Pico substrate (Pierce).

Adenovirus Infections

Adenoviruses were generated using the pAdEasy system (He, Zhou et al. 1998). All concentrated viruses were titered by performing serial dilutions of the concentrated virus and counting the number of GFP-expressing 293 cells after 18–24 h. The following adenoviruses co-expressing GFP were used: full length

TGFβR3 (FL), TGFβR3 missing the cytoplasmic domain (CYTO) or the last 3 amino acids (Δ3), or GIPC. Cells were plated in collagen coated 6 well dishes at a density of 200,000 cells per well in immorto media overnight at 33˚C. The following day, virus was added directly to the cells at a final concentration of 10^8 PFU/ml and allowed to incubate for an additional 24 hours. The next day cells were plated for invasion or proliferation assays as described above.

Transfections

siRNA

Cells were plated at a density of 200,000 per well of 6-well plate. The following day cells were transfected with 2µg siRNA (Ambion) and 8 µl Xtreme siRNA Transfection Reagent (Roche). Sequences for siRNA used are as follows: GIPC1: *sense* 5'-GCAGUGUGAUUGACCACAUtt-3', *anti-sense* 5'-AUGUGGUCAAUCACACUGCct-3'. At 48 hours post-transfection cells were harvested for qRT-PCR to confirm knockdown of Gipc1(sense, 5'-TGGTTCAGGCCCACAA-3'; anti-sense, 5'-TCTCTAGCAAGTCATCCACC-3'), or used directly for invasion assays. Where overexpression of TGFβR3 was done in conjunction with knockdown of GIPC1, cells were transfected with siRNA, then infected with adenovirus 24 hours after, and plated for invasion assays 24 hours after that.

Plasmids

Cells were plated at a density of 50,000 per well of 6-well plate. The following day cells were transfected with 2µg pcDNA3.1 vector alone or expressing full length TGFβR3-F), TGFβR3-CYTO or TGFβR3- Δ3 and 8 µl FugeneHD Transfection Reagent (Roche). After 48 hours, cells were harvested for western blot analysis.

Statistical analysis

Paired student t-test was used to establish significance. Data are presented as the average of three experiments ± SEM for one littermate pair, unless otherwise specified. P-values of < 0.05 were considered significant.

Results

Epicardial cells in *Tgfbr3*$^{-/-}$ embryos display decreased proliferation and invasion

Deletion of *Tgfbr3* in the mouse results in death at E14.5 due to failed coronary vessel development that is characterized by an abnormal epicardium, increased subepicardial space, and poorly developed, dysmorphic vessels (Compton, Potash et al. 2007). These observations suggest that although the epicardium is formed in *Tgfbr3*$^{-/-}$ embryos, aberrant epicardial cell behavior may underlie the failure of coronary vessel development. Therefore we chose to measure epicardial cell proliferation, apoptosis, and invasion *in vivo* as an initial attempt to determine the mechanisms responsible for failed coronary vessel development. To determine the rate of epicardial cell proliferation, pregnant *Tgfbr3*$^{+/-}$ mice were injected with BrdU and embryos harvested at E12.5 and E13.5, a time when the epicardium covers the heart and epicardial cell EMT is evident. Embryos were sectioned and immunostained for BrdU (Figure 10A). Epicardial cells were counted and the percent of BrdU positive cells determined. No difference was noted at E12.5, however at E13.5 epicardial cells in *Tgfbr3*$^{+/+}$ embryos showed significantly more proliferation than *Tgfbr3*$^{-/-}$ littermates (25.3% $\pm$ 0.88% vs 15.7% $\pm$ 1.58%, p=0.012; n=3) (Figure 10B).

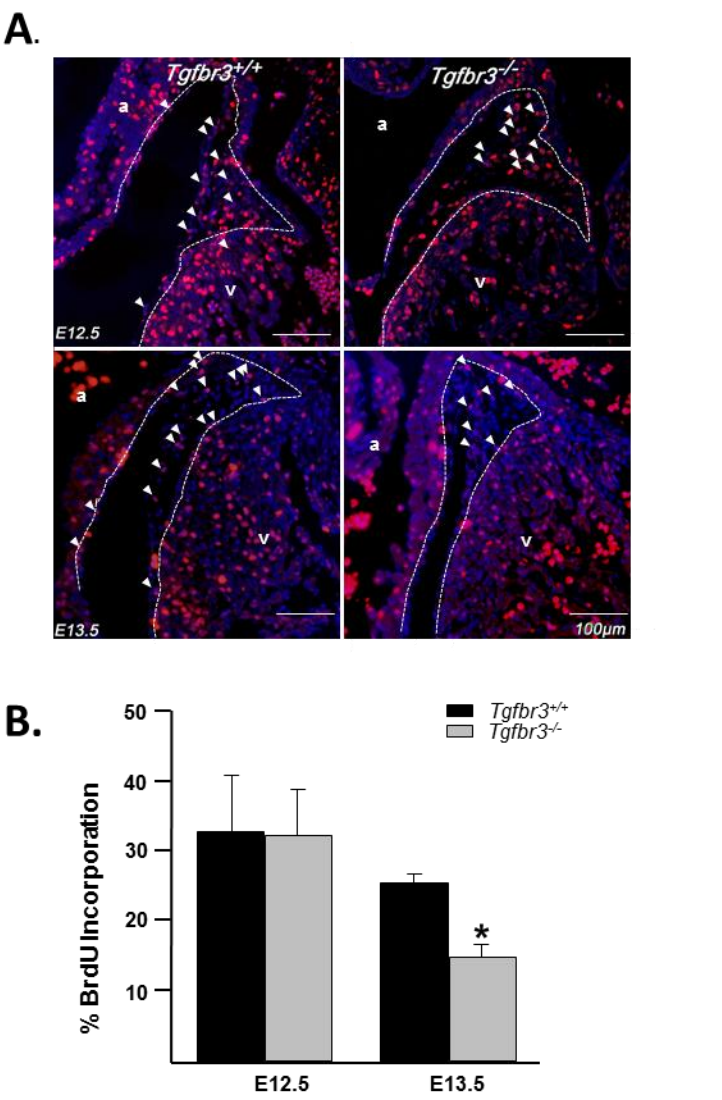

Figure 10 Epicardial cells in *Tgfbr3*$^{-/-}$ embryos show decreased proliferation (A) Heart sections from E12.5 and E13.5 embryos stained for BrdU. Representative BrdU positive cells are indicated by solid arrowheads. White dashed line demarcates myocardium from the epicardium and subepicardial space. (B) Percent proliferation is the number of BrdU positive cells per total number of DAPI stained nuclei (n= 3 embryos per genotype, per stage (*p<0.05)). cells (n=3 embryos per genotype (*p<0.05)). (a=atria, v=ventricle)

Apoptosis was assessed in E12.5 and E13.5 littermate embryos by TUNEL analysis. We noted a very low rate of apoptosis in *Tgfbr3*$^{+/+}$ embryos (< 4%) and no significant difference between genotypes (Figure 11). After the epicardium covers the surface of the heart *in vivo*, a subset of epicardial cells undergo EMT and invade the subepicardial space with some cells continuing into the myocardium (Olivey, Compton et al. 2004). We assessed epicardial cell invasion in E13.5 embryos by detecting the epicardial cell marker WT1 (Moore, McInnes et al. 1999). *Tgfbr3*$^{-/-}$ embryos display a significantly lower number of WT-1 positive cells that invade the subepicardial space or the myocardium (20.4% ± 3.71) compared to *Tgfbr3*$^{+/+}$ littermates (31.0% ± 2.87) (Figure 12 A and B; Figure 13 A and B). These data suggest that both decreased cell proliferation and decreased cell invasion contribute to failed coronary vessel development in *Tgfbr3*$^{-/-}$ mice.

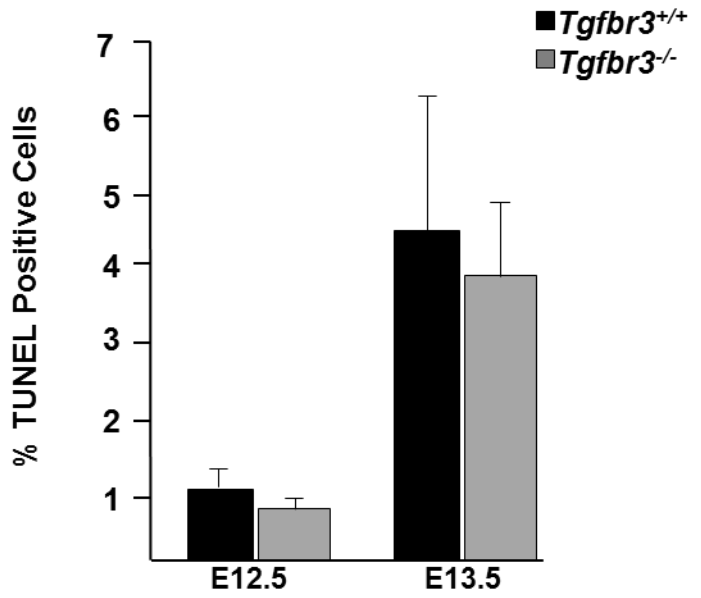

Figure 11 *Tgfbr3*$^{-/-}$ cells have similar apoptosis rate *in vivo* E12.5 and E13.5 embryos were genotyped, embedded, and *Tgfbr3*$^{+/+}$ and *Tgfbr3*$^{-/-}$ littermate embryos were sectioned. TUNEL staining was performed on sections through the heart and the nuclei stained with DAPI. The total number of nuclei and the number of TUNEL positive nuclei were determined in representative sections of the epicardium to determine the percentage of apoptotic cells present. The percentage of apoptosis in *Tgfbr3*$^{-/-}$ epicardial cells was not significantly different from that of *Tgfbr3*$^{+/+}$ littermates at either E12.5 or 13.5.

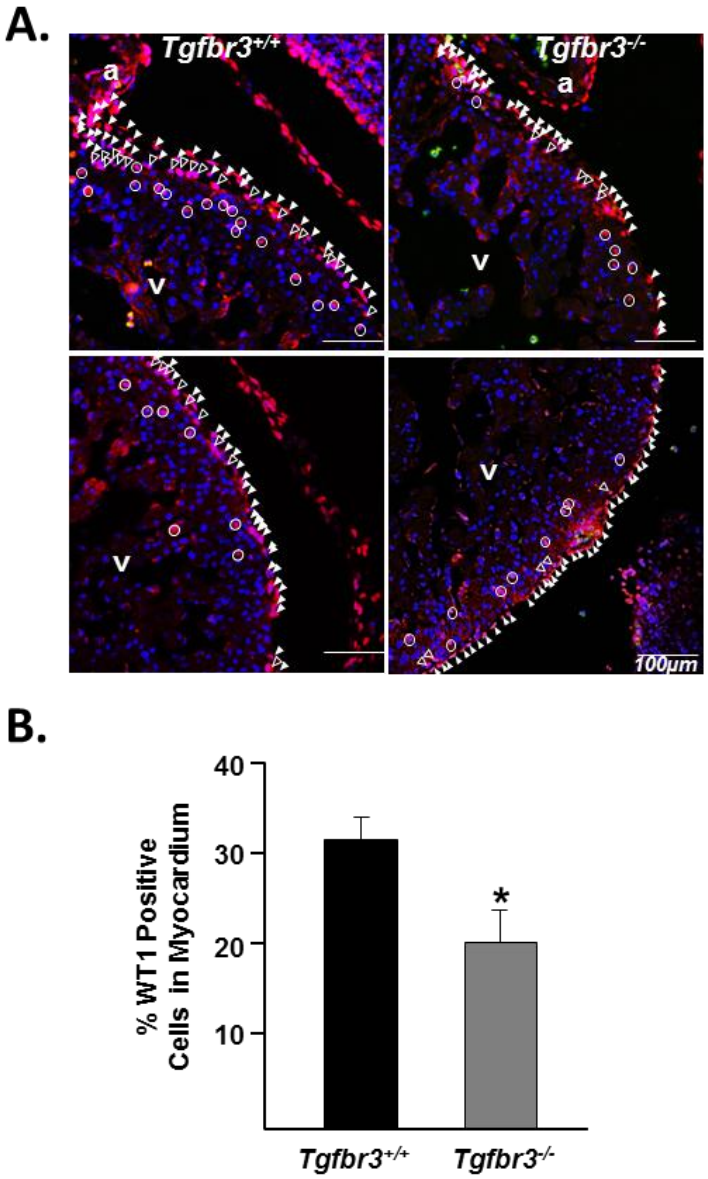

Figure 12 Epicardial cells in *Tgfbr3*$^{-/-}$ embryos show decreased myocardial invasion Sections stained for WT1 in E13.5 hearts. Representative WT1 positive mesenchymal cells are identified by the open circles. Representative cells in the epicardium are indicated by solid arrowheads, while epicardially derived mesenchymal cells in the subepicardial space are identified by the open arrowheads. (D) Percent invasion into myocardium is calculated as the number of WT1 positive mesenchymal cells per total WT1 positive cells (n=3 embryos per genotype (*$p<0.05$)). (a=atria, v=ventricle)

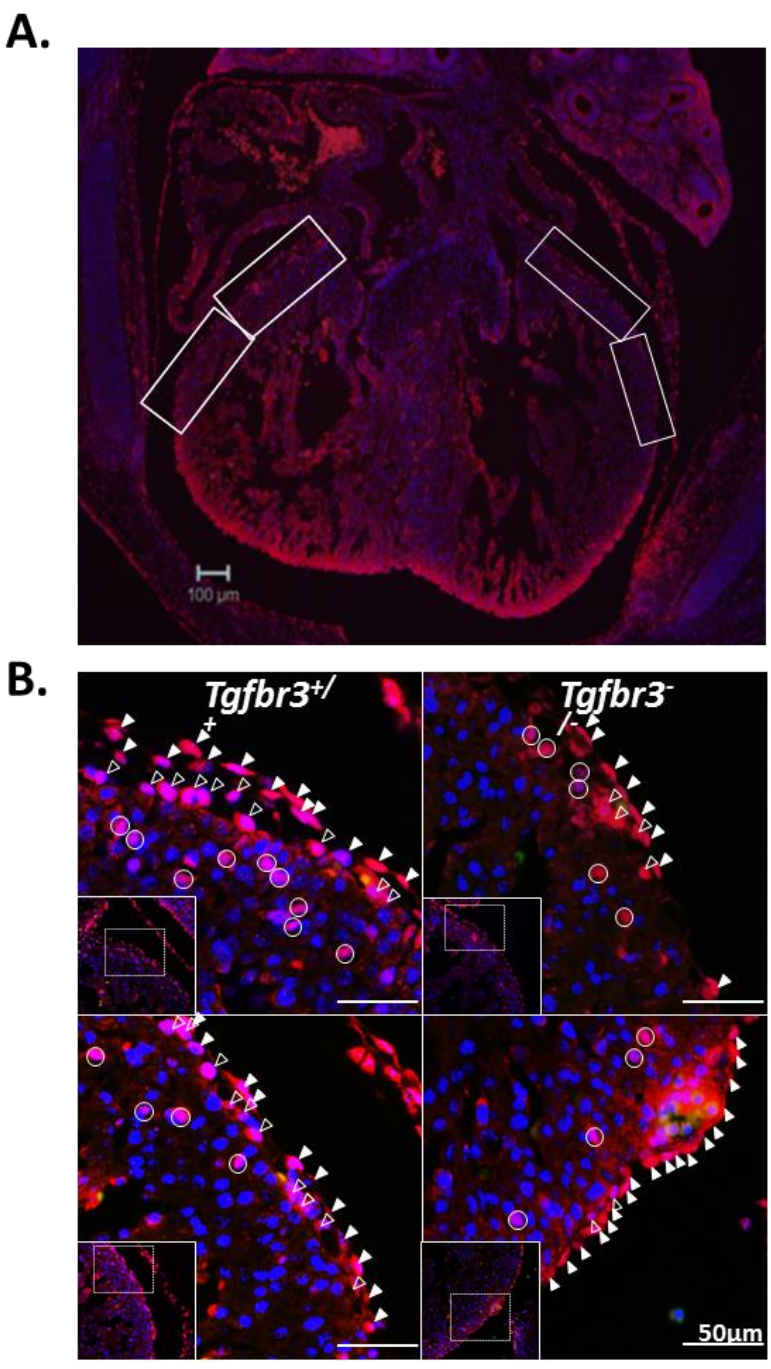

Figure 13 WT1 staining (A) Areas of the right and left ventricles (boxed area) used to assess proliferation and invasion using WT-1 staining as presented in Figure 12A and B. (B) Magnified view of sections in Figure 12A depicting WT1 positive cells

Tgfbr3$^{-/-}$ epicardial cells display decreased proliferation and invasion *in vitro*

Given the alterations in epicardial cell proliferation and invasion noted in *Tgfbr3*$^{-/-}$ embryos, we developed immortalized epicardial cell lines from *Tgfbr3*$^{+/+}$ and *Tgfbr3*$^{-/-}$ embryos that would allow us to probe TGFβR3 regulation of epicardial cell behavior *in vitro*. Since we have previously immortalized epicardial cells from *Tgfbr3*$^{+/+}$ embryos and shown that these cells behave similarly to freshly isolated primary cells (Austin, Compton et al. 2008), we used this same approach to generate and characterize epicardial cells from *Tgfbr3*$^{+/+}$ and *Tgfbr3*$^{-/-}$ littermate pair embryos. We first measured the proliferation rates of *Tgfbr3*$^{+/+}$ and *Tgfbr3*$^{-/-}$ epicardial cells. As measured by BrdU incorporation, *Tgfbr3*$^{+/+}$ cells exhibit proliferation rates that peak at 48 hours and decline to basal levels by 72 hours. *Tgfbr3*$^{-/-}$ cells show a significantly reduced rate of proliferation that is sustained throughout the time course examined (Figure 14 A and B). We used an MTS assay as a second independent approach to confirm this initial observation. *Tgfbr3*$^{-/-}$ cells had a cell density 50% lower at 48 hours and 62% lower at 72 hours, indicating an overall lower rate of proliferation throughout the time course of the experiment (Figure 14C). We measured apoptosis *in vitro* through Caspase 3/7 activity and trypan blue exclusion (Figure 15 A and B). *Tgfbr3*$^{-/-}$ cells have an elevated level of apoptosis at all-time points as measured by both methods. This increase in apoptosis was not seen *in vivo*. This may be partially explained by the inherent low levels of apoptosis that would make detecting small

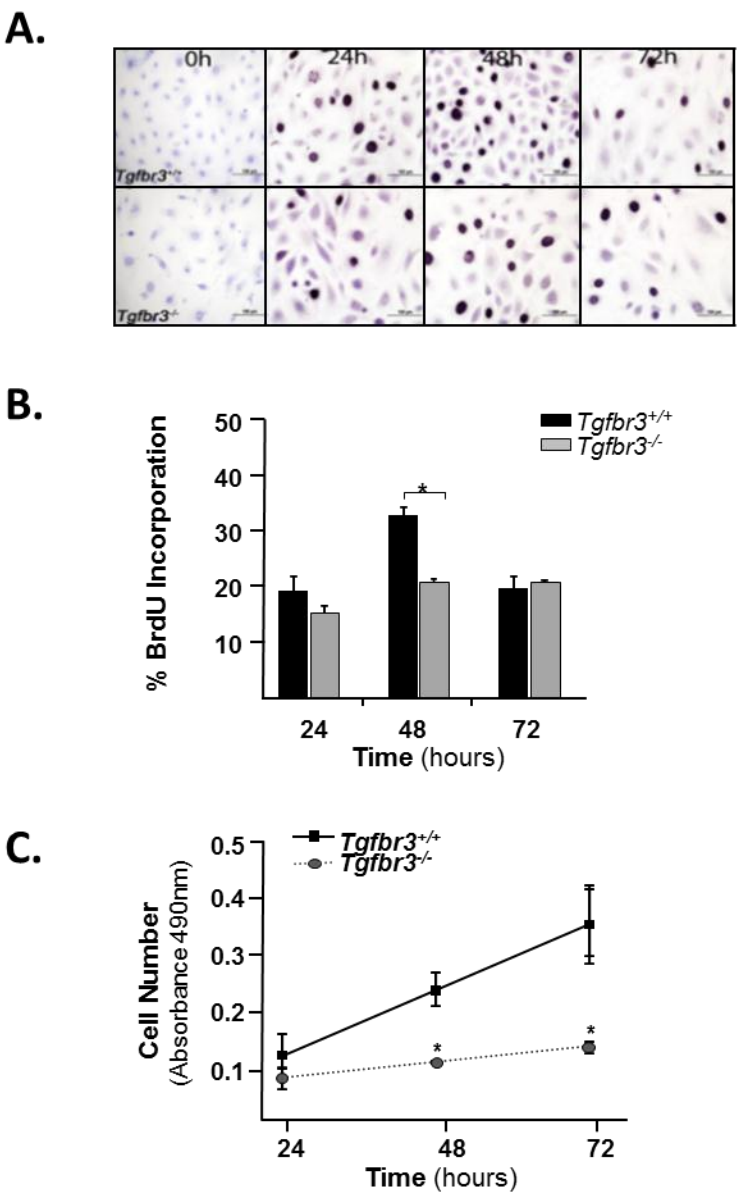

Figure 14 Cultured *Tgfbr3*$^{-/-}$ epicardial cells show decreased proliferation (A) Photomicrographs of cells incubated with BrdU and fixed at 24, 48 and 72h after initial seeding on 4-well collagen coated slides. (B) Quantitation of percent BrdU incorporation (n=3,*p=0.001) (C) Measurement of cell number by MTS assay (experiments were repeated 3 times in triplicate, results for one littermate pair shown, *p<0.05).

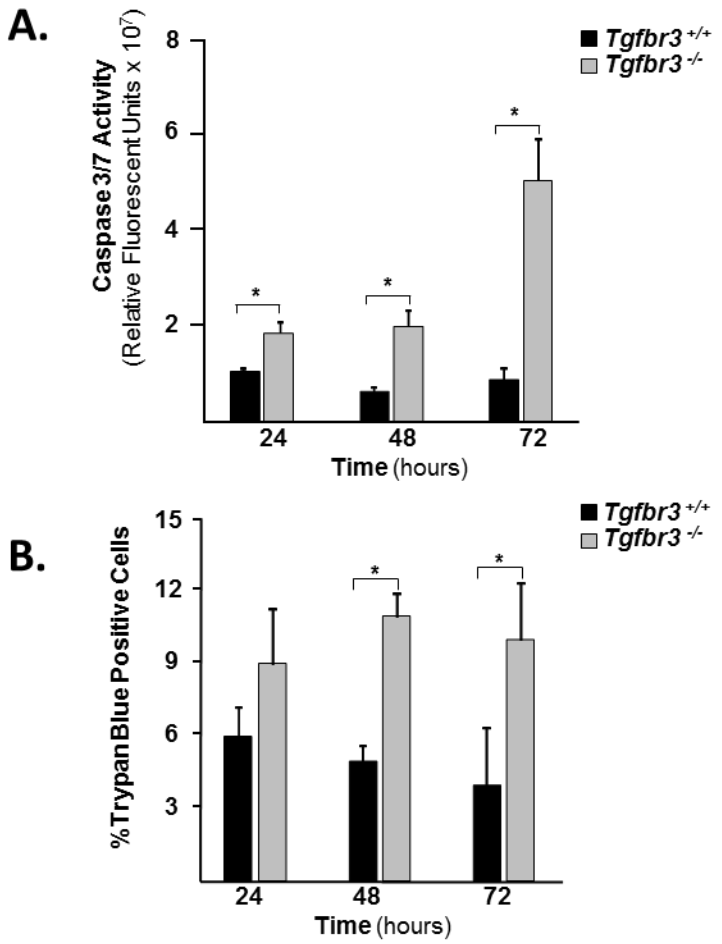

Figure 15 *Tgfbr3*$^{-/-}$ epicardial cells have increased apoptosis rate *in vitro* *(A)* Cells were incubated with a Caspase 3/7 pro-fluorescent substrate at 24, 48, and 72 hours after initially seeding in triplicate in a 96-well plate. Product formation was detected by measuring the fluorescence of each well. (*$p<0.05$). Experiments were repeated 3 times in triplicate for multiple littermates. (B) Trypan blue exclusion was used as a second independent measure of apoptosis. The proportion of trypan blue positive cells to total cells was calculated. Experiments were repeated three times (*$p<0.05$).

changes in apoptosis difficult. Alternatively, in vitro cells may respond to the stress inherent in culture by increasing apoptosis while cells *in vivo*, absent this stress, may have unaltered rates of apoptosis. To examine epicardial cell invasion we used a modified Boyden Chamber assay as a model system. Incubation of *Tgfbr3*$^{+/+}$ cells with either 250pM TGFβ1 or TGFβ2 induces a 7 and 6 fold increase in cell invasion over vehicle, respectively. In contrast, epicardial cells from *Tgfbr3*$^{-/-}$ littermates incubated with either TGFβ1 or TGFβ2 induced only a 2-fold increase in invasion (Figure 16 A and B). The decreased proliferation and invasion seen in *Tgfbr3*$^{-/-}$ epicardial cells *in vitro* support the use of these cells as a model system to elucidate the mechanisms by which the loss of TGFβR3 alters proliferation and invasion *in vivo*.

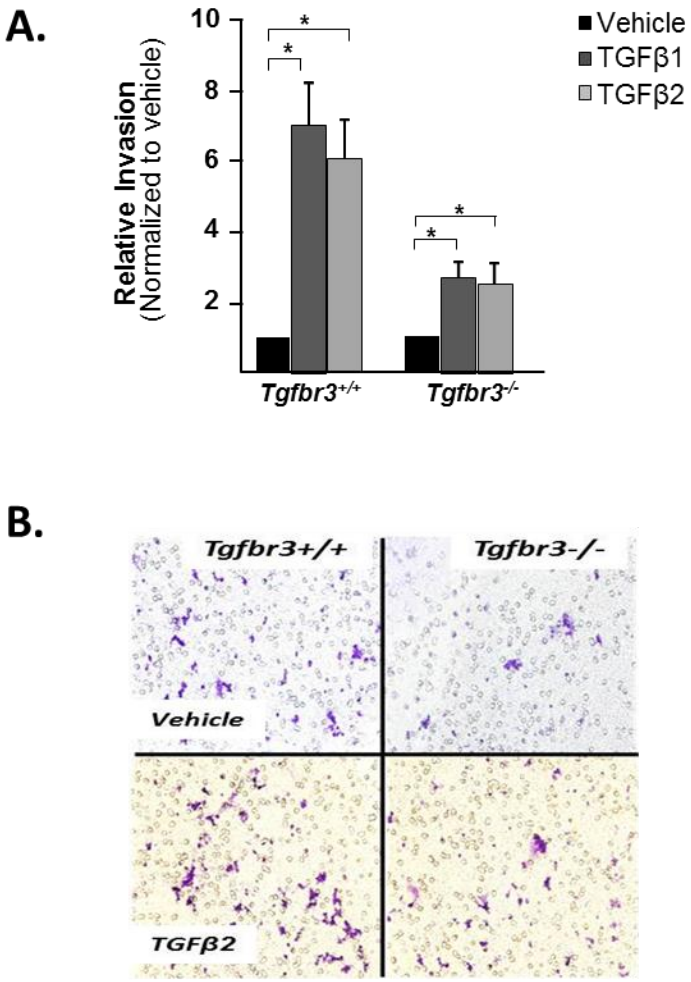

Figure 16 Cultured *Tgfbr3*$^{-/-}$ epicardial cells show decreased invasion A modified Boyden chamber assay was used to quantify invasion. (A) Quantitation of invasion (n=3, replicates of 6 for multiple littermates,*=p<0.05). (B) Duplicate membranes were stained with crystal violet. Experiments were repeated three times (*p=0.05).

Since *Tgfbr3*$^{-/-}$ epicardial cells show decreased invasion *in vitro* and *in vivo*, we asked whether *Tgfbr3*$^{-/-}$ cells displayed impaired motility in a 2 dimensional assay that does not require matrix invasion. We used an *in vitro* wound healing assay to initially probe epicardial cell motility. *Tgfbr3*$^{+/+}$ cells close a wound by 48 hours. However cells from *Tgfbr3*$^{-/-}$ littermates require an additional 24 hours (Figure 17 A and B). Since wound closure may be affected by both cell motility and cell proliferation, we used time lapse video microscopy to determine the role of motility directly in the delay of wound healing. Four littermate cell line pairs were compared, and for each pair multiple independent time lapse recordings were used to compute average motility. In these 2-dimensional motility assays, *Tgfbr3*$^{-/-}$ cells from one littermate pair display a slightly faster motility rate (13%; $p<0.001$) (Figure 18 A). The motility of *Tgfbr3*$^{+/+}$ and *Tgfbr3*$^{-/-}$ cells substantially increases on hard substrates: cells move on collagen coated glass threefold faster than on the surface of a collagen gel (Figure 18B). However, in each case altered cell motility could not explain the delayed wound healing in *Tgfbr3*$^{-/-}$ cells, thus decreased wound healing is likely due to decreased rates of proliferation.

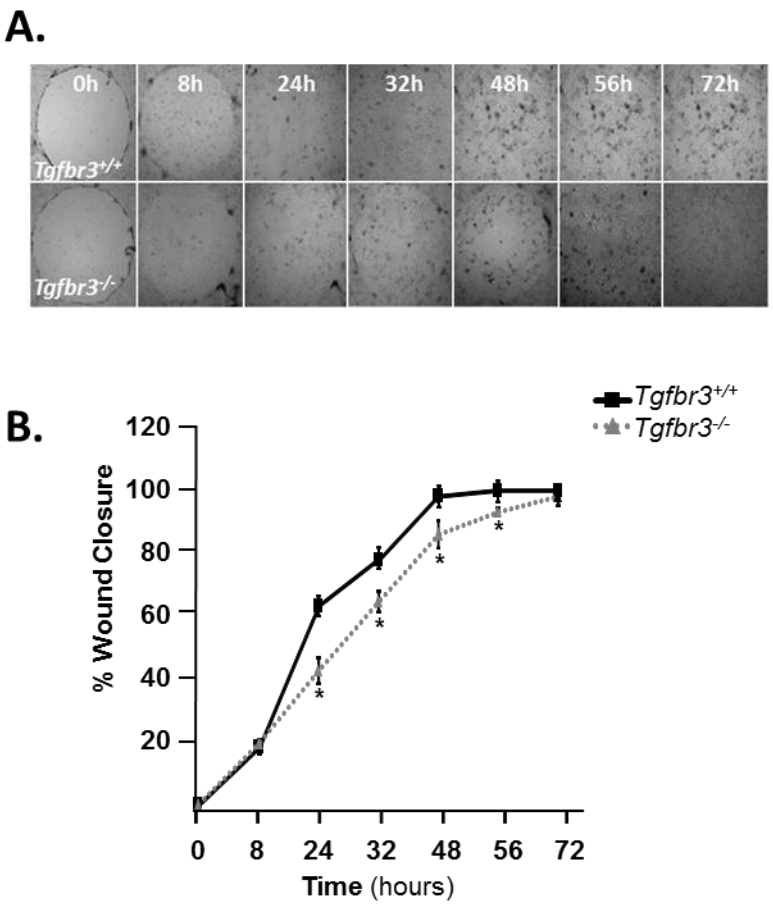

Figure 17 *Tgfbr3*$^{-/-}$ cells display decreased wound healing (A) Wound Healing *in vitro:* Confluent cell monolayers were wounded using a rotating silicon tip and photographed over 72 hours to monitor wound closure. The denuded area was measured using ImageJ software. % wound closure relative to the initial wound area was calculated. *Tgfbr3*$^{+/+}$ cells completely close the wound by 48 hours after wounding. *Tgfbr3*$^{-/-}$ cells required an additional 24 hours to completely close the wound (n=3, *p< 0.05).

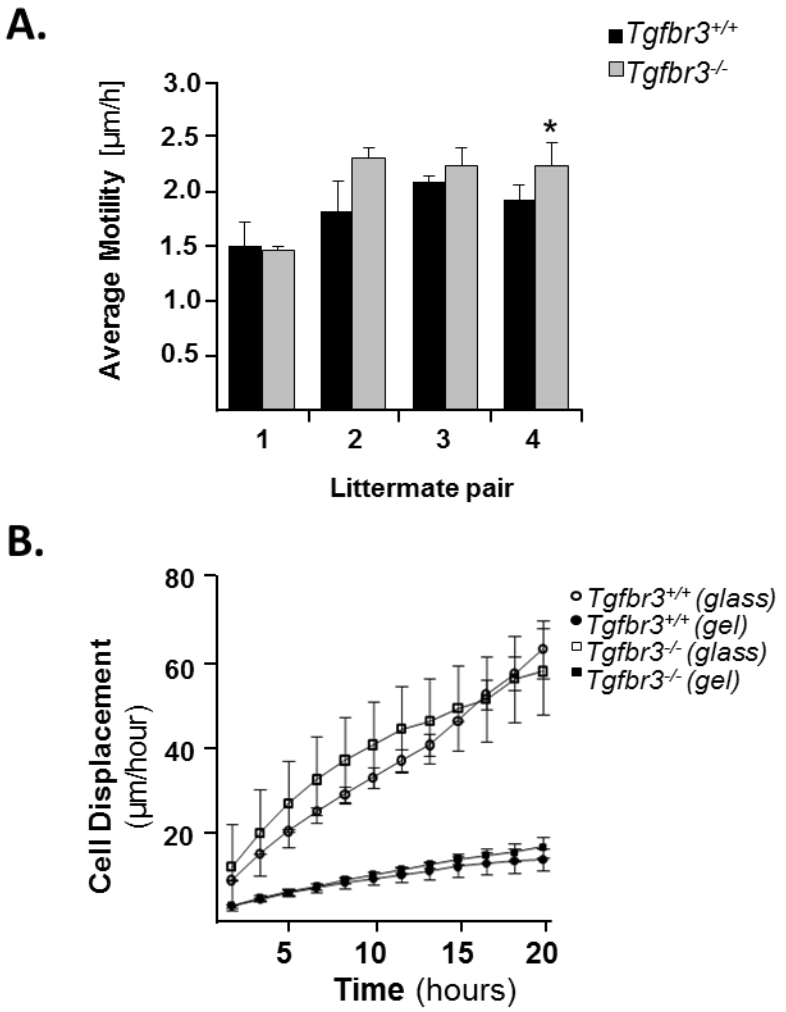

Figure 18 *Tgfbr3*$^{-/-}$ cells display decreased motility (A) Two dimensional motility of cells obtained from *Tgfbr3*$^{+/+}$ and *Tgfbr3*$^{-/-}$ cells. Four cell line pairs are compared, and for each pair multiple independent time lapse recordings are used to compute average motility. Error bars represent the standard deviation derived from the comparison of multiple measurements performed on the given cell line (*$p<0.05$) (B) Mean cell displacements values using video microscopy. The difference between genotypes is not significant

Tgfbr3$^{-/-}$ epicardial cells can undergo EMT and smooth muscle differentiation in response to TGFβ1 or TGFβ2

Epicardial cells give rise to the vascular smooth muscle cells that are required for vessel stabilization and maintenance (Mikawa and Gourdie 1996). Analysis of *Tgfbr3*$^{-/-}$ embryos suggest that epicardial cells do give rise to smooth muscle cells *in vivo* (Compton, Potash et al. 2007) but, given the importance of this cell type in the stabilization and maintenance of the coronary vessels, we chose to directly test for any requirement of TGFβR3 in epicardial cell differentiation into smooth muscle. We have previously shown that TGFβ1 or TGFβ2 induces loss of epithelial character and smooth muscle differentiation in *Tgfbr3*$^{+/+}$ epicardial cells (Austin, Compton et al. 2008). Here, immunostaining revealed that both *Tgfbr3*$^{+/+}$ and *Tgfbr3*$^{-/-}$ cells have abundant expression of the tight junction protein zonula occludens-1 (ZO-1) at the cell borders (Figure 19A). This pattern of ZO-1 expression is characteristic of epithelial cells (González-Mariscal, Betanzos et al. 2000). In both *Tgfbr3*$^{+/+}$ and *Tgfbr3*$^{-/-}$ cells, 250 pM TGFβ1 or TGFβ2 caused the loss of cell border localization of ZO-1 indicative of the loss of epithelial character. These data are consistent with the analysis of *Tgfbr3*$^{-/-}$ embryos which show that epicardial cells can undergo EMT evident by the appearance of epicardially derived cells in the subepicardial space. Loss of epithelial character was accompanied by the appearance of the smooth muscle marker SM22α in stress fibers (Figure 19B). Smooth muscle marker expression was confirmed by qRT-PCR, and both TGFβ1 and TGFβ2 significantly induced the expression of

SM22α, SMα-actin (SMαA), and calponin in *Tgfbr3*$^{-/-}$ cells (Figure 19 C and D). Together, these data demonstrate that *Tgfbr3* is not required for the loss of epithelial character or smooth muscle differentiation in epicardial cells and supports the conclusion that loss of the ability of epicardial cells to differentiate into smooth muscle is not a component of the phenotype of the *Tgfbr3*$^{-/-}$ mouse.

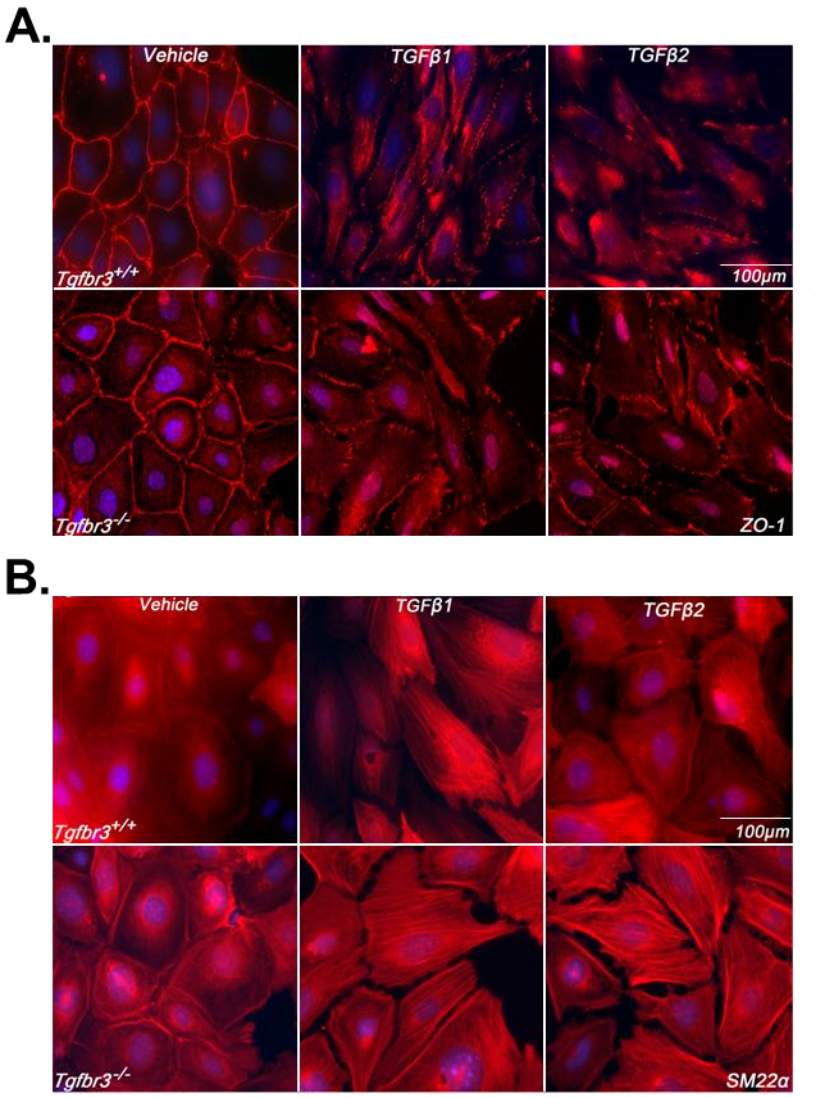
A.
Vehicle
TGFβ1
TGFβ2
Tgfbr3+/+
100μm
Tgfbr3-/-
ZO-1
B.
Vehicle
TGFβ1
TGFβ2
Tgfbr3+/+
100μm
Tgfbr3-/-
SM22α
C.
Tgfbr3+/+
Vehicle
TGFβ1
TGFβ2
Fold Induction
10
8
6
4
2
SM22α
SMαA
CALPONIN
D.
Tgfbr3-/-
Vehicle
TGFβ1
TGFβ2
Fold Induction
10
8
6
4
2
SM22α
SMαA
CALPONIN

Figure 19 Cultured *Tgfbr3*$^{-/-}$ epicardial cells can undergo EMT and smooth muscle differentiation *Tgfbr3*$^{+/+}$ and *Tgfbr3*$^{-/-}$ cells were incubated with vehicle, 250 pM TGFβ1 or TGFβ2 for 72 hours. (A) Immunohistochemistry: *Tgfbr3*$^{+/+}$ (top) and *Tgfbr3*$^{-/-}$ (bottom) cells incubated with vehicle localize the epithelial marker, ZO-1 to cell margins. TGFβ1 or TGFβ2 induces loss of cell-cell contact and loss of ZO-1 from cell margins. (B) *Tgfbr3*$^{+/+}$ (top) and *Tgfbr3*$^{-/-}$ (bottom) cells incubated with vehicle do not show SM22α in stress fibers. TGFβ1 or TGFβ2 induces SM22α expression in stress fibers in both genotypes. (C and D) Induction of the smooth muscle markers, SM22α, SMαA, and Calponin was evaluated using qRT-PCR analysis (n=3; *$p<0.05$)

Loss of TGFβR3 results in decreased responsiveness to not only TGFβ1 and TGFβ2 but to other key regulators of cell invasion

Since the loss of *Tgfbr3* results in decreased cell invasion due to decreased TGFβ responsiveness, and several other growth factors have been shown to mediate epicardial EMT and myocardial invasion (Morabito, Dettman et al. 2001; Tomanek, Zheng et al. 2001; Tomanek, Holifield et al. 2002; Mellgren, Smith et al. 2008; Craig, Parker et al. 2010), we next asked if loss of *Tgfbr3* altered responsiveness to other key regulators of cell invasion. High molecular weight hyaluronic acid (HMW-HA), a major component of the ECM in the developing heart(Camenisch, Spicer et al. 2000), has recently been implicated in mediating epicardial EMT and invasion (Craig, Parker et al. 2010). Furthermore, TGFβ2 has been reported to regulate HAS-2 expression, the gene responsible for hyaluronic acid synthesis (Craig, Austin et al. 2010).Given the decreased responsiveness to TGFβ2-induced invasion observed in *Tgfbr3*$^{-/-}$ cells *in vitro* and the role of HMW-HA in regulating epicardial cell behavior, we assessed the ability of *Tgfbr3*$^{+/+}$ and *Tgfbr3*$^{-/-}$ cells to invade collagen gels in response to HMW-HA. *Tgfbr3*$^{+/+}$ and *Tgfbr3*$^{-/-}$ cells were incubated with 0, 50, 75, 150 or 300 µg/ml HMW-HA, and cellular invasion analyzed. *Tgfbr3*$^{+/+}$ cells show a concentration dependent increase in invasion with HMW-HA, however, *Tgfbr3*$^{-/-}$ cells do not (Figure 20A). To determine whether the loss of responsiveness to HMW-HA correlated with loss of HA receptor expression, we detected levels of the HA receptors, LYVE1 and CD44, using qRT-PCR and Western blot analysis. Protein and mRNA levels

of both receptors are not significantly different between genotypes; hence decreased responsiveness to HMW-HA does not correlate with loss of HA receptor expression (Figure 20B).

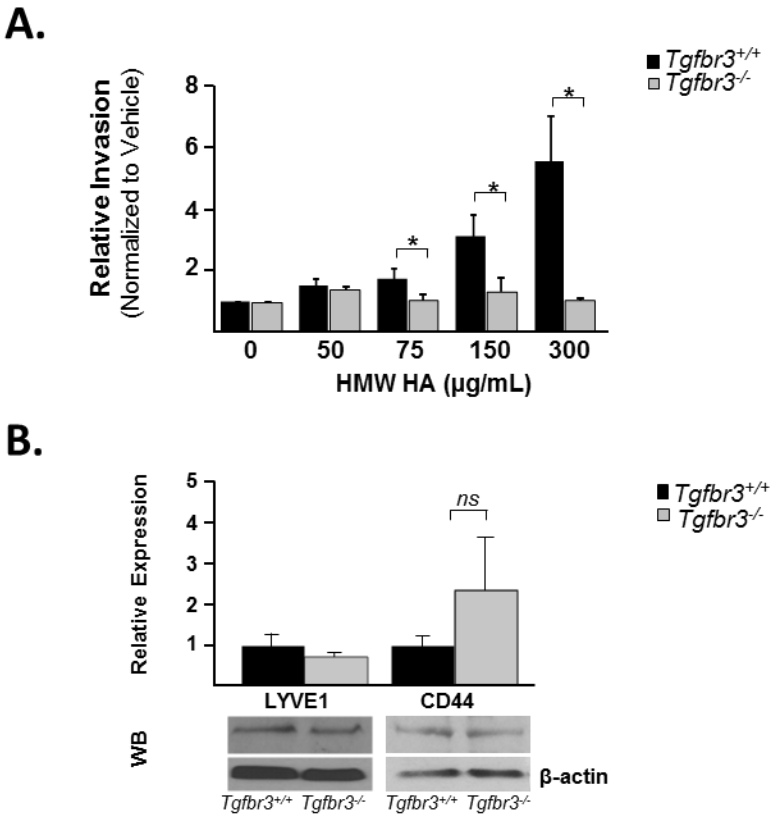

Figure 20 Loss of *Tgfbr3* results in decreased response to HMW-HA Invasion was analyzed as described in Figure 16. (A) Concentration response *Tgfbr3*$^{+/+}$ and *Tgfbr3* $^{-/-}$ littermates with HMW-HA. (B) Expression analysis using qRT-PCR (top) and western blot (bottom) comparing LYVE1 and CD44 levels in *Tgfbr3*$^{+/+}$ and *Tgfbr3*$^{-/-}$ littermates.

Additional factors that mediate epicardial EMT and myocardial invasion include FGF2, PDGFAA, PDGFBB, EGF, and VEGF (Morabito, Dettman et al. 2001; Tomanek, Zheng et al. 2001; Tomanek, Holifield et al. 2002; Mellgren, Smith et al. 2008). Therefore, to determine whether there is a global defect in the ability of *Tgfbr3*$^{-/-}$ cells to execute invasive cell motility, we assessed whether responsiveness to any of these factors was altered in *Tgfbr3*$^{-/-}$ cells. Response to PDGFAA, PDGFBB, EGF, and VEGF is unaltered between genotypes, however *Tgfbr3*$^{-/-}$ littermates display a decreased ability to invade in response to FGF2 (1.5- fold relative to vehicle) , a potent inducer of epicardial cell EMT and invasion *in vitro* (Morabito, Dettman et al. 2001), when compared to *Tgfbr3*$^{+/+}$ controls (2.25- fold relative to vehicle) (Figure 21A). Analysis of receptor expression using qRT-PCR revealed no difference in FGF receptor expression (Figure 21B).Collectively, these data suggests that *Tgfbr3*$^{-/-}$ cells are competent to execute invasive cell motility and reveal that TGFβR3 plays a central role in regulating responsiveness not only to members of the TGFβ family but select mediators of epicardial cell function such as HMW-HA and FGF2.

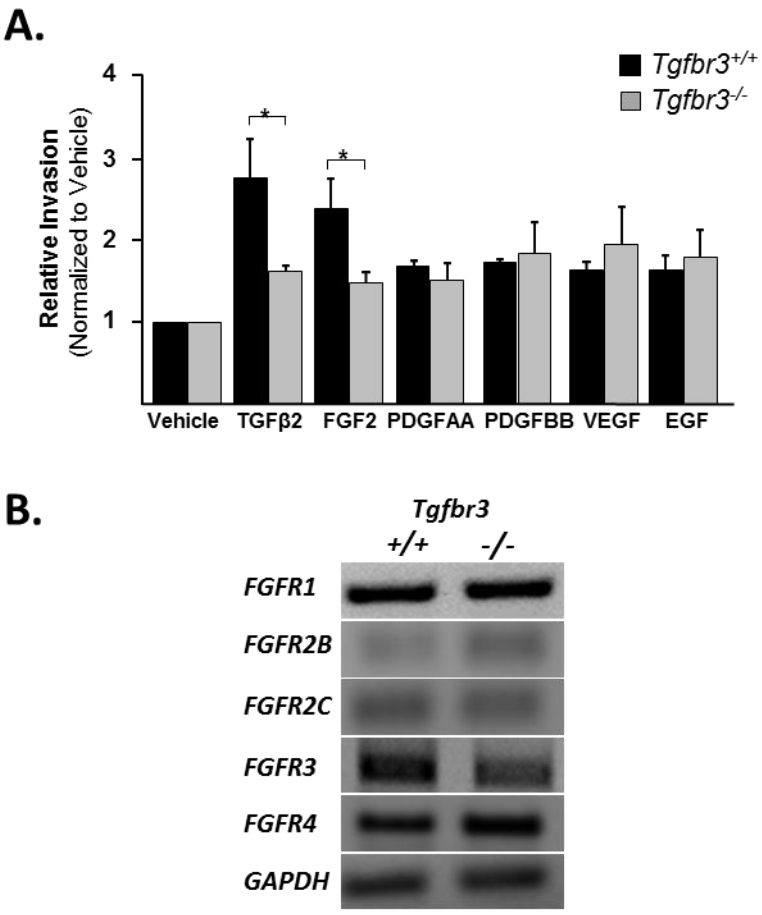

Figure 21 Loss of *Tgfbr3* results in decreased response to FGF-2. Invasion was analyzed as described in Figure 16. (A) Incubation with vehicle, 250pM TGFβ2, or 10ng/ml of FGF2, PDGFAA, PDGFBB, VEGF or EGF. (n=3, replicates of 6, for multiple littermates,*=$p<0.05$). (B) Expression analysis using qRT-PCR comparing FGFR levels in *Tgfbr3*$^{+/+}$ and *Tgfbr3*$^{-/-}$ littermates.

Non-canonical signaling through TGFβR3 interaction with GIPC is required for invasion

The mechanisms by which TGFβR3 signals are largely unknown. The cytoplasmic domain of TGFβR3 is not required to present ligand to TGFβR1 and TGFβR2 to augment canonical signaling (Blobe, Schiemann et al. 2001). Targeting TGFβR3 in mice (Compton, Potash et al. 2007) and cardiac cushion explants (Brown, Boyer et al. 1999) suggests a unique and non-redundant role for TGFβR3 in addition to ligand presentation. To determine a potential role of the cytoplasmic domain of TGFβR3 in regulating proliferation and invasion, we expressed TGFβR3 mutants missing portions of the cytoplasmic domain (Figure 22A). The cytoplasmic domain of TGFβR3 lacks enzymatic activity but the 3 C-terminal amino acids bind the scaffolding protein GIPC1 (Blobe, Liu et al. 2001). We overexpressed in *Tgfbr3*$^{-/-}$ cells either full length TGFβR3 (FL), TGFβR3 lacking the entire cytoplasmic domain (CYTO) or TGFβR3 lacking only the 3 C-terminal amino acids (Δ3) (Figure 22 B-E). Overexpression of TGFβR3 FL in *Tgfbr3*$^{-/-}$ cells rescued both TGFβ, HMW-HA, and FGF-2 mediated cellular invasion relative to vehicle incubated, GFP expressing cells (Figure 23A) and proliferation (Figure 23B). In contrast, overexpression of either TGFβR3 CYTO or Δ3 did not rescue proliferation (Figure 23B). or invasion in *Tgfbr3*$^{-/-}$ cells (Figure 23A). These data demonstrate that the cytoplasmic domain, and specifically the 3 C-terminal amino acids, are required for the regulation of TGFβR3-mediated proliferation and invasion by epicardial cells.

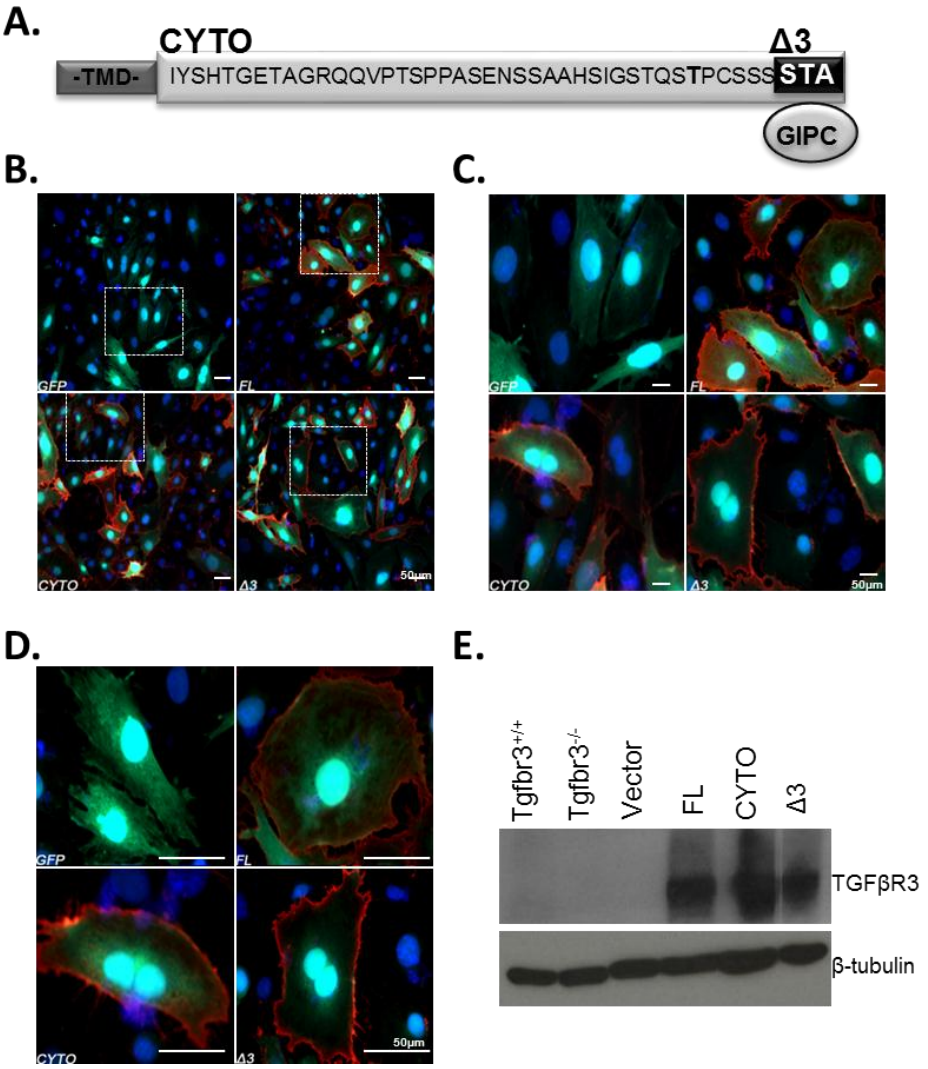

Figure 22 Expression of TGFβR3 isoforms in epicardial cells (A) TGFβR3 contains a 43 amino acid cytoplasmic domain whose C-terminal 3 amino acids, STA, bind GIPC. (B-D) Expression of adenoviral constructs and sub-cellular localization. *Tgfbr3*$^{-/-}$ epicardial cells were infected with adenovirus co-expressing GFP and either full length TGFβR3 (FL), TGFβR3 missing the entire cytoplasmic domain (CYTO) or the 3-terminal amino acids (Δ3). Cells were stained for TGFβR3. Photomicrographs were taken at 20X , C and D were magnified from these original photomicrographs for clarity. (E) Western blot using antibody specific to human TGFβR3 to confirm expression levels in *Tgfbr3*$^{-/-}$ epicardial cells transfected with either pcDNA3.1, TGFβR3-FL, TGFβR3-CYTO, or TGFβR3-Δ3. *Tgfbr3*$^{+/+}$ and *Tgfbr3*$^{-/-}$ cells were used as controls. This human-specific antisera does not recognize the mouse protein.

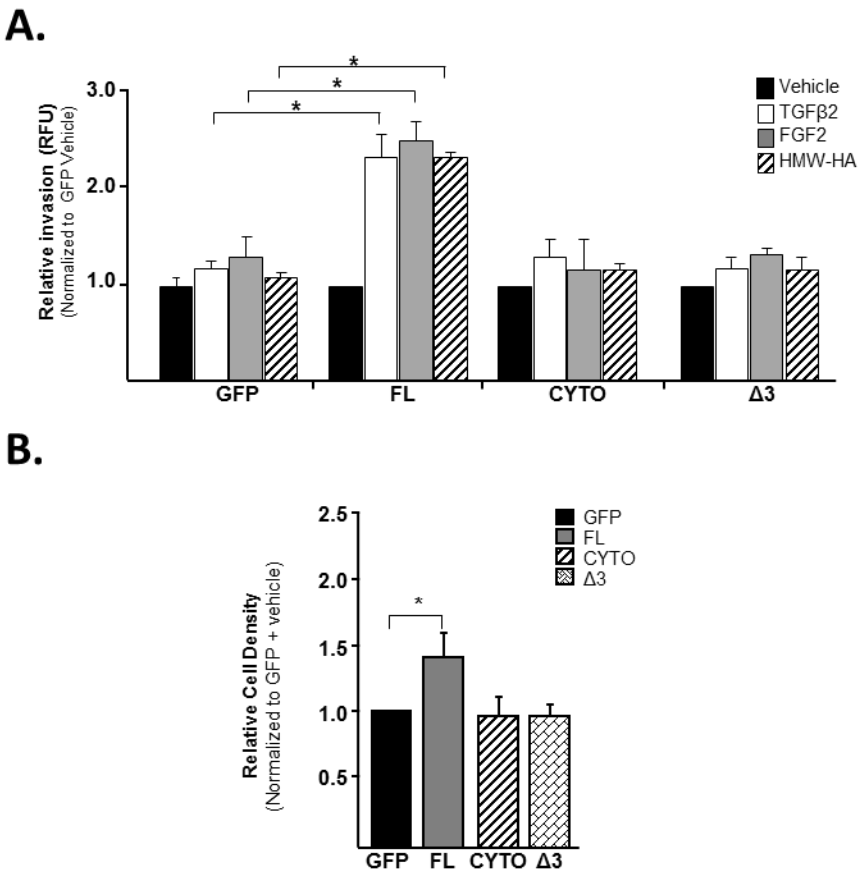

Figure 23 The cytoplasmic domain of TGFβR3 is required for invasion *Tgfbr3*$^{-/-}$ epicardial cells infected with adenovirus co-expressing GFP and either FL, CYTO or Δ3 receptor and (A) incubated with vehicle, 250 pM TGFβ2, 10ng/ml FGF-2 or 300 μg/ml HMW-HA for invasion assay. (B) MTS assay to determine which residues are required for proliferation.(n=3, replicates of 6,*=$p<0.05$).

The interaction between TGFβR3 and GIPC1, through the 3 C-terminal amino acids, has been reported to regulate cellular invasion in breast cancer cell lines (Lee, Hempel et al. 2009). Therefore, we assessed the role of GIPC in proliferation and invasion by overexpressing GIPC in *Tgfbr3*$^{+/+}$ and *Tgfbr3*$^{-/-}$ cells. Three isoforms of GIPC exist and we found GIPC1 is the predominant form in epicardial cells. Overexpression of GIPC1 had no effect on proliferation rate irrespective of genotype (Figure 24B). Overexpression of GIPC1 enhanced cellular invasion by *Tgfbr3*$^{+/+}$ cells but did not rescue deficient invasive cell motility by *Tgfbr3*$^{-/-}$ epicardial cells (Figure 24A). Knockdown of GIPC1 (Figure 25A) with either one of two specific siRNA constructs in *Tgfbr3*$^{+/+}$ epicardial cells reduced TGFβ2, HMW-HA, and FGF-2-induced invasion to levels comparable to those observed in *Tgfbr3*$^{-/-}$ cells (Figure 25B) while having no effect on cellular proliferation rates (Figure 25C). To directly establish that TGFβR3-mediated invasion in response to TGFβ2, FGF-2, and HMW-HA requires GIPC, we overexpressed TGFβR3-FL in *Tgfbr3*$^{-/-}$ cells, knocked down GIPC1, and analyzed TGFβ2, FGF-2, and HMW-HA mediated invasion (Figure 26). The addition of GIPC1 siRNA to cells overexpressing TGFβR3-FL significantly inhibited the ability of TGFβR3-FL to mediate TGFβ2, FGF-2 or HMW-HA-induced invasion. These data support the requirement of GIPC for TGFβR3-mediated invasion in response to TGFβ2, HMW-HA, and FGF-2.

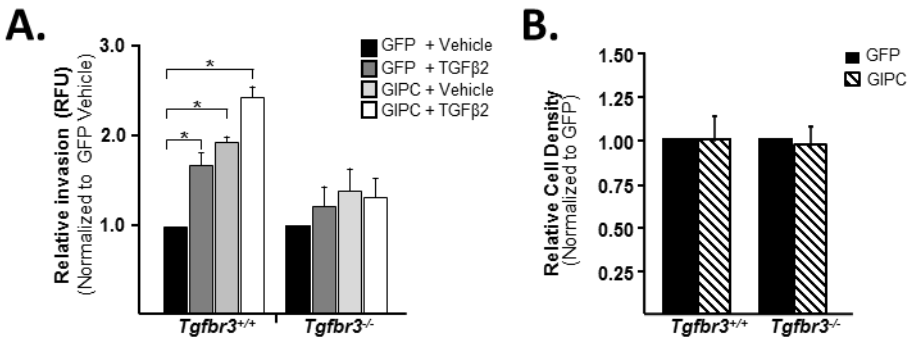

Figure 24 GIPC overexpression is insufficient to rescue invasion in *Tgfbr3*$^{-/-}$ cells (A) Invasion assay: *Tgfbr3*$^{+/+}$ or *Tgfbr3*$^{-/-}$ cells infected with adenovirus co-expressing GFP and GIPC1 and incubated with vehicle or 250 pM TGFβ2. (n=3, replicates of 6,*=$p<0.05$). (B) Cells were infected as above and subjected to an MTS assay to determine the effect on cell number. (n=3, replicates of 3,*=$p<0.05$).

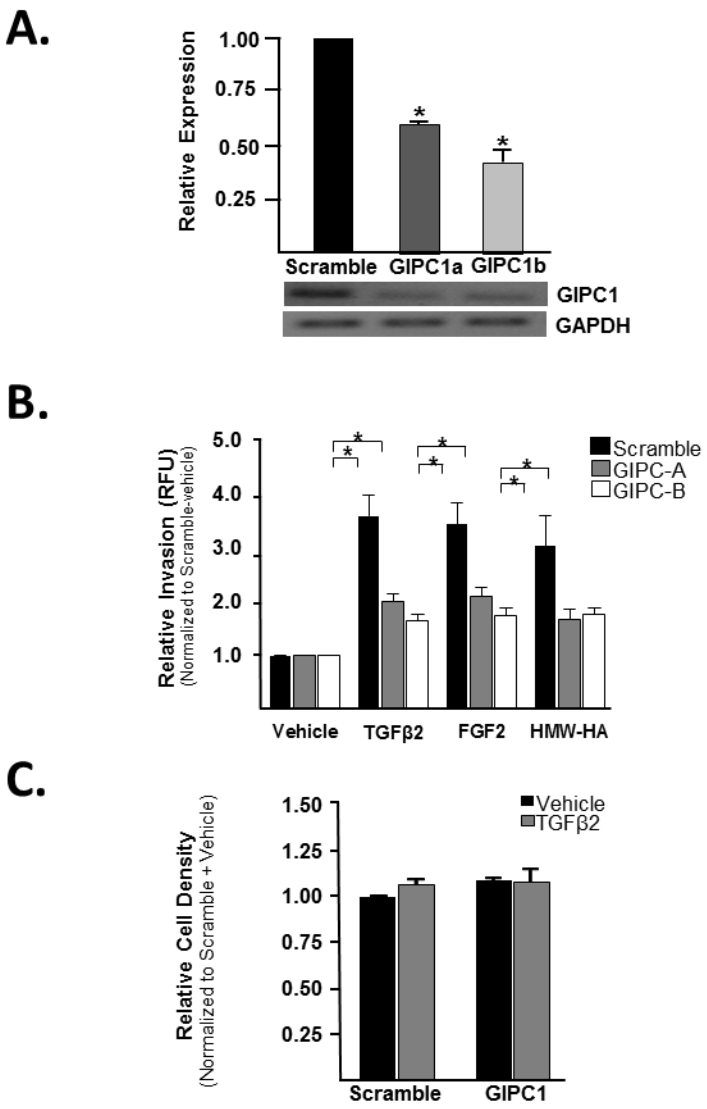

Figure 25 GIPC is required for TGFβ2, FGF-2 and HMW-HA-induced invasion *Tgfbr3*$^{+/+}$ cells transfected with siRNA directed against GIPC1. (A) Expression of GIPC1 mRNA to confirm knockdown (n=3; $p<0.05$). (B) Invasion assay: After transfection with siRNA, cells were incubated with vehicle, 250 pM TGFβ2, 10ng/ml FGF-2 or 300 µg/ml HMW-HA (n=3, replicates of 6,*=$p<0.05$ (C) MTS assay: Cell number was determined following transfection of siRNA. (n=3, replicates of 3,*=$p<0.05$)

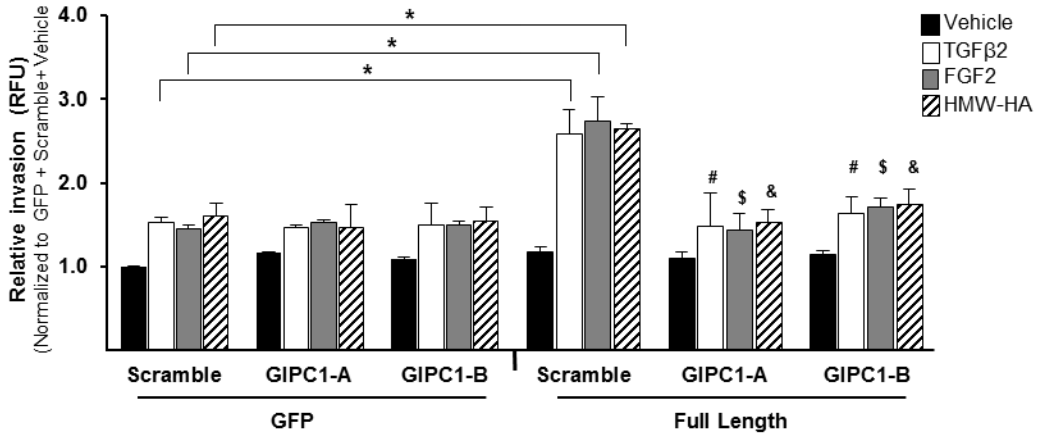

Figure 26 interaction of TGFβR3 and GIPC is required for invasion Invasion was analyzed as previously described. *Tgfbr3*$^{-/-}$ cells infected with adenovirus expressing GFP or FL receptor, transfected with siRNA to GIPC1, and incubated with vehicle, 250 pM TGFβ2, 10ng/ml FGF-2, or 300 µg/ml HMW-HA. (n=3, replicates of 4). $p<0.05$ *[GFP+scramble+ligand] vs. [FL+scramble+ligand]; #[FL+scramble+ TGFβ2] vs. [FL+GIPCsiRNA+TGFβ2]; $[FL+scramble+FGF2] vs. [FL+GIPCsiRNA+ FGF2]; &[FL+scramble+HMW-HA] vs. [FL+GIPCsiRNA+ HMW-HA];

Discussion

The loss of *Tgfbr3* in mice results in failed coronary vessel development (Compton, Potash et al. 2007) but the mechanisms by which TGFβR3 signals and regulates this process are largely unknown. Here we show that the loss of TGFβR3 is associated with decreased proliferation and invasion in both epicardial cells and the epicardium of intact embryos. Surprisingly, the decreased invasion of epicardial cells is seen in response to FGF2 and HMW-HA, known regulators of epicardial cell behavior and coronary vessel development (Pennisi and Mikawa 2009; Craig, Parker et al. 2010) in addition to TGFβ1 and TGFβ2. The responsiveness to these ligands in *Tgfbr3*$^{-/-}$ cells was found to be dependent on the 3 terminal amino acids of the cytoplasmic domain of TGFβR3 and interaction with GIPC indicating that TGFβR3 is signaling via a mechanism distinct from ligand presentation and activation of canonical TGFβ signaling. Based on our observations we propose that failed coronary vessel development in *Tgfbr3*$^{-/-}$ mice is due to decreased delivery of epicardially derived cells that are required to participate in coronary vessel development. We suggest that altered behavior in *Tgfbr3*$^{-/-}$ cells *in vivo* is at least partially due to the loss of signaling from FGF2 and HMW-HA as well as TGFβ. Since TGFβR3 signaling requires a specific cytoplasmic domain and the interacting protein GIPC to support epicardial cell invasion and responsiveness to TGFβ, FGF2, and HMW-HA, we propose that failed interaction between TGFβR3 and GIPC in the

Tgfbr3$^{-/-}$ embryo is responsible for failed coronary vessel development (Figure 27).

Our results showing that decreased proliferation and invasion are associated with failed coronary vessel development suggest that the time window during which cells must be delivered to the heart to participate in coronary vessel development is relatively narrow. A decrease in the number of cells available to participate in vessel formation may be tolerated in other vascular beds, but the dependence of embryo viability on coronary vessel formation by E15.0 does not allow sufficient time for the continued production and delivery of lower numbers of cells to rescue coronary vessel development. This is supported by several other gene knockouts that affect coronary vessel development that have reported altered proliferation, apoptosis, or invasion in the epicardium, epicardial-derived cells, or myocardium (Li, Waldo et al. 2002; Lavine, White et al. 2006; Mellgren, Smith et al. 2008; Sridurongrit, Larsson et al. 2008; Rhee, Zhao et al. 2009). Understanding the pathways that regulate epicardial cell proliferation and invasion during development has become increasingly important as a mounting amount of evidence demonstrate that pathways that regulate epicardial cell development are reinitiated during heart regeneration. Injury models in zebrafish uncovered a novel role for the epicardium in the regeneration of myocardium accompanied by the activation of developmental genes throughout the epicardium, epicardial cell EMT, and the appearance of new vessels (Lepilina, Coon et al. 2006). Mammals possess less regenerative capacity than zebrafish

but analysis of the response of the epicardium to injury reveals striking similarities (Smart, Risebro et al. 2007; Cai, Martin et al. 2008; Zhou, Ma et al. 2008; Bock-Marquette, Shrivastava et al. 2009; Christoffels, Grieskamp et al. 2009; Rentschler and Epstein 2011). For example in mice, a novel population of cells derived from the epicardium have been found to increase after myocardial infarction or aortic banding consistent with a role in injury response (Russell, Goetsch et al. 2011). These data suggest that understanding the factors that regulate epicardial cell proliferation and invasion may provide the opportunity to target the epicardium to modulate the response to injury in adults.

We had the surprising result that loss of TGFβR3 also altered responsiveness to both HMW-HA and FGF2 despite unchanged levels of their respective receptors. This result was specific to HMW-HA and FGF2 since epicardial cell invasion in response to PDGFAA, PDGFBB, VEGF, and EGF is unaffected by the loss of TGFβR3. Both HMW-HA and FGF2 are important regulators of epicardial cell invasion (Morabito, Dettman et al. 2001; Craig, Parker et al. 2010). The loss of responsiveness of epicardial cells to FGF2 and HMW-HA, in addition to TGFβ1 and TGFβ2, may explain how the loss of a single gene, which disrupts several potential signaling pathways, so dramatically, alters the morphology of the epicardium and myocardium in *Tgfbr3*$^{-/-}$ embryos. Altered myocardial morphology and decreased myocardial proliferation is noted in a number of mouse models where gene deletion alters the epicardium (Kwee, Baldwin et al. 1995; Mahtab, Wijffels et al. 2008; Sridurongrit, Larsson et al. 2008) and likely reflects the well

documented requirement of intact epicardial-myocardial interaction (Kwee, Baldwin et al. 1995; Yang, Rayburn et al. 1995; Tevosian, Deconinck et al. 2000; Crispino, Lodish et al. 2001; Lavine, Yu et al. 2005; Merki, Zamora et al. 2005; Olivey and Svensson 2010) to support myocardial thickening (Wu, Lee et al. 1999; Weeke-Klimp, Bax et al. 2010). Decreased myocardial proliferation has also been reported in *Tgfbr3*$^{-/-}$ embryos (Stenvers, Tursky et al. 2003). Our results suggest a dysregulation of the ability of *Tgfbr3*$^{-/-}$ cells to respond to several known regulators of epicardial and coronary vessel development (Pennisi and Mikawa 2009; Craig, Parker et al. 2010) and establishes TGFβR3 as a regulator of multiple signals that direct epicardial cell behavior.

Examination of the ability to rescue the deficits seen in *Tgfbr3*$^{-/-}$ cells by TGFβR3 mutants indicates a role for noncanonical TGFβ signaling in the regulation of epicardial cell proliferation and invasion. The expression of TGFβR3-CYTO or TGFβR3-Δ3 is unable to rescue demonstrating the requirement of the cytoplasmic domain, and specifically the 3 C-terminal amino acids, for signaling. Importantly, the cytoplasmic domain of TGFβR3 is not required for ligand presentation and signaling via the canonical TGFβ pathway (Blobe, Liu et al. 2001). How can the rescue of FGF2 and HMW-HA be explained? These ligands could bind TGFβR3 and initiate signaling or these ligands could activate signaling through their respective receptors that share a common downstream mediator that is lost in *Tgfbr3*$^{-/-}$ cells. In support of directly signaling through TGFβR3, it has been reported that FGF2 can bind to TGFβR3

(Andres, DeFalcis et al. 1992) and more recent data in valvular interstitial cells demonstrates a functional link between FGF2 binding and TGFβR3 activation (Han and Gotlieb 2011). In contrast, HMW-HA has not been reported to bind TGFβR3 consistent with the idea that TGFβ, FGF2, and HMW-HA may share a common downstream mediator that is dysregulated in the absence of TGFβR3.

The inability of TGFβR3-Δ3 to rescue identified a potential mediator of this noncanonical pathway downstream of TGFβR3. The scaffolding protein GIPC1 requires these same 3 C-terminal amino acids to bind TGFβR3 (Blobe, Liu et al. 2001). Interaction between TGFβR3 and GIPC1 in cancer cell lines regulates cell migration and invasion (Lee, Hempel et al. 2009), while the targeted deletion of GIPC1, or synectin, in mice has been shown to attenuate the growth and branching of coronary arterioles (Dedkov, Thomas et al. 2007). In endothelial cells, the interaction of GIPC1 with syndecan-4, a co-receptor for FGF2, (Tkachenko, Elfenbein et al. 2006) or endoglin, a coreceptor for TGFβ, (Lee, Ray et al. 2008) has been shown to regulate migration. Consistent with the known role of the 3 C terminal amino acids of TGFβR3 in GIPC binding (Blobe, Liu et al. 2001), siRNA directed against GIPC1 decreased invasion of $Tgfbr3^{+/+}$ cells in response to TGFβ2, FGF2, or HMW-HA, phenocopying loss of Tgfbr3. Further, siRNA directed against GIPC1 prevented rescue of invasion by TGFβR3-FL in *Tgfbr3*$^{-/-}$ cells. Taken together, our data in epicardial cells are most consistent with the interaction between the 3 C-terminal amino acids of the cytoplasmic domain of TGFβR3 and GIPC being required for the regulation of invasion. We conclude that TGFβR3 signaling via a noncanonical signaling

pathway that includes interaction with GIPC1 plays a key role in epicardial cell function during coronary vessel development and may provide a potential novel target for therapies directed at the epicardium and epicardial derivatives.

In summary, *Tgfbr3*$^{-/-}$ mice have failed coronary vessel development accompanied by hyperplasia of the subepicardial layer (Compton, Potash et al. 2007) indicating that epicardial cells can undergo EMT and enter the subepicardial matrix. Based on our observations we propose that failed coronary vessel development in *Tgfbr3*$^{-/-}$ mice is at least partly due to decreased epicardial cell proliferation and mesenchymal cell invasion which limits the number of cells available to participate in coronary vessel development (Figure 27). We had the unexpected result that *Tgfbr3*$^{-/-}$ epicardial cells have decreased responsiveness to FGF2 and HA in addition to TGFβ and we suggest that altered epicardial cell behavior in *Tgfbr3*$^{-/-}$ cells is at least partially due to the loss of signaling from these cues. Surprisingly, we found that TGFβR3 signaling requires a specific cytoplasmic domain and the interacting protein GIPC to support epicardial cells invasion and responsiveness to TGFβ, FGF2, and HMW-HA. We propose that this failed interaction in the *Tgfbr3*$^{-/-}$ embryo is responsible for failed coronary vessel development.

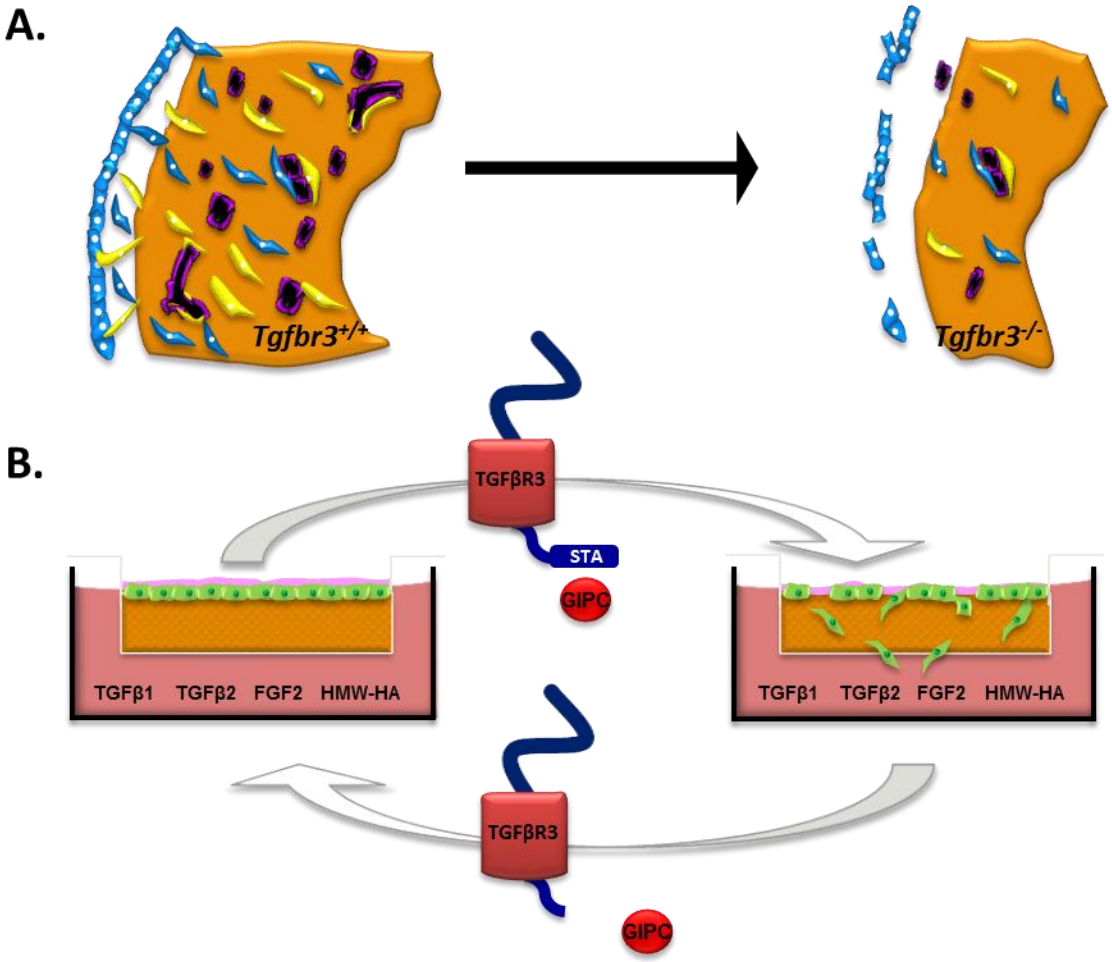
A.
Tgfbr3+/+
Tgfbr3-/-
B.
TGFβR3
STA
GIPC
TGFβ1 TGFβ2 FGF2 HMW-HA
TGFβ1 TGFβ2 FGF2 HMW-HA
TGFβR3
GIPC

Figure 27 Model of TGFβR3 Regulation of Epicardial Cell Behavior (A) In *Tgfbr3*$^{+/+}$ hearts (left), the epicardium forms a continuous epicardial layer that is tightly opposed to the myocardium. Epicardial-derived cells (EPDC's) undergo EMT and invade the subepicardial space. Some of these cells invade the myocardium and become smooth muscle cells (yellow) and cardiac fibroblasts (blue) while endothelial cells (purple) are contributed by the sinus venosus. In *Tgfbr3*$^{-/-}$ hearts (right), decreased proliferation of epicardial cells and an impaired ability of these cells to invade results in fewer cells to participate in vessel development. (B) *In vitro,* the invasion deficit in *Tgfbr3*$^{-/-}$ cells seen in response TGFβ1, TGFβ2 FGF2 and HMW-HA can be rescued by TGFβR3-FL which allows interaction with GIPC. Expression of TGFβR3-Δ3 which lacks GIPC binding site, or targeting of GIPC, does not rescue invasion. These data suggest that TGFβR3 and GIPC interaction are also required for regulating epicardial cell behavior *in vivo*.

CHAPTER III

TGFβ AND BMP-2 REGULATE EPICARDIAL CELL INVASION VIA TGFβR3 ACTIVATION OF THE PAR6/SMURF1/RHOA PATHWAY

Introduction

Epithelial to mesenchymal transformation (EMT) is an important process during embryonic development and disease progression (Azhar, Schultz Jel et al. 2003; Choi and Diehl 2009; Yu, Ruest et al. 2009; Cardiff 2010). TGFβ plays a critical role in regulating EMT in both of these settings (Taylor, Parvani et al. 2010) and is particularly relevant in cardiovascular development during heart valve formation and coronary vessel development (Azhar, Schultz Jel et al. 2003; Olivey, Compton et al. 2004; Desgrosellier, Mundell et al. 2005; Delaughter, Saint-Jean et al. 2011). Coronary vessel development is initiated when a group of mesothelial cells termed the proepicardium are transferred to the surface of the heart to form the epicardium (Viragh and Challice 1981; Manner 1993; Olivey, Compton et al. 2004; Tomanek 2005). A subset of these cells undergoes epithelial to mesenchymal transformation (EMT) and invades the subepicardial space with some cells continuing into the myocardium. Cells may then differentiate into one of several cell lineages including vascular smooth muscle cells and cardiac fibroblasts (Mikawa and Fischman 1992; Poelmann, Gittenberger-de Groot et al. 1993).

Targeting of Tgfbr3 in mice is embryonic lethal at E14.5 due to failed coronary vessel development (Compton, Potash et al. 2007). Although the roles of the serine-threonine kinase containing Type I (TGFβR1 or ALK5) and Type II (TGFβR2) receptors in TGFβ signaling are well understood (Kretzschmar and Massague 1998) there remain significant gaps in our understanding of how the wide array of TGFβ-induced responses are signaled and regulated, particularly with respect to the contributions of TGFβR3. TGFβR3 binds TGFβ1 and TGFβ3 and is required for the high affinity binding of TGFβ2 (Lopez-Casillas, Wrana et al. 1993). TGFβR3 also binds and signals in response to BMP2(Kirkbride, Townsend et al. 2008) and functions as an inhibin receptor (Wiater, Harrison et al. 2006). After TGFβ binding to TGFβR3, TGFβR3 presents ligand to the Type I (TGFβR1) and Type II (TGFβR2) TGFβ Receptors to augment signaling through the canonical signaling pathway that requires the phosphorylation and nuclear translocation of the Smads (Derynck and Zhang 2003). TGFβR3 contains a highly conserved, 43 amino acid intracellular domain with no identified catalytic activity (Lopez-Casillas, Cheifetz et al. 1991; Wang, Lin et al. 1991). The cytoplasmic domain is not required for the ability of TGFβR3 to present ligand to TGFβR1 and TGFβR2 and augment canonical signaling (Blobe, Liu et al. 2001). TGFβR3 is postulated to play a unique and non-redundant role in TGFβ signaling in addition to ligand presentation based on the results of targeting TGFβR3 in mice (Compton, Potash et al. 2007) and cardiac cushion explants (Brown, Boyer et al. 1999). Regulation of the migration and invasion of several cancer cell lines, as well as in epicardial (Sanchez, Hill et al. 2011) and endothelial (Townsend, in

press) cells, has been shown to require the cytoplasmic domain of TGFβR3 (Lee, Hempel et al. 2009; Mythreye and Blobe 2009) suggesting the presence of a non-canonical signaling pathway activated by TGFβR3.

Our laboratory has recently reported that the Par6/Smurf1/RhoA pathway mediates EMT in atrioventricular (AV) cushion endocardial cells which contribute to the heart valves (Townsend, Wrana et al. 2008; Townsend, Robinson et al. 2011). The Par6/Smurf1/RhoA pathway aids in the maintanence of epithelial cell polarity and is activated in a Smad-independent manner to induce loss of epithelial character and EMT (Ozdamar, Bose et al. 2005). The Par6 pathway has been demonstrated to play a key role in the control of morphological transformation in breast cancer metastasis (Viloria-Petit, David et al. 2009; Viloria-Petit and Wrana 2010). Par6 was initially described in *C.elegans* as a mediator of apical-basal polarity (Watts, Etemad-Moghadam et al. 1996) and is localized with TGFβR1 or ALK5 at the tight junctions by occludin (Bose and Wrana 2006). Upon TGFβ stimulation, TGFβR2 phosphorylates Par6 which then recruits the E3 ubiquitin ligase, Smurf1 (Wang, Zhang et al. 2003). Smurf1 in turn targets RhoA for degradation allowing dissolution of tight junctions and subsequently EMT (Wang 2006). We established that BMP-2 binds and signals via TGFβR3 in endocardial cells (Kirkbride, Townsend et al. 2008) and that BMP2 activates the Par6/Smurf1/RhoA pathway in a TGFβR3-dependent manner (Townsend, Robinson et al. 2011).

TGFβR3 is also expressed in epicardial cells which are major contributors to the coronary vessels, and *Tgfbr3*$^{-/-}$ mice die at E14.5 due to failed coronary vessel development (Compton, Potash et al. 2007) associated with decreased invasion by the epicardial-derived mesenchymal cells (Sanchez, Hill et al. 2011). *In vitro, Tgfbr3*$^{-/-}$ epicardial cells lose epithelial character in response to TGFβ but have a diminished ability to undergo TGFβ-induced invasion into a collagen gel *in vitro* (Sanchez, Hill et al. 2011). Given the role of the Par6/Smurf1/RhoA pathway in mediating TGFβ and BMP2-induced EMT in endocardial cushions and the requirement of TGFβR3 for this process, we investigated the role of Par6/Smurf1/RhoA in epicardial cell invasion *in vitro* and demonstrate that the Par6/Smurf1/RhoA pathway is operant in epicardial cells. Surprisingly, TGFβR3 is not required to access this pathway in epicardial cells to mediate loss of epithelial character but TGFβR3 is required for both TGFβ and BMP2-induced invasion.

Experimental Procedures

Cell Culture

Immortalized epicardial cell lines were obtained as previously described (Austin, Compton et al. 2008). To maintain the immortalized state, cells were grown in immorto media: DMEM containing 10% FBS (fetal bovine serum), 100 U/ml Penicillin/Streptomycin (P/S), 1X Insulin-Transferrin-Selenium (ITS;1 µg/ml insulin, 5.5 x 10^{-4}µg/ml transferrin, 0.677 µg /ml selenium), and 10U/ml (interferon γ) INFγ at 33°C. For experiments, the T antigen was silenced by culturing at 37˚C in the absence of ITS and INFγ. E11.5 epicardial cells were used in all experiments unless otherwise specified.

Growth Factors and Inhibitors

TGFβ1, TGFβ2, and BMP2 were purchased from R&D Systems and were reconstituted in 4mM HCl/0.01% BSA. TGFβ1 and TGFβ2 were used at 250 pM. SB431452 was purchased from Sigma and Cal 616451 was purchased from Calbiochem and used at 2.5µM and 150 nM, respectively.

Adenovirus Infections

Adenoviruses were generated using the pAdEasy system (He, Zhou et al. 1998). All concentrated viruses were titered by performing serial dilutions of the concentrated virus and counting the number of GFP-expressing 293 cells after

18–24 h. The following adenoviruses co-expressing GFP were used: full length TGFβR3 (FL), constitutively active Alk5 (caAlk5), wild-type Par6 (WTPar6), dominant negative Par6 (dnPar6), Smurf1, constitutively active RhoA (caRhoA), dominant negative Rhoa (dnRhoA), constitutively active cdc42 (cacdc42), dominant negative cdc42 (dncdc42), constitutively active Rac1 (caRac1), dominant negative Rac1 (dnRac1). Epicardial cells were plated in collagen coated 6 well dishes at a density of 200,000 cells per well in immorto media overnight at 33˚C. The following day, virus was added directly to the cells at a final concentration of 10^8 PFU/ml and allowed to incubate for an additional 24 hours. The next day cells were plated for invasion, proliferation or qRT-PCR analysis as described below.

Transfections

Cells were plated at a density of 200,000 per well of 6-well plate. The following day cells were transfected with 2µg siRNA (Ambion) and 8 µl Xtreme siRNA Transfection Reagent (Roche). Cells were incubated for an additional 48 hours before proceeding with experiments. Sequences for siRNA used are as follows:

siRNA	Sense 5'→3'	Anti-Sense 5'→3'
Scramble	CUCCTUGTCAATUUACCGCtt	AAGCGGTAAATTGACAAGGag
ALK5-A	CAAACGCGCUGACAUCUAUtt	AUAGAUGUCAGCGCGUUUGaa
ALK5-B	GAGUAGGCACUAAAAGGUAtt	UACCUUUUAGUGCCUACUCtg
PAR6-A	GUAUCUUCAUUUCUCGAAUtt	AUUCGAGAAAUGAAGAUACct
PAR6-B	CUCUGUCACGGAAGAAAAAtt	UUUUUCUUCCGUGACAGAGtg
SMURF1-A	GGAACUAGAGCUGAUAAUAtt	UAUUAUCAGCUCUAGUUCCtt
SMURF1-B	GAUCAACCCAGAUUCUUCUtt	AGAAGAAUCUGGGUUGAUCtg
RhoA-A	AGCCCUGAUAGUUUAGAAAtt	UUUCUAAACUAUCAGGGCUgt
RhoA-B	CAGCCCUGAUAGUUUAGAAtt	UUCUAAACUAUCAGGGCUGtc

Immunohistochemistry

Tgfbr3$^{+/+}$ cells were plated at a density of 25,000 cells per well in one well of a 4-well collagen coated chamber slide and allowed to adhere overnight at 37˚C. The following day virus was added to each well and 24 hours later the media was replaced with DMEM containing 5% FBS. After a 72 hour incubation period at 37˚C, cells were fixed in 2% parafomaldehyde (PFA) for 30 min and permeabilized with PBS and 0.2% Triton X-100 for 5 min at room temperature. Cells immunostained for ZO-1 were blocked with 2% bovine serum albumin (BSA) in PBS for 1 hr and incubated with dilute primary antibody (ZO-1, 2µg/ml, Zymed) overnight at 4˚C. Primary antibody was detected with goat anti-rabbit cy3 secondary antibody (1:800; Jackson ImmunoResearch). Nuclei were stained with 4',6-diamidino-2-phenylinodole (DAPI; Sigma). Photomicrographs were captured with Nikon Eclipse TE2000-E microscope and QED imagining software.

Invasion Assay

To determine the invasive potential of immortalized epicardial cells, a modified Boyden chamber assay was employed. Collagen gels were prepared as described (Craig, Parker et al. 2010). Briefly, cells were fluorescently labeled with CalceinAM (BD Biosciences) and then plated at 12,000 cells per well in DMEM containing 0.5% FBS (fetal bovine serum) in the top chamber (4-6 replicates/treatment group). Cells were then allowed to settle overnight at 37˚C. For wells receiving growth factor treatment the following day DMEM containing 20% FBS +/- 250 pM TGFβ1 or TGFβ2) was added to the bottom chamber. Wells receiving inhibitor treatment, growth factor plus inhibitor were added to

bottom well as described above. In addition, cells were treated with inhibitor in the top well in 0.5% DMEM + FBS. All treatment groups were incubated for an additional 24 hours at 37˚C. The top insert was then removed and placed in a plate containing 0.25% Trypsin/2.21 mM-EDTA in HBSS (CellGro). Cells were allowed to detach from the membrane into the trypsin containing plate, which was then read using SpectraMax 96-well plate reader (Ex: 485, Em: 538, Cutoff: 530; sensitivity: 30)

Proliferation Assay

Proliferation was determined using and MTS assay, which relies on the *in vivo* reduction of MTS tetrazolium to a colored formazan product by NADPH in metabolically active cells. The product formed is read at 490nm and is directly proportional to the number of living cells in culture. Cells were plated in triplicate in a 96-well plate at a density of 5,000 cells/well in 100 µl of DMEM containing 10% FBS and 100U/ml P/S overnight at 37˚C. At 48h post-plating, 20 µl of substrate (Promega: Cell Titer 96 Aqueous Solution) was added to each well. Colorimetric reaction was allowed to proceed for 30 minutes at 37˚C, followed by reading at 490nm.

qRT-PCR

To confirm gene knockdown we used qRT-PCR. For siRNA studies, RNA was collected 48 hours after transfection. Total RNA was isolated using the TRIzol reagent (Invitrogen) according to the manufacturer's protocol. cDNA was

generated from 1ug total RNA using oligo-dT primers and Superscript III polymerase (Invitrogen). Real-time PCR analysis was done with iQ SYBR Green Supermix (Bio-Rad) in the Bio-Rad iCycler for 40 cycles. The expression levels are calculated using the $\Delta\Delta C_T$ method. The threshold cycle (C_T) represents the PCR cycle at which an increase of the reporter fluorescence above the baseline is first detected. The fold change in expression levels, R, is calculated as follows: $R=2^{-\Delta\Delta CT}$ (where $R = 2^{(\Delta CT\ treated-\Delta CT\ control)}$). This method normalizes the abundance of all transcripts to the constitutive expression level of *GAPDH* RNA. Primer pairs to confirm gene knockdown are as follows:

Gene	Sense primer (5'→3')	Anti-sense primer (5'→3')
Alk5	CCTTCTGATCCATCGGTTGA	CCATTGGCATACCAGCAT
Par6g	CCTTGCTTCGAGTCTTCAT	GCTGATGTTGAGGTGGG
Smurf1	CTTCAAGGCTCTGCAAGG	GCTTCTCATAGGACTCATAGGG
RhoA	GACAGGAAGATTATGACCGC	TGGACAGAAATGCTTGACTTC

Statistical analysis

Paired student t-test was used to establish significance. Data are presented as the average of experiments ± SEM. P-values of < 0.05 were considered significant.

Results

ALK5 is sufficient to drive epicardial EMT and invasion

Par6 and ALK5 are co-localized at tight junctions by occludin (Ozdamar, Bose et al. 2005) where ligand binding induces ALK5 to phosphorylate Par6 initiating the activation of the Par6/Smurf1/RhoA pathway (Ozdamar, Bose et al. 2005). We have previously shown that ALK5 is required and sufficient for the loss of epithelial character in epicardial cells (Austin, Compton et al. 2008) (Figure 28A). Here, we sought to determine whether ALK5 is required for TGFβ-induced invasion into a collagen gel using a modified Boyden Chamber Assay. Cells were incubated with vehicle or vehicle plus one of two structurally dissimilar small molecule inhibitors of ALK5 kinase activity, 2.5 μM SB431452 or 150 nM Calbiochem 616451 (Figure 28B). Incubation with 250 pM TGFβ2 induced invasion 2.7-fold over vehicle incubated cells. The ability of TGFβ2 to induce invasion was abrogated with the addition of either inhibitor (Figure 28B). To confirm these results we used two independent siRNA constructs targeting ALK5 with GC-matched siRNA as a control. Cells transfected with control siRNA and incubated with either 250 pM TGFβ1 or TGFβ2 induced a 2.7 and 2.2-fold invasion relative to control siRNA + vehicle incubated cells. Addition of either siRNA targeting ALK5 inhibited the ability of TGFβ1 or TGFβ2 to induce invasion (Figure 28C). Together these data demonstrate that ALK5 is required for TGFβ-induced invasion in epicardial cells.

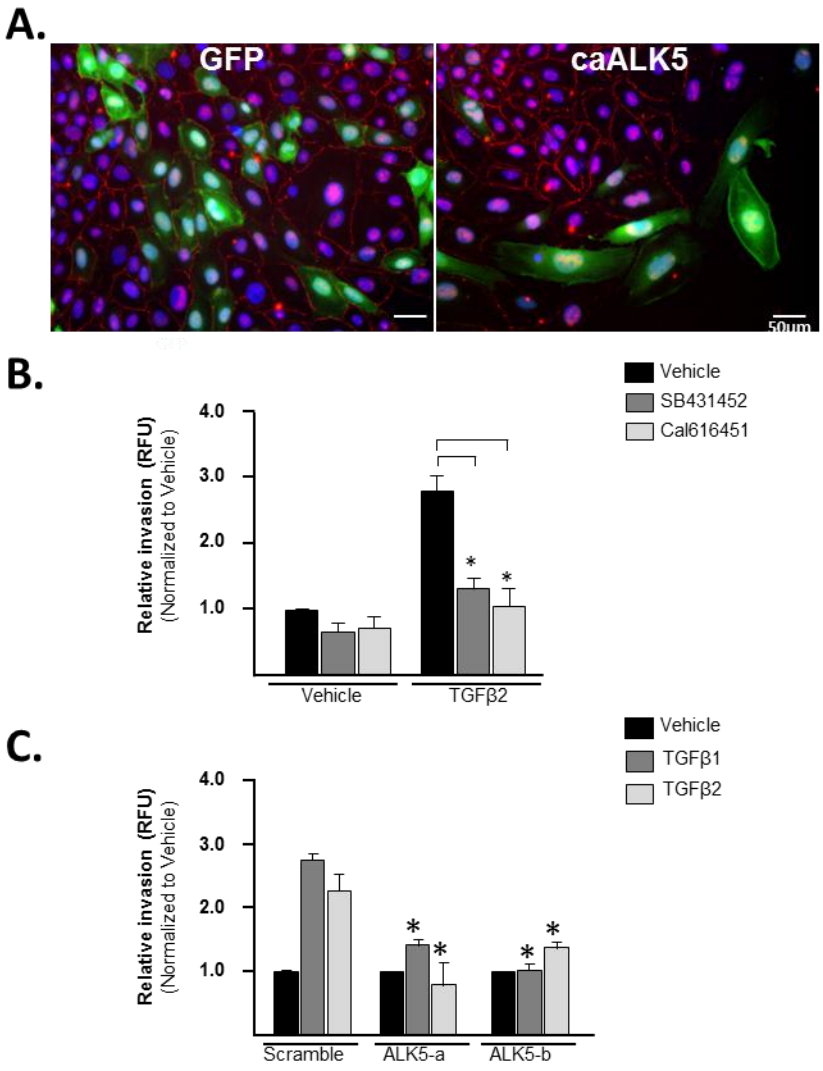

Figure 28 ALK5 is required for epicardial cell invasion (A) Tgfbr3+/+ cells infected with adenovirus expressing GFP alone (left) or GFP and caALK5 (right), and immunostained for the tight junction protein, ZO-1. (B and C) Quantitation of TGFβ-induced invasion using a modified Boyden chamber assay in the presence of either: (C) ALK5 inhibitors, SB431452 (2.5μM) or Cal616451 (150 nM) or (D) siRNA targeting ALK5 (n=3; *p<0.05)

Par6 is sufficient and required to drive epicardial EMT and invasion

We next used overexpression of wildtype Par6 (WTPar6) or dominant negative Par6 (dnPar6) determine whether Par6 activity regulates epithelial character and invasion in epicardial cells. We used immunohistochemistry to score for the loss of epithelial character by analyzing the redistribution of the tight junction protein, zonula occludens-1 (ZO-1). We infected cells with adenovirus co-expressing GFP alone or GFP and either wildtype Par6 (WTPar6) or dominant negative Par6 (dnPar6). GFP expressing cells demonstrated ZO-1 at cell-cell junctions while the addition of 250 pM TGFβ2 caused the loss of ZO-1 from cell-cell junctions. Overexpression of WTPar6 induced loss of ZO-1 from cell-cell junctions in the absence of ligand to an extent similar to that seen in cells incubated with TGFβ2. In contrast, cells expressing dnPar6 retained expression of ZO-1 at cell-cell junctions even in the presence of 250 pM TGFβ2 (Figure 29A). These data indicate that Par6 is sufficient and required for epicardial EMT. To address the role Par6 in epicardial invasion cells were infected with adenovirus co-expressing GFP alone or GFP and WTPar6 or dnPar6. GFP expressing cells incubated with 250 pM TGFβ2 showed a 3-fold change in invasion relative to vehicle incubated cells (Figure 29B). Expression of WTPar6 alone was sufficient to induce ~5.8-fold change in invasion relative to GFP infected, vehicle incubated cells. Addition of TGFβ2 to WTPar6 expressing cells did not further stimulate invasion. Expression of dnPar6, inhibited the ability of TGFβ2 to induce invasion (Figure 29B). To address the possibility that the increased number of cells invading seen in

WTPar6 infected cells was due to altered cell proliferation, we used the MTS assay to measure cell number in GFP, WTPar6 and dnPar6 infected cells (Figure 29C). No difference in cell number was noted in any of the groups. To further confirm the role of Par6 in TGFβ2 induced invasion, we used two independent siRNA constructs to target Par6. Cells transfected with Control siRNA and incubated with either TGFβ1 or TGFβ2 induced ~2 and 2.6 fold invasion, respectively. Transfection with either construct targeting Par6 completely abolished the ability of either TGFβ1 or TGFβ2 to induce invasion cells (Figure 29D). Neither of the siRNA's had an effect on cell number (Figure 29E). Collectively, these data indicate that Par6 is sufficient and required for the loss of epithelial character and invasion in epicardial cells.

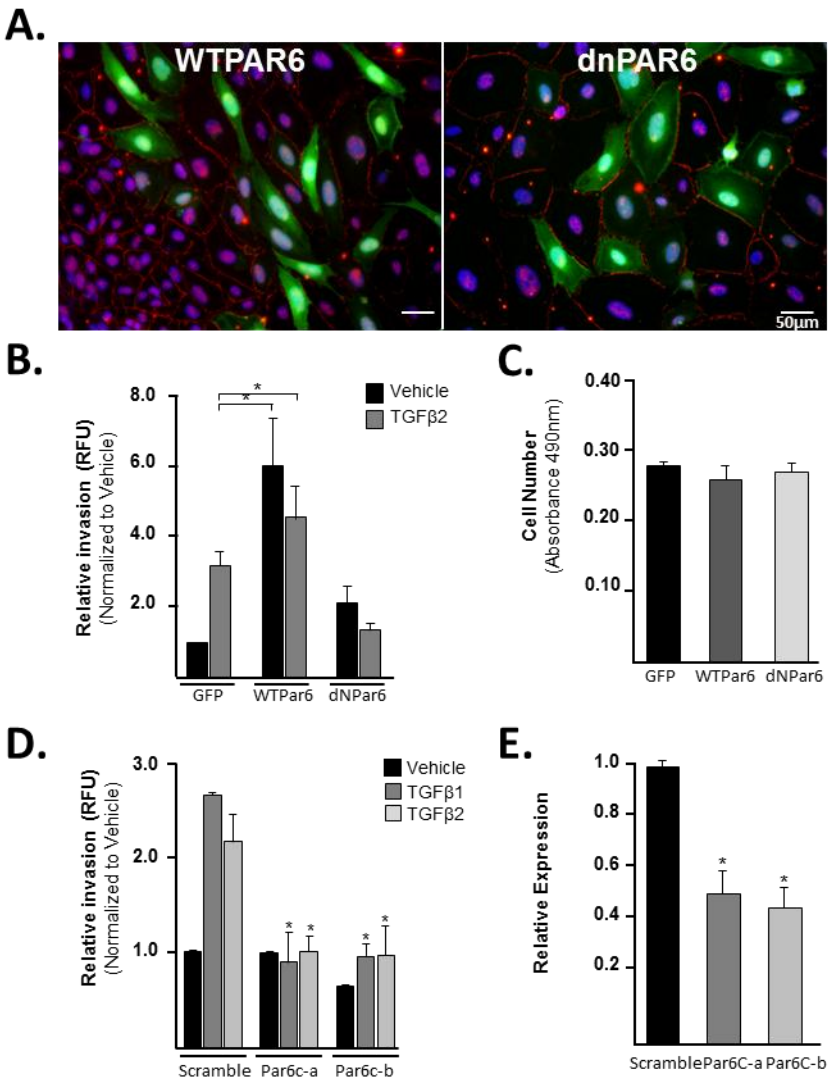

Figure 29 Par6 is required and sufficient for epicardial cell invasion *Tgfbr3*$^{+/+}$ cells infected with adenovirus expressing GFP + WTPar6 or GFP+ dnPar6 (A-C). (A) Immunohistochemistry to visualize redistribution of ZO-1. (B) Quantitation of invasion (C.) Quantitation of cell number using MTS assay. *Tgfbr3*$^{+/+}$ cells transfected with siRNA targeting Par6 (D, E). (D.) Quantitation of invasion (E.) Relative expression levels as measured by qRT-PCR. (n=3; *p<0.05)

Smurf1 is sufficient to drive epicardial EMT and invasion Having established that Par6 is operant in epicardial cells and functions in epicardial EMT and invasion, we next investigated the role of Smurf1, which is activated by Par6 in this pathway. Overexpression of Smurf1 was sufficient to induce redistribution of ZO1 (Figure 30A) and invasion (Figure 30B). Smurf1 overexpression induced a 3-fold change in invasion over GFP expressing, vehicle incubated cells (Figure 30B), while having no effect on cell number (Figure 30C). Knockdown of Smurf1 using two independent siRNA constructs abolished TGFβ1 and TGFβ2 induced invasion (Figure 30D) and did not alter cell number (Figure 30E). These studies demonstrate that Smurf1 is sufficient for loss of epithelial character and required and sufficient for invasion, consistent with a role downstream of Par6.

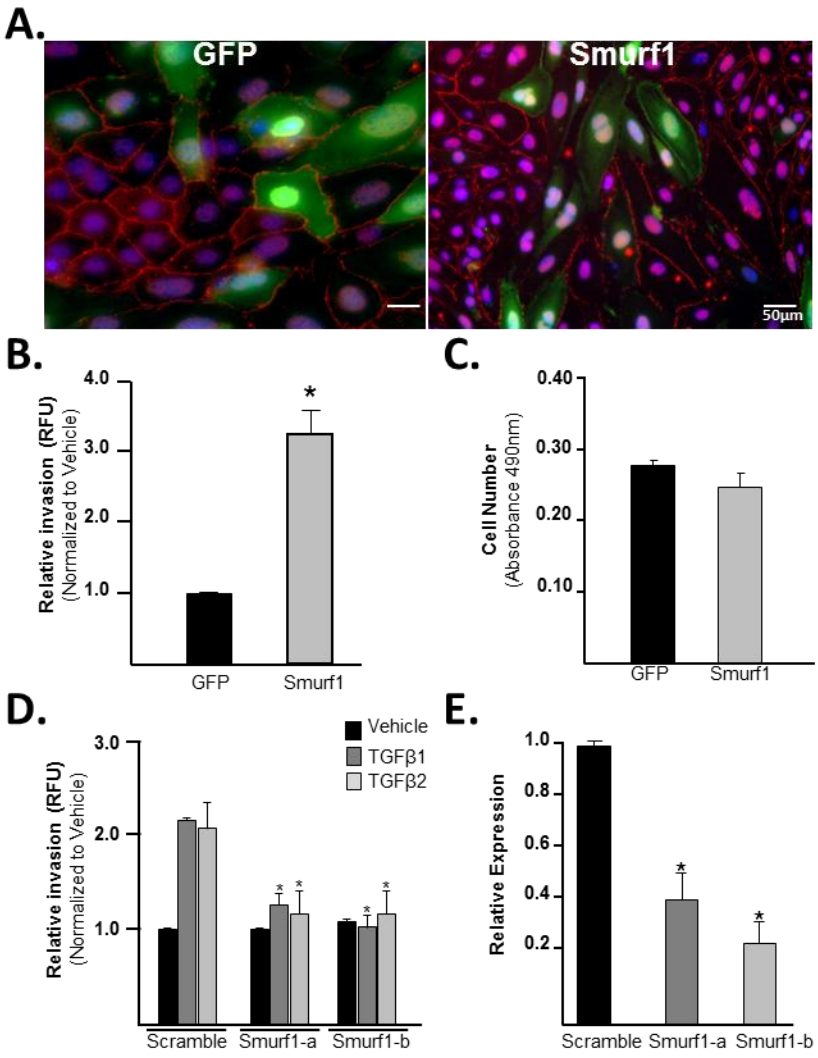

Figure 30 Smurf1 is required and sufficient for epicardial cell invasion *Tgfbr3*$^{+/+}$ cells infected with adenovirus co-expressing GFP alone or GFP+ Smurf1 (A-C). (A) Immunohistochemistry to visualize redistribution of ZO-1. (B) Quantitation of invasion. (C) Quantitation of cell number using MTS assay.*Tgfbr3*$^{+/+}$ cells transfected with siRNA targeting Smurf1 (D,E). (D) Quantitation of invasion. (E.) Relative expression levels as measured by qRT-PCR. (n=3; *p<0.05)

RhoA activity regulates epicardial EMT and invasion

Once activated, Smurf1 targets RhoA for degradation leading to EMT in NMuMG and endocardial cells (Ozdamar, Bose et al. 2005; Townsend, Wrana et al. 2008). To determine the role of RhoA activity in epicardial EMT we infected cells with adenovirus expressing either dominant negative (dn) or constitutively active (ca) RhoA. Cells expressing caRhoA retained epithelial character as determined by the presence of ZO1 at the tight junctions, whereas cells expressing dnRhoA induced redistribution of ZO1 (Figure 31A). Overexpression of dnRhoA induced invasion independent of ligand addition whereas caRhoA abolished TGFβ2-induced invasion (Figure 31B). Expression of either dnRhoA or caRhoA did not affect cell number (Figure 31C). Knockdown of RhoA using two independent siRNA support our initial observation and indicate that RhoA stability is required to maintain epithelial character while degradation of RhoA promotes loss of epithelial character and drives invasion (Figure 31D). Targeting RhoA by siRNA did not affect cell number (Figure 31E). Given that multiple GTPases have been implicated in regulating cytoskeletal rearrangement (Bayless and Davis 2002; Edlund, Landstrom et al. 2002; Derangeon, Bourmeyster et al. 2008), and that the small GTPases, Cdc42 and Rac1, have been reported to act in concert with RhoA to mediate intracellular signaling (Wang and Beier 2005; Wojciak-Stothard, Tsang et al. 2005), we asked whether these other two small GTPases could be playing a role in epicardial cell invasion. To discern the roles of these GTPases on epicardial invasion, we overexpressed ca- or dn- Cdc42 or Rac1. Neither

isoforms of the GTPases had any effect on relative invasion levels (Figure 32A and B) or cell number (Figure 32C). Therefore, these GTPases do not participate in epicardial cell invasion. Taken together these data support the role for Par6/Smurf1/RhoA being operant in epicardial cells to regulate loss of epithelial character and cell invasion.

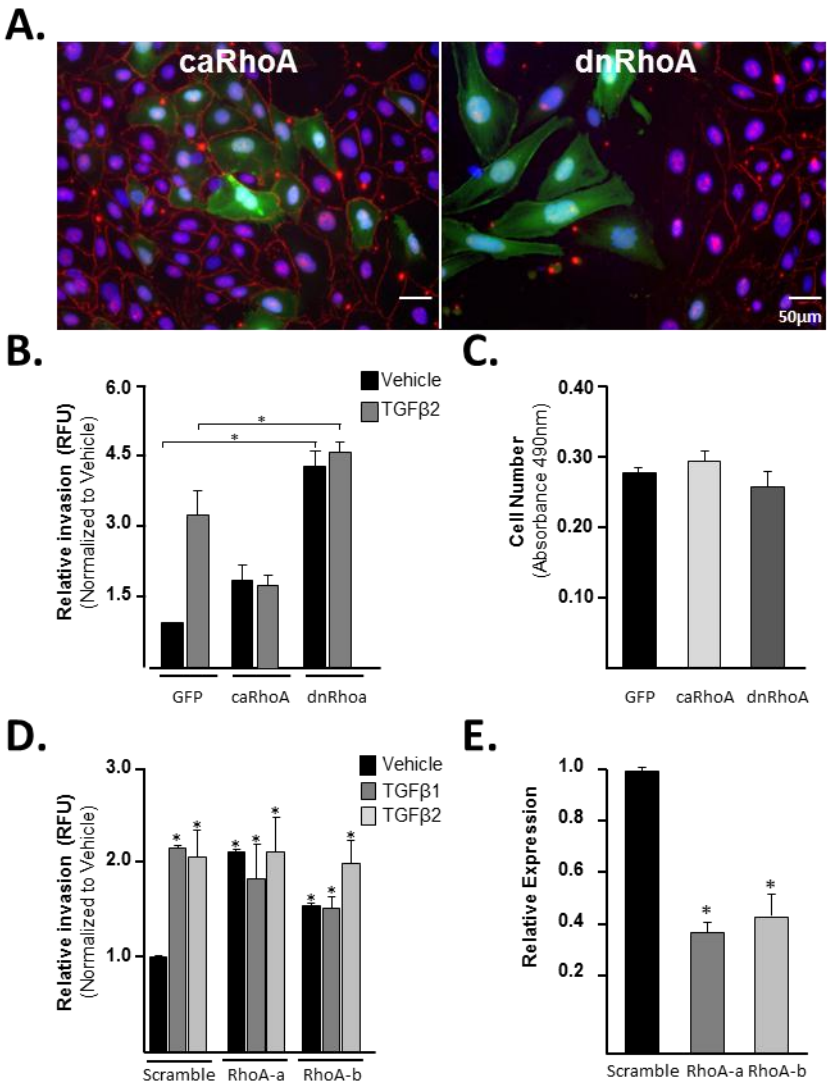

Figure 31 RhoA degradation is required and sufficient for epicardial cell invasion *Tgfbr3*$^{+/+}$ cells infected with adenovirus co-expressing GFP+caRhoA or GFP+dnRhoA. Immunohistochemistry to visualize redistribution of ZO-1. (B) Quantitation of invasion.(C) Quantitation of cell number using MTS assay. *Tgfbr3*$^{+/+}$ cells transfected with siRNA targeting RhoA (D,E). (D).Quantitation of invasion. (E.) Relative expression levels as measured by qRT-PCR. (n=3; *p<0.05)

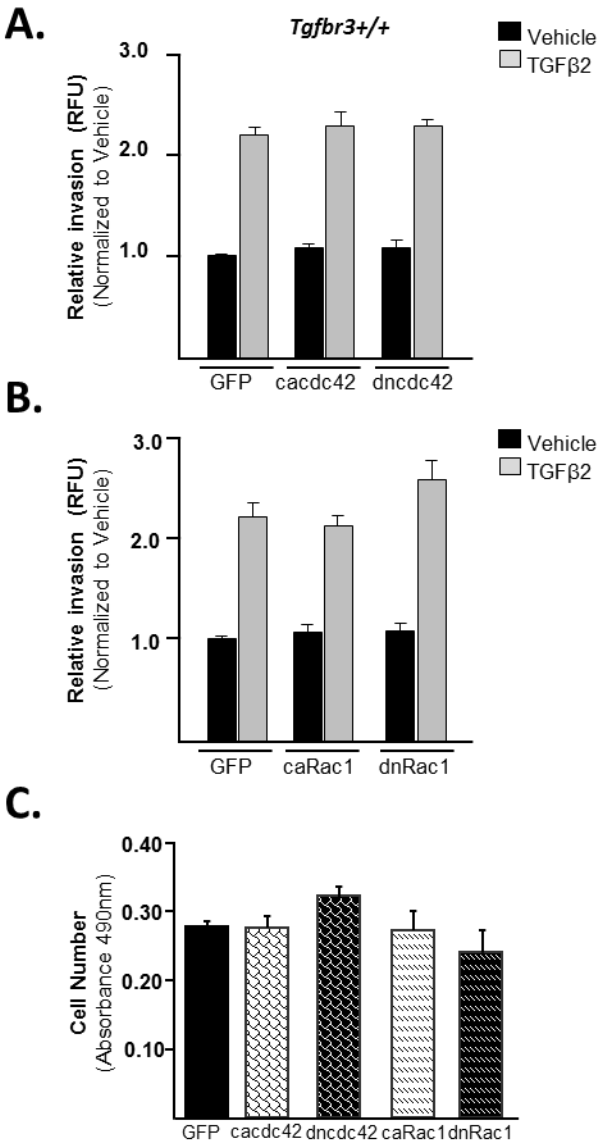

Figure 32 Cdc42 and Rac1 are not required for epicardial cell invasion *Tgfbr3*$^{+/+}$ cells infected with adenovirus co-expressing GFP+caCdc42, GFP+dnCdc42, GFP+caRac1 or GFP+dnRac1. (A, B) Quantitation of invasion using a modified Boyden chamber assay. (C.) Quantitation of cell number using MTS assay. (n=3; *p<0.05)

BMP-2 can access the Par6/Smurf1/RhoA pathway in epicardial cells

Given that TGFβ and BMP-2 both access the Par6/Smurf1/RhoA pathway in endocardial cells via TGFβR3 (Townsend, Robinson et al. 2011) we next asked whether BMP-2 acts through the Par6/Smurf1/RhoA pathway to regulate invasion. We targeted each member of the Par6 pathway in *Tgfbr3*$^{+/+}$ epicardial cells with two independent siRNA constructs as described above. In all cases, transfection with scrambled siRNA followed by incubation with 5nM BMP-2 induced ~ 2.25 fold invasion relative to vehicle incubated cells. Knockdown of ALK5, Par6 or Smurf1 with each siRNA abolished the ability of BMP-2 to induce invasion (Figure 33 A, B, C). Knockdown of RhoA resulted in levels of cell invasion that were not increased by the addition of BMP-2 (Figure 33D). These data indicate that in epicardial cells, as in endocardial cells, the Par6/Smurf1/RhoA pathway can be accessed by both TGFβ and BMP-2.

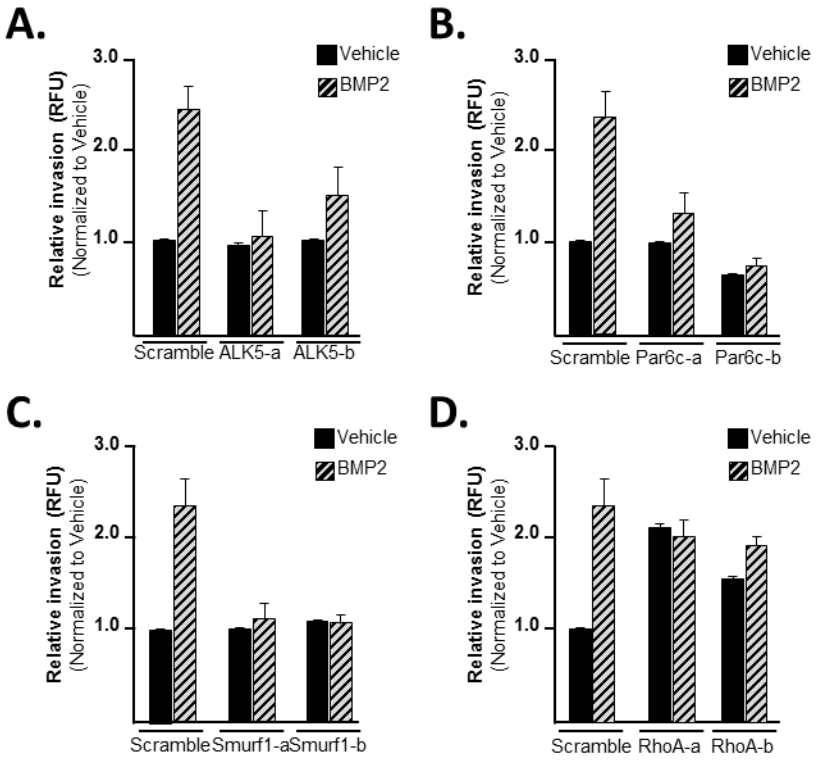

Figure 33 BMP2 can induce invasion through the Par6/Smurf1/RhoA Cells were transfected with siRNA targeting (A.)ALK5, (B.)Par6, (C.)Smurf1,or (D.)RhoA, and their ability to invade a collagen gel in response to 5nM BMP2 was assessed using a modified Boyden chamber assay. (n=3; *p<0.05)

TGFβR3 regulates access to the Par6/Smurf1/RhoA pathway by TGFβ and BMP-2 in epicardial cells

Given that TGFβ and BMP-2 both require TGFβR3 to access the Par6/Smurf1/RhoA pathway in endocardial cells (Townsend, Robinson et al. 2011) we sought to determine whether access to this pathway in epicardial cells required TGFβR3. We took advantage of our existing *Tgfbr3*$^{-/-}$ immortalized epicardial cells to determine if the Par6/Smurf1/RhoA pathway is downstream of TGFβR3. Overexpression of full length TGFβR3 (FL-TGFβR3) in *Tgfbr3*$^{-/-}$ cells was coupled with knock down of ALK5, Par6 or Smurf1 and scoring the ability of epicardial cells to invade in response to TGFβ2 or BMP-2. GFP-infected *Tgfbr3*$^{-/-}$ cells transfected with control siRNA and incubated with TGFβ2 or BMP-2 exhibited low levels of invasion (1.54 and 1.49-fold, respectively) relative to vehicle incubated cells (Figure 34A). In contrast, cells infected with FL-TGFβR3 and transfected with control siRNA showed higher levels of invasion (2.22 and 2.17-fold, respectively) when incubated with TGFβ2 or BMP-2 (Figure 34A). Cells infected with FL-TGFβR3 and transfected with siRNA targeting ALK5 (Figure 34A), Par6 (Figure 34B), or Smurf1 (Figure 34C) reduced the ability of FL-TGFβR3 to rescue responsiveness to TGFβ2 or BMP-2-induced invasion.

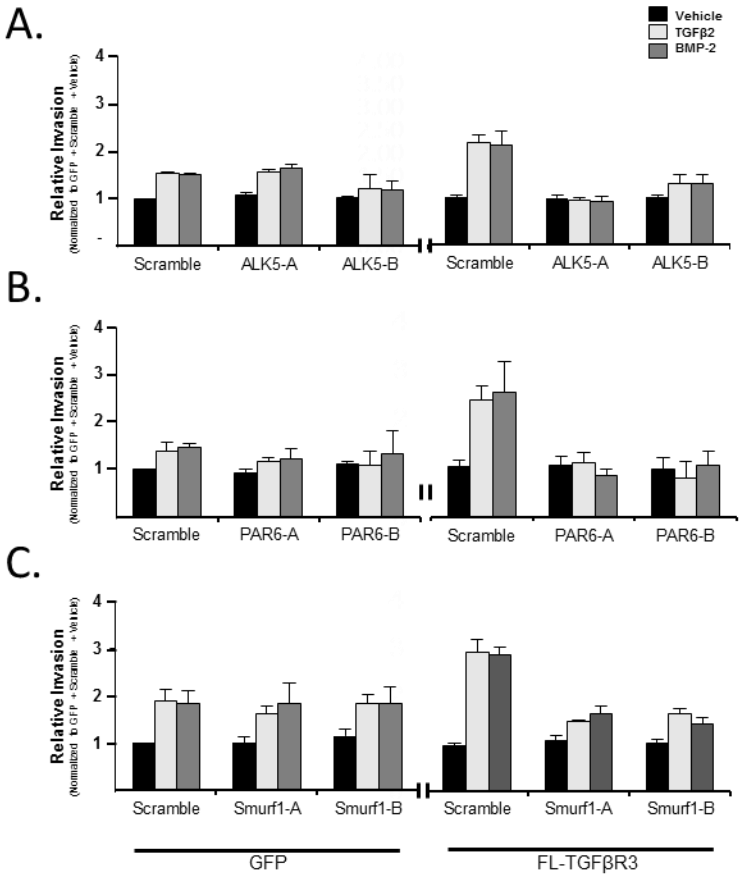

Figure 34 TGFβR3 regulates access to the Par6/Smurf1/RhoA pathway by TGFβ2 and BMP2 in epicardial cells Quantitation of invasion using a modified Boyden chamber assay. *Tgfbr3*$^{-/-}$ cells infected with adenovirus expressing GFP or GFP+FL-TGFβR3 followed by transfection with siRNA directed at (A.) ALK5, (B.)Par6 or (C.) Smurf1 and incubation with TGFβ2 or BMP-2 to access the ability of epicardial cells to invade collagen gel. (n=3; *p<0.05)

Overexpression of WTPar6, Smurf1 or dnRhoA was sufficient to induce invasion in *Tgfbr3*$^{-/-}$ cells, although to a lesser extent than in wildtype cells, demonstrating that the pathway components are present in the absence of *Tgfbr3* in these cells (Figure 35A). There was no effect on cell number (Figure 35B). Expression of dnPar6 or caRhoA did not induce changes in invasion or cell number (Figure 35B). Together these data establish that TGFβR3 is required in epicardial cells to access the Par6/Smurf1/RhoA pathway in response to TGFβ2 or BMP-2.

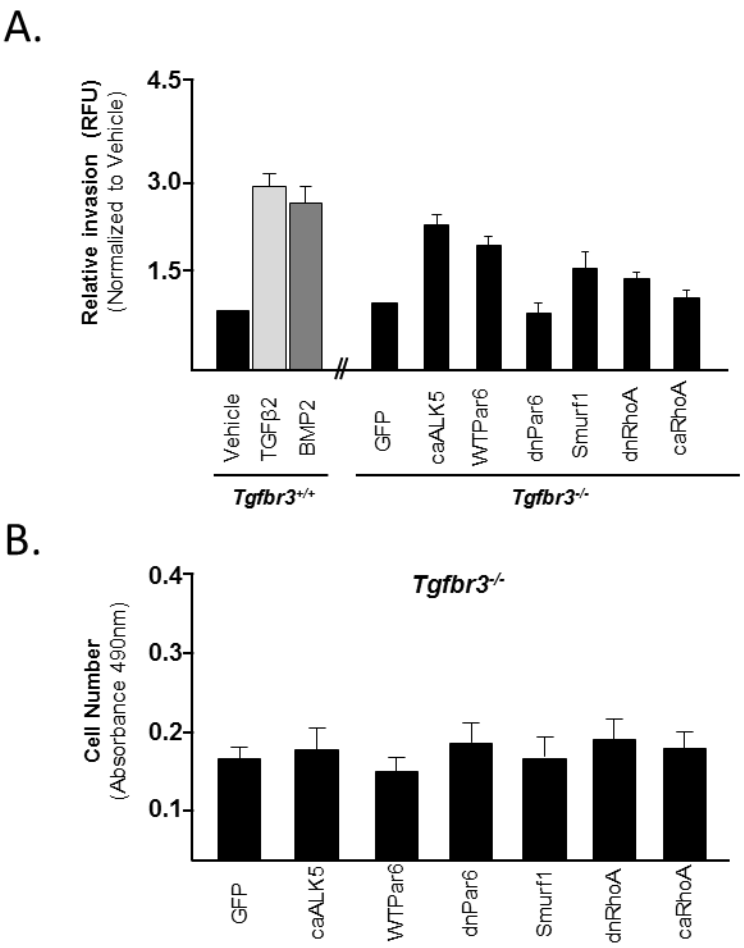

Figure 35 *Tgfbr3*$^{-/-}$ cells have a reduced ability to access the Par6/Smurf1/RhoA pathway *Tgfbr3*$^{-/-}$ cells infected with adenovirus co-expressing GFP and caALK5, WTPar6, dnPar6, Smurf1, caRhoA or dnRhoA (A) Quantitation of invasion using a modified Boyden chamber assay (B) Quantitation of cell number using MTS assay. (n=3; *$p<0.05$)

Discussion

Here we demonstrate that in epicardial cells both TGFβ2 and BMP2 require TGFβR3 to access the Par6/Smurf1/RhoA pathway via ALK5 to mediate cell invasion. This establishes a novel pathway downstream of TGFβR3 in epicardial cells that contributes to coronary vessel formation by regulating the delivery of epicardially-derived mesenchyme to the subepicardial space and myocardium. Loss of TGFβR3 results in failed coronary vessel formation (Compton, Potash et al. 2007) associated with decreased mesenchymal cell invasion (Sanchez, Hill et al. 2011)., but the molecular mechanisms regulating cell invasion downstream of TGFβR3 have been unclear. Recently we reported that epicardial cell invasion *in vitro* requires both the specific cytoplasmic residues of TGFβR3 that bind the scaffolding protein, GAIP-interacting protein, C terminus (GIPC) as well as GIPC (Sanchez, Hill et al. 2011). The data presented here suggests that integration of GIPC signaling and TGFβR3-dependent regulation of the Par6/Smurf1/RhoA together mediate epicardial cell invasion. In endocardial cells, TGFβR3 is required to activate the Par6/Smurf1/RhoA pathway by TGFβ2 and BMP2 to induce EMT and invasion (Townsend, Robinson et al. 2011). This activity in endocardial cells is similarly dependent on the cytoplasmic domain of TGFβR3 and GIPC (Townsend 2011). While these findings in epicardial and endothelial cells are consistent and suggest a general mechanism for TGFβR3-mediated regulation of EMT, how these two pathways intersect is not currently known.

Although to our knowledge no prior report has addressed the role of Par6 or Smurf1 in epicardial cell EMT, invasion, or differentiation there is considerable data on the role of ALK5. We have previously established that ALK5 is required and sufficient to drive EMT and smooth muscle differentiation in epicardial cells (Compton, Potash et al. 2006; Austin, Compton et al. 2008). ALK5 is also required but not sufficient for cell transformation and invasion in endocardial cells (Lai, Beason et al. 2000; Desgrosellier, Mundell et al. 2005) downstream of TGFβ2 and BMP2 (Kirkbride, Townsend et al. 2008; Townsend, Wrana et al. 2008). ALK5 signaling has also been shown to be particularly important for proper formation of the epicardium during cardiac development *in vivo*. Mice with conditional deletion of *Alk5* from the epicardium survive until birth but the coronary arteries display a defective smooth muscle layer and epicardial cells cultured from these mice fail to undergo TGFβ-induced EMT *in vitro* (Sridurongrit, Larsson et al. 2008). These data confirm the role of ALK5 in mediating epicardial cell EMT and invasion but also suggest that additional mechanisms are available *in vivo* to at least partially rescue epicardial cell invasion. These additional mechanisms may include signaling initiated by HA(Craig, Austin et al. 2010; Craig, Parker et al. 2010)), PDGF (Mellgren, Smith et al. 2008), or FGF (Pennisi and Mikawa 2009) which have all been demonstrated to regulate epicardial cell invasion (Olivey and Svensson 2010).

Par6 has been shown regulate cell polarity through interaction with the small GTPases, Cdc42 and Rac1 (Joberty, Petersen et al. 2000; Lin, Edwards et al.

2000) and TGFβR3 has been reported to regulate directional persistence through its interaction with Cdc42 (Mythreye and Blobe 2009). However, neither constitutively active nor dominant negative forms of these small GTPases interfered with the ability of epicardial cells to respond to TGFβ2 or BMP-2 induced invasion. In contrast, both dnRhoA and siRNA targeting RhoA induced epicardial cell invasion while caRhoA inhibited TGFβ2-stimulated invasion. These results in epicardial cells are consistent with those seen in endocardial cells where TGFβR3 is required for cell transformation and invasion in response to TGFβ2 or BMP-2 (Kirkbride, Townsend et al. 2008; Townsend, Robinson et al. 2011). The introduction of dnRhoA or siRNA to ventricular endocardial cells induced cell transformation and invasion while caRhoA did not (Townsend, Wrana et al. 2008). Constitutively active or dominant negative forms of Cdc42 and Rac1 were without effect on transformation or invasion. These findings, along with the fact that neither Cdc42 nor Rac1 are substrates for Smurf1 (Wang, Ogunjimi et al. 2006), support the hypothesis that TGFβ2 and BMP-2 induced invasion is mediated through RhoA degradation in response to Par6 activation of Smurf1 as has been described in NMuMG cells (Ozdamar, Bose et al. 2005).

The integration of TGFβ2 and BMP-2 signaling through TGFβR3 is especially relevant to interpret the phenotype of the *Tgfbr3*$^{-/-}$ mouse. The consideration of the mechanisms that underlie the failed coronary vessel development seen in *Tgfbr3*$^{-/-}$ mice must now include the contribution of BMP-2 signaling through TGFβR3 as well as the previously recognized role of the TGFβ's in signaling via

TGFβR3. Similarly, a potential role for TGFβR3, as well as the canonical BMP signaling receptors, may be considered in understanding the reported roles of BMP-2 in development. For example, *Bmp2*$^{-/-}$ mice have deficits in endocardial EMT (Ma, Lu et al. 2005; Rivera-Feliciano and Tabin 2006) and in proepicardial explants, BMP2 in cooperation with FGF2, regulates differentiation into myocardial or epicardial lineage (Kruithof, van Wijk et al. 2006). TGFβR3 is expressed in both of these tissues which would allow for a contribution by TGFβR3 to BMP-2 signaling ((Brown, Boyer et al. 1999), unpublished).

Par6 has been shown to play a significant role in cancer metastasis. Blockade of Par6 activity maintains the epithelial character of nontransformed mammary cells and decreases protrusions from transformed mammary cells (Viloria-Petit, David et al. 2009). In an orthotopic model of breast cancer metastasis the inhibition of Par6 activity enhanced the epithelial character of tumor cells and decreased metastasis (Viloria-Petit, David et al. 2009). These data suggests a central role for Par6 signaling in tumor progression and metastasis. Data in epicardial cells presented here suggest that TGFβR3 must be considered as a possible regulator of Par6 in tumor metastasis, especially given abundant data demonstrating that TGFβR3 regulates tumor cell migration (Gatza, Oh et al. 2010; Gatza, Holtzhausen et al. 2011; Lambert, Huang et al. 2011). Similarly BMP-2, in addition to TGFβ, may access Par6 in tumor cells via TGFβR3. In summary, we demonstrate that TGFβ2 and BMP2 in epicardial cells signal can assess the Par6/Smurf1/RhoA pathway via TGFβR3 to mediate epicardial cell invasion

during coronary vessel formation. These data force us reconsider the roles and contributions of these ligands with respect to activation of canonical signaling pathways versus signaling through TGFβR3 in both development and disease.

CHAPTER IV

SUMMARY AND CONCLUSIONS

As coronary heart disease continues to be the leading cause of death in developed countries, there is a need to uncover novel therapeutic targets that will aid in the prevention and treatment of such disease. A new potential area of treatment proposes targeting the developmental pathways involved in embryonic cardiovascular development in the adult heart following injury. The re-initiation of pathways involved during coronary vessel formation, in particular, has been postulated as an area of interest. Our laboratory has focused on understanding the contributions of the Type III TGFβ Receptor during coronary vessel development, as deletion of this receptor results in failed coronary vessel formation. Here I have revealed the molecular mechanism for failed coronary development in *Tgfbr3*$^{-/-}$ and provide data supporting a unique and non-redundant role in for TGFβR3 in TGFβ signaling.

Analysis of E13.5 embryos reveals a lower rate of epicardial cell proliferation and decreased epicardially-derived cell invasion in *Tgfbr3*$^{-/-}$ hearts. Similarly, *Tgfbr3*$^{-/-}$ epicardial cells *in vitro* show decreased proliferation and decreased invasion in response to TGFβ1 and TGFβ2. Unexpectedly, loss of TGFβR3 also decreases responsiveness to two other important regulators of epicardial cell behavior, FGF2 and HMW-HA.

The deficits observed *in vivo* and *in vitro,* presented an opportunity to explore the molecular mechanisms of TGFβR3 signaling in the epicardium. Restoring full length TGFβR3 in *Tgfbr3*$^{-/-}$ cells rescued deficits in invasion *in vitro* in response TGFβ1 and TGFβ2 as well as FGF2 and HMW-HA. Further, expression of TGFβR3 missing the 3 C-terminal amino acids that are required to interact with the scaffolding protein GIPC1 did not rescue any of the deficits. Overexpression of GIPC1 alone in *Tgfbr3*$^{-/-}$ cells did not rescue invasion whereas knockdown of GIPC1 in *Tgfbr3*$^{+/+}$ cells decreased invasion in response to TGFβ2, FGF2, and HMW-HA. Together, these data uncover a novel mechanism for TGFβ signaling in epicardial cells that regulates growth factor responsiveness. Disruption of TGFβR3 interaction with GIPC1 results in dysregulation of epicardial cell proliferation and invasion and contributes to failed coronary vessel development in *Tgfbr3*$^{-/-}$ mice.

The ability of TGFβR3 to rescue FGF2 and HMW-HA-induced invasion was certainly a perplexing finding. We postulate that either these ligands bind TGFβR3 and initiate signaling or they activate signaling through their respective receptors that share a common downstream mediator that is lost in *Tgfbr3*$^{-/-}$ cells. What is known is that although TGFβR3 has only a 43 amino acid, non-enzymatic cytoplasmic domain, it is required for signaling during coronary vessel development. Although we have uncovered that GIPC interaction with TGFβR3's cytoplasmic domain is critical to respond to these growth factors, future studies should focus on identifying how TGFβR3, through GIPC, relays extracellular

signals. Does GIPC bring other receptors (FGFR, CD44, and LYVE1) in close proximity to TGFβR3, thus allowing crosstalk of these pathways? Or does GIPC internalize TGFβR3 to allow the formation of signaling hubs as is the case for internalization of G protein coupled receptors and subsequent MAPK recruitment?

Our laboratory recently demonstrated that the Par6/Smurf1/RhoA pathway can mediate EMT in atrioventricular cushion endocardial cells(Townsend, Robinson et al. 2011), which contribute to the heart valves. Access of either TGFβ2 or BMP-2 to this pathway is dependent on TGFβR3. Given, the importance of the Par6/Smurf1/RhoA pathway in epithelial homeostasis, and the role of TGFβR3 in the epicardium, we investigated the functionality of this pathway in these coronary vessel precursor cells. Targeting of ALK5 in *Tgfbr3*$^{+/+}$ cells inhibited EMT and invasion. Overexpression of wild-type (wt) Par6, but not dominant negative (dn) Par6, induced EMT and invasion while targeting Par6 by siRNA inhibited EMT and invasion. Overexpression of Smurf1 and dnRhoA induced EMT and invasion. Targeting of Smurf1 by siRNA or overexpression of caRhoA inhibited EMT and invasion. In *Tgfbr3*$^{-/-}$ epicardial cells which have a decreased ability to invade collagen gels in response to TGFβ2, overexpression of wtPar6, Smurf1, or dnRhoA had a diminished ability to induce invasion. Overexpression of TGFβR3 in *Tgfbr3*$^{-/-}$ cells, followed by siRNA targeting Par6 or Smurf1, diminished the ability of TGFβR3 to rescue invasion demonstrating that the

Par6/Smurf1/RhoA pathway is activated downstream of TGFβR3 in epicardial cells.

While uncovering a novel signaling pathway involved in coronary vessel development is certainly important, the finding that TGFβR3 regulates access of TGFβ-2 and BMP-2 to this pathway broadens our understanding of TGFβ signaling for several reasons: First, my results emphasizes the relevance of non-Smad signaling. Although not presented here, Smad1 or Smad3 overexpression is not sufficient to induce invasion in epicardial cells (unpublished). These results are consistent with previous reports where blocking components of the Smad pathway while overexpressing Par6 pathway were unable to revert mesenchymal character activated by the Par6 pathway(Viloria-Petit and Wrana 2010). Second, our results highlight the role of TGFβR3 in TGFβ signaling which has long been overshadowed by TGFβR1 and TGFβR2. This forces us to reconsider therapeutic targets not only during coronary vessel development, but during cancer progression, where both TGFβR3 and the Par6/Smurf1/RhoA have been reported to promote tumorgenesis.

The past decade has significantly advanced our knowledge of TGFβR3 signaling during development and disease progression. Regulation of cell migration, invasion and proliferation has been a recurrent role for TGFβR3, and several mechanisms have been described: TGFβR3 can regulate directional persistence by regulating Cdc42 activity (Mythreye and Blobe 2009); here we showed that

TGFβR3-dependent invasion is mediated through RhoA. Migration of cancer cells has also been shown to require TGFβR3-dependent regulation of NFκB activity (Criswell and Arteaga 2007; You, How et al. 2009). NFκB activity is reduced in *Tgfbr3*$^{-/-}$ cells and inhibiting NFκB in *Tgfbr3*$^{+/+}$ cells inhibits invasion (unpublished). Regulation of Cdc42 and NFκB activity is mediated through interaction of TGFβR3 with β-arrestin2 (You, How et al. 2009). The cytoplasmic domain of TGFβR3's also regulates proliferation through Smad3 and p38 signaling (You, Bruinsma et al. 2007), and we have shown that regulation of proliferation in epicardial cells requires interaction with GIPC. Nonetheless, there are significant gaps in our understanding of TGFβR3 signaling: How are all these signals integrated? Are all pathways accessible in every cell type? What determines whether TGFβR3 regulates migration, invasion or proliferation in any given cell? What effect does stabilization on the cellular membrane by GIPC versus internalization by β-arrestin2 have on accessing these diverse pathways? Does modification of TGFβR3's extracellular domain determine ligand binding? Does this in turn determine what pathways are activated? What role does ectodomain shedding play in all of these processes? Differential ALK activation has been an important role for endoglin in regulating endothelial behavior. Given the similarity between endoglin and TGFβR3, could TGFβR3 have a similar function in non-endothelial cells?

In summary, I have revealed a molecular mechanism for failed coronary development in *Tgfbr3*$^{-/-}$ mice and provide data supporting a unique and non-redundant role in for TGFβR3 in TGFβ signaling. My studies have revealed new directions for investigation into the role of this important growth factor family in development and disease.

LITERATURE CITED

Andres, J. L., D. DeFalcis, et al. (1992). "Binding of two growth factor families to separate domains of the proteoglycan betaglycan." The Journal of biological chemistry **267**(9): 5927-5930.

Attisano, L. and J. L. Wrana (2002). "Signal transduction by the TGF-beta superfamily." Science **296**(5573): 1646-1647.

Attisano, L., J. L. Wrana, et al. (1994). "TGF-beta receptors and actions." Biochim Biophys Acta **1222**(1): 71-80.

Austin, A. F., L. A. Compton, et al. (2008). "Primary and immortalized mouse epicardial cells undergo differentiation in response to TGFbeta." Dev Dyn **237**(2): 366-376.

Austin, A. F., L. A. Compton, et al. (2008). "Primary and immortalized mouse epicardial cells undergo differentiation in response to TGFbeta." Developmental dynamics : an official publication of the American Association of Anatomists **237**(2): 366-376.

Azhar, M., J. Schultz Jel, et al. (2003). "Transforming growth factor beta in cardiovascular development and function." Cytokine Growth Factor Rev **14**(5): 391-407.

Bai, S., X. Shi, et al. (2000). "Smad6 as a transcriptional corepressor." J Biol Chem **275**(12): 8267-8270.

Bakin, A. V., C. Rinehart, et al. (2002). "p38 mitogen-activated protein kinase is required for TGFbeta-mediated fibroblastic transdifferentiation and cell migration." J Cell Sci **115**(Pt 15): 3193-3206.

Bakin, A. V., A. K. Tomlinson, et al. (2000). "Phosphatidylinositol 3-Kinase Function Is Required for Transforming Growth Factor beta -mediated Epithelial to Mesenchymal Transition and Cell Migration." J. Biol. Chem. **275**(47): 36803-36810.

Barbara, N. P., J. L. Wrana, et al. (1999). "Endoglin is an accessory protein that interacts with the signaling receptor complex of multiple members of the transforming growth factor-beta superfamily." J Biol Chem **274**(2): 584-594.

Barnett, J. V. and J. S. Desgrosellier (2003). "Early events in valvulogenesis: a signaling perspective." Birth Defects Res Part C Embryo Today **69**(1): 58-72.

Barnett, J. V., A. Moustakas, et al. (1994). "Cloning and developmental expression of the chick type II and type III TGF beta receptors." Dev Dyn **199**(1): 12-27.

Bassing, C. H., J. M. Yingling, et al. (1994). "A transforming growth factor beta type I receptor that signals to activate gene expression." Science **263**(5143): 87-89.

Bassing, C. H., J. M. Yingling, et al. (1994). "Receptors for the TGF-beta ligand family." Vitam Horm **48**: 111-156.

Bayless, K. J. and G. E. Davis (2002). "The Cdc42 and Rac1 GTPases are required for capillary lumen formation in three-dimensional extracellular matrices." J Cell Sci **115**(6): 1123-1136.

Bennett, H. S. (1936). "The development of the blood supply to the heart in the embryo pig." Am J Anat **60**: 27-53.

Bhowmick, N. A., M. Ghiassi, et al. (2001). "Transforming Growth Factor-{beta}1 Mediates Epithelial to Mesenchymal Transdifferentiation through a RhoA-dependent Mechanism." Mol. Biol. Cell **12**(1): 27-36.

Bierie, B. and H. L. Moses (2006). "Tumour microenvironment: TGFbeta: the molecular Jekyll and Hyde of cancer." Nat Rev Cancer **6**(7): 506-520.

Blobe, G. C., X. Liu, et al. (2001). "A novel mechanism for regulating transforming growth factor beta (TGF-beta) signaling. Functional modulation of type III TGF-beta receptor expression through interaction with the PDZ domain protein, GIPC." J Biol Chem **276**(43): 39608-39617.

Blobe, G. C., W. P. Schiemann, et al. (2001). "Functional roles for the cytoplasmic domain of the type III transforming growth factor beta receptor in regulating transforming growth factor beta signaling." The Journal of biological chemistry **276**(27): 24627-24637.

Blobe, G. C., W. P. Schiemann, et al. (2001). "Functional roles for the cytoplasmic domain of the type III transforming growth factor beta receptor in regulating transforming growth factor beta signaling." J Biol Chem **276**(27): 24627-24637.

Bock-Marquette, I., S. Shrivastava, et al. (2009). "Thymosin beta4 mediated PKC activation is essential to initiate the embryonic coronary developmental program and epicardial progenitor cell activation in adult mice in vivo." Journal of molecular and cellular cardiology **46**(5): 728-738.

Bose, R. and J. L. Wrana (2006). "Regulation of Par6 by extracellular signals." Curr Opin Cell Biol **18**(2): 206-212.

Brown, C. B., A. S. Boyer, et al. (1996). "Antibodies to the Type II TGFbeta receptor block cell activation and migration during atrioventricular cushion transformation in the heart." Dev Biol **174**(2): 248-257.

Brown, C. B., A. S. Boyer, et al. (1999). "Requirement of type III TGF-beta receptor for endocardial cell transformation in the heart." Science **283**(5410): 2080-2082.

Cai, C. L., J. C. Martin, et al. (2008). "A myocardial lineage derives from Tbx18 epicardial cells." Nature **454**(7200): 104-108.

Camenisch, T. D., A. P. Spicer, et al. (2000). "Disruption of hyaluronan synthase-2 abrogates normal cardiac morphogenesis and hyaluronan-mediated transformation of epithelium to mesenchyme." The Journal of clinical investigation **106**(3): 349-360.

Cardiff, R. D. (2010). "The pathology of EMT in mouse mammary tumorigenesis." J Mammary Gland Biol Neoplasia **15**(2): 225-233.

Chang, H., D. Huylebroeck, et al. (1999). "Smad5 knockout mice die at mid-gestation due to multiple embryonic and extraembryonic defects." Development **126**(8): 1631-1642.

Cheifetz, S., T. Bellon, et al. (1992). "Endoglin is a component of the transforming growth factor-beta receptor system in human endothelial cells." J Biol Chem **267**(27): 19027-19030.

Cheifetz, S., H. Hernandez, et al. (1990). "Distinct transforming growth factor-beta (TGF-beta) receptor subsets as determinants of cellular responsiveness to three TGF-beta isoforms." J Biol Chem **265**(33): 20533-20538.

Chen, W., K. C. Kirkbride, et al. (2003). "Beta-arrestin 2 mediates endocytosis of type III TGF-beta receptor and down-regulation of its signaling." Science **301**(5638): 1394-1397.

Choi, S. S. and A. M. Diehl (2009). "Epithelial-to-mesenchymal transitions in the liver." Hepatology **50**(6): 2007-2013.

Christoffels, V. M., T. Grieskamp, et al. (2009). "Tbx18 and the fate of epicardial progenitors." Nature **458**(7240): E8-9; discussion E9-10.

Compton, L. A., D. A. Potash, et al. (2007). "Coronary Vessel Development Is Dependent on the Type III Transforming Growth Factor {beta} Receptor." Circ Res **101**(8): 784-791.

Compton, L. A., D. A. Potash, et al. (2006). "Transforming growth factor-beta induces loss of epithelial character and smooth muscle cell differentiation in epicardial cells." Dev Dyn **235**(1): 82-93.

Craig, E. A., A. F. Austin, et al. (2010). "TGFbeta2-mediated production of hyaluronan is important for the induction of epicardial cell differentiation and invasion." Exp Cell Res.

Craig, E. A., P. Parker, et al. (2010). "Involvement of the MEKK1 signaling pathway in the regulation of epicardial cell behavior by hyaluronan." Cellular signalling **22**(6): 968-976.

Craig, E. A., P. Parker, et al. (2010). "Involvement of the MEKK1 signaling pathway in the regulation of epicardial cell behavior by hyaluronan." Cell Signal **22**(6): 968-976.

Crispino, J. D., M. B. Lodish, et al. (2001). "Proper coronary vascular development and heart morphogenesis depend on interaction of GATA-4 with FOG cofactors." Genes & development **15**(7): 839-844.

Crispino, J. D., M. B. Lodish, et al. (2001). "Proper coronary vascular development and heart morphogenesis depend on interaction of GATA-4 with FOG cofactors." Genes Dev **15**(7): 839-844.

Criswell, T. L. and C. L. Arteaga (2007). "Modulation of NF{kappa}B Activity and E-cadherin by the Type III Transforming Growth Factor beta Receptor Regulates Cell Growth and Motility." J. Biol. Chem. **282**(44): 32491-32500.

Datto, M. B., J. P. Frederick, et al. (1999). "Targeted disruption of Smad3 reveals an essential role in transforming growth factor beta-mediated signal transduction." Mol Cell Biol **19**(4): 2495-2504.

Deaton, R. A., C. Su, et al. (2005). "Transforming growth factor-beta1-induced expression of smooth muscle marker genes involves activation of PKN and p38 MAPK." J Biol Chem **280**(35): 31172-31181.

Dedkov, E. I., M. T. Thomas, et al. (2007). "Synectin/syndecan-4 regulate coronary arteriolar growth during development." Dev Dyn **236**(7): 2004-2010.

Delaughter, D. M., L. Saint-Jean, et al. (2011). "What chick and mouse models have taught us about the role of the endocardium in congenital heart disease." Birth defects research. Part A, Clinical and molecular teratology **91**(6): 511-525.

Derangeon, M., N. Bourmeyster, et al. (2008). "RhoA GTPase and F-actin dynamically regulate the permeability of Cx43-made channels in rat cardiac myocytes." J Biol Chem **283**(45): 30754-30765.

Derynck, R. and Y. E. Zhang "Smad-dependent and Smad-independent pathways in TGF-[beta] family signalling."

Derynck, R. and Y. E. Zhang (2003). "Smad-dependent and Smad-independent pathways in TGF-[beta] family signalling." Nature **425**(6958): 577.

Desgrosellier, J. S., N. A. Mundell, et al. (2005). "Activin receptor-like kinase 2 and Smad6 regulate epithelial-mesenchymal transformation during cardiac valve formation." Dev Biol **280**(1): 201-210.

Dettman, R. W., W. Denetclaw, Jr., et al. (1998). "Common epicardial origin of coronary vascular smooth muscle, perivascular fibroblasts, and intermyocardial fibroblasts in the avian heart." Dev Biol **193**(2): 169-181.

Dickson, M. C., J. S. Martin, et al. (1995). "Defective haematopoiesis and vasculogenesis in transforming growth factor-beta 1 knock out mice." Development **121**(6): 1845-1854.

Ebner, R., R. H. Chen, et al. (1993). "Cloning of a type I TGF-beta receptor and its effect on TGF-beta binding to the type II receptor." Science **260**(5112): 1344-1348.

Edlund, S., M. Landstrom, et al. (2002). "Transforming Growth Factor-beta -induced Mobilization of Actin Cytoskeleton Requires Signaling by Small GTPases Cdc42 and RhoA." Mol. Biol. Cell **13**(3): 902-914.

Engel, M. E., M. A. McDonnell, et al. (1999). "Interdependent SMAD and JNK signaling in transforming growth factor-beta-mediated transcription." J Biol Chem **274**(52): 37413-37420.

Gao, L. and I. G. Macara (2004). "Isoforms of the polarity protein par6 have distinct functions." J Biol Chem **279**(40): 41557-41562.

Gatza, C. E., A. Holtzhausen, et al. (2011). "Type III TGF-beta Receptor Enhances Colon Cancer Cell Migration and Anchorage-Independent Growth." Neoplasia **13**(8): 758-770.

Gatza, C. E., S. Y. Oh, et al. (2010). "Roles for the type III TGF-beta receptor in human cancer." Cellular signalling **22**(8): 1163-1174.

Gittenberger-de Groot, A. C., M. P. Vrancken Peeters, et al. (2000). "Epicardial outgrowth inhibition leads to compensatory mesothelial outflow tract collar and abnormal cardiac septation and coronary formation." Circ Res **87**(11): 969-971.

Goldsmith, J. B. and H. W. Butler (1973). "The development of the cardiac-coronary circulatory system." Am J Anat **60**(2): 185-201.

González-Mariscal, L., A. Betanzos, et al. (2000). "MAGUK proteins: structure and role in the tight junction." Seminars in Cell & Developmental Biology **11**(4): 315-324.

Goumans, M. J., G. Valdimarsdottir, et al. (2003). "Activin receptor-like kinase (ALK)1 is an antagonistic mediator of lateral TGFbeta/ALK5 signaling." Mol Cell **12**(4): 817-828.

Goumans, M. J., G. Valdimarsdottir, et al. (2002). "Balancing the activation state of the endothelium via two distinct TGF-beta type I receptors." Embo J **21**(7): 1743-1753.

Grant, R. T. (1926). "Development of the cardiac coronary vessels in the rabbit." Heart **13**: 261-271.

Gu, Z., E. M. Reynolds, et al. (1999). "The type I serine/threonine kinase receptor ActRIA (ALK2) is required for gastrulation of the mouse embryo." Development **126**(11): 2551-2561.

Gurevich, V. V. and E. V. Gurevich (2003). "The new face of active receptor bound arrestin attracts new partners." Structure (Camb) **11**(9): 1037-1042.
Han, L. and A. I. Gotlieb (2011). "Fibroblast growth factor-2 promotes in vitro mitral valve interstitial cell repair through transforming growth factor-beta/Smad signaling." The American journal of pathology **178**(1): 119-127.
Hata, A., G. Lagna, et al. (1998). "Smad6 inhibits BMP/Smad1 signaling by specifically competing with the Smad4 tumor suppressor." Genes Dev **12**(2): 186-197.
He, T.-C., S. Zhou, et al. (1998). "A simplified system for generating recombinant adenoviruses." Proceedings of the National Academy of Sciences of the United States of America **95**(5): 2509-2514.
Heallen, T., M. Zhang, et al. (2011). "Hippo pathway inhibits Wnt signaling to restrain cardiomyocyte proliferation and heart size." Science **332**(6028): 458-461.
Hellermann, J. P., S. J. Jacobsen, et al. (2005). "Heart failure after myocardial infarction: clinical presentation and survival." Eur J Heart Fail **7**(1): 119-125.
Ho, E. and Y. Shimada (1978). "Formation of the epicardium studied with the scanning electron microscope." Dev Biol **66**(2): 579-585.
Huang, X., X. Gao, et al. (2008). "Coronary development is regulated by ATP-dependent SWI/SNF chromatin remodeling component BAF180." Dev Biol **319**(2): 258-266.
Ishida, W., T. Hamamoto, et al. (2000). "Smad6 is a Smad1/5-induced smad inhibitor. Characterization of bone morphogenetic protein-responsive element in the mouse Smad6 promoter." J Biol Chem **275**(9): 6075-6079.
Jiao, K., M. Langworthy, et al. (2006). "Tgfbeta signaling is required for atrioventricular cushion mesenchyme remodeling during in vivo cardiac development." Development **133**(22): 4585-4593.
Joberty, G., C. Petersen, et al. (2000). "The cell-polarity protein Par6 links Par3 and atypical protein kinase C to Cdc42." Nat Cell Biol **2**(8): 531-539.
Kaartinen, V., M. Dudas, et al. (2004). "Cardiac outflow tract defects in mice lacking ALK2 in neural crest cells." Development **131**(14): 3481-3490.
Kaartinen, V., J. W. Voncken, et al. (1995). "Abnormal lung development and cleft palate in mice lacking TGF-beta 3 indicates defects of epithelial-mesenchymal interaction." Nat Genet **11**(4): 415-421.
Kimura, N., R. Matsuo, et al. (2000). "BMP2-induced apoptosis is mediated by activation of the TAK1-p38 kinase pathway that is negatively regulated by Smad6." J Biol Chem **275**(23): 17647-17652.
Kirkbride, K. C., T. A. Townsend, et al. (2008). "Bone morphogenetic proteins signal through the transforming growth factor-beta type III receptor." J. Biol. Chem.: M704883200.
Kirkbride, K. C., T. A. Townsend, et al. (2008). "Bone morphogenetic proteins signal through the transforming growth factor-beta type III receptor." J Biol Chem **283**(12): 7628-7637.
Kirschner, K. M., N. Wagner, et al. (2006). "The Wilms tumor suppressor Wt1 promotes cell adhesion through transcriptional activation of the alpha4integrin gene." J Biol Chem **281**(42): 31930-31939.
Komiyama, M., K. Ito, et al. (1987). "Origin and development of the epicardium in the mouse embryo." Anat Embryol (Berl) **176**(2): 183-189.

Kretzschmar, M. and J. Massague (1998). "SMADs: mediators and regulators of TGF-beta signaling." Curr Opin Genet Dev **8**(1): 103-111.

Kruithof, B. P., B. van Wijk, et al. (2006). "BMP and FGF regulate the differentiation of multipotential pericardial mesoderm into the myocardial or epicardial lineage." Dev Biol **295**(2): 507-522.

Kuhn, H. J. and G. Liebherr (1988). "The early development of the epicardium in Tupaia belangeri." Anat Embryol (Berl) **177**(3): 225-234.

Kwee, L., H. S. Baldwin, et al. (1995). "Defective development of the embryonic and extraembryonic circulatory systems in vascular cell adhesion molecule (VCAM-1) deficient mice." Development **121**(2): 489-503.

Lai, Y. T., K. B. Beason, et al. (2000). "Activin receptor-like kinase 2 can mediate atrioventricular cushion transformation." Dev Biol **222**(1): 1-11.

Lambert, K. E., H. Huang, et al. (2011). "The type III transforming growth factor-beta receptor inhibits proliferation, migration, and adhesion in human myeloma cells." Molecular biology of the cell **22**(9): 1463-1472.

Langlois, D., M. Hneino, et al. (2010). "Conditional inactivation of TGF-beta type II receptor in smooth muscle cells and epicardium causes lethal aortic and cardiac defects." Transgenic Res **19**(6): 1069-1082.

Lavine, K. J., F. Long, et al. (2008). "Hedgehog signaling to distinct cell types differentially regulates coronary artery and vein development." Development **135**(18): 3161-3171.

Lavine, K. J., A. C. White, et al. (2006). "Fibroblast growth factor signals regulate a wave of Hedgehog activation that is essential for coronary vascular development." Genes Dev **20**(12): 1651-1666.

Lavine, K. J., K. Yu, et al. (2005). "Endocardial and epicardial derived FGF signals regulate myocardial proliferation and differentiation in vivo." Developmental cell **8**(1): 85-95.

Lavine, K. J., K. Yu, et al. (2005). "Endocardial and epicardial derived FGF signals regulate myocardial proliferation and differentiation in vivo." Dev Cell **8**(1): 85-95.

Lee, J. D., N. Hempel, et al. "The type III TGF-{beta} receptor suppresses breast cancer progression through GIPC-mediated inhibition of TGF-{beta} signaling." Carcinogenesis **31**(2): 175-183.

Lee, J. D., N. Hempel, et al. (2009). "The type III TGF-{beta} receptor suppresses breast cancer progression through GIPC-mediated inhibition of TGF-{beta} signaling." Carcinogenesis **31**(2): 175-183.

Lee, N. Y. and G. C. Blobe (2007). "The interaction of endoglin with beta-arrestin2 regulates transforming growth factor-beta-mediated ERK activation and migration in endothelial cells." J Biol Chem **282**(29): 21507-21517.

Lee, N. Y., B. Ray, et al. (2008). "Endoglin promotes transforming growth factor beta-mediated Smad 1/5/8 signaling and inhibits endothelial cell migration through its association with GIPC." J Biol Chem **283**(47): 32527-32533.

Lepilina, A., A. N. Coon, et al. (2006). "A dynamic epicardial injury response supports progenitor cell activity during zebrafish heart regeneration." Cell **127**(3): 607-619.

Lewis, K. A., P. C. Gray, et al. (2000). "Betaglycan binds inhibin and can mediate functional antagonism of activin signalling." Nature **404**(6776): 411-414.

Li, W. E., K. Waldo, et al. (2002). "An essential role for connexin43 gap junctions in mouse coronary artery development." Development **129**(8): 2031-2042.
Lie-Venema, H., A. C. Gittenberger-de Groot, et al. (2003). "Ets-1 and Ets-2 transcription factors are essential for normal coronary and myocardial development in chicken embryos." Circ Res **92**(7): 749-756.
Lin, D., A. S. Edwards, et al. (2000). "A mammalian PAR-3-PAR-6 complex implicated in Cdc42/Rac1 and aPKC signalling and cell polarity." Nat Cell Biol **2**(8): 540-547.
Lin, H. Y. and A. Moustakas (1994). "TGF-beta receptors: structure and function." Cell Mol Biol (Noisy-le-grand) **40**(3): 337-349.
Lin, H. Y., X. F. Wang, et al. (1992). "Expression cloning of the TGF-beta type II receptor, a functional transmembrane serine/threonine kinase." Cell **68**(4): 775-785.
Lloyd-Jones, D., R. J. Adams, et al. (2010). "Heart Disease and Stroke Statistics--2010 Update: A Report From the American Heart Association." Circulation **121**(7): e46-215.
Lopez-Casillas, F., S. Cheifetz, et al. (1991). "Structure and expression of the membrane proteoglycan betaglycan, a component of the TGF-beta receptor system." Cell **67**(4): 785-795.
Lopez-Casillas, F., J. L. Wrana, et al. (1993). "Betaglycan presents ligand to the TGF beta signaling receptor." Cell **73**(7): 1435-1444.
Lu, J. R., T. A. McKinsey, et al. (1999). "FOG-2, a heart- and brain-enriched cofactor for GATA transcription factors." Mol Cell Biol **19**(6): 4495-4502.
Ma, L., M. F. Lu, et al. (2005). "Bmp2 is essential for cardiac cushion epithelial-mesenchymal transition and myocardial patterning." Development **132**(24): 5601-5611.
Mahtab, E. A., M. C. Wijffels, et al. (2008). "Cardiac malformations and myocardial abnormalities in podoplanin knockout mouse embryos: Correlation with abnormal epicardial development." Dev Dyn **237**(3): 847-857.
Mahtab, E. A., M. C. Wijffels, et al. (2008). "Cardiac malformations and myocardial abnormalities in podoplanin knockout mouse embryos: Correlation with abnormal epicardial development." Developmental dynamics : an official publication of the American Association of Anatomists **237**(3): 847-857.
Manner, J. (1993). "Experimental study on the formation of the epicardium in chick embryos." Anat Embryol (Berl) **187**(3): 281-289.
Massague, J. and R. R. Gomis (2006). "The logic of TGFbeta signaling." FEBS Lett **580**(12): 2811-2820.
Massague, J. and F. Weis-Garcia (1996). "Serine/threonine kinase receptors: mediators of transforming growth factor beta family signals." Cancer Surv **27**: 41-64.
Mellgren, A. M., C. L. Smith, et al. (2008). "Platelet-derived growth factor receptor beta signaling is required for efficient epicardial cell migration and development of two distinct coronary vascular smooth muscle cell populations." Circ Res **103**(12): 1393-1401.
Merki, E., M. Zamora, et al. (2005). "Epicardial retinoid X receptor alpha is required for myocardial growth and coronary artery formation." Proc Natl Acad Sci U S A **102**(51): 18455-18460.

Mikawa, T. and D. A. Fischman (1992). "Retroviral analysis of cardiac morphogenesis: discontinuous formation of coronary vessels." Proc Natl Acad Sci U S A **89**(20): 9504-9508.

Mikawa, T. and R. G. Gourdie (1996). "Pericardial mesoderm generates a population of coronary smooth muscle cells migrating into the heart along with ingrowth of the epicardial organ." Dev Biol **174**(2): 221-232.

Mishina, Y., R. Crombie, et al. (1999). "Multiple roles for activin-like kinase-2 signaling during mouse embryogenesis." Dev Biol **213**(2): 314-326.

Miyazawa, K., M. Shinozaki, et al. (2002). "Two major Smad pathways in TGF-beta superfamily signalling." Genes Cells **7**(12): 1191-1204.

Miyazono, K., H. Ichijo, et al. (1993). "Transforming growth factor-beta: latent forms, binding proteins and receptors." Growth Factors **8**(1): 11-22.

Molin, D. G., U. Bartram, et al. (2003). "Expression patterns of Tgfbeta1-3 associate with myocardialisation of the outflow tract and the development of the epicardium and the fibrous heart skeleton." Dev Dyn **227**(3): 431-444.

Moore, A., L. McInnes, et al. (1999). "YAC complementation shows a requirement for Wt1 in the development of epicardium, adrenal gland and throughout nephrogenesis." Development **126**(9): 1845-1857.

Morabito, C. J., R. W. Dettman, et al. (2001). "Positive and negative regulation of epicardial-mesenchymal transformation during avian heart development." Dev Biol **234**(1): 204-215.

Muders, M. H., P. K. Vohra, et al. (2009). "Targeting GIPC/synectin in pancreatic cancer inhibits tumor growth." Clin Cancer Res **15**(12): 4095-4103.

Mulder, K. M. (2000). "Role of Ras and Mapks in TGFbeta signaling." Cytokine Growth Factor Rev **11**(1-2): 23-35.

Munoz-Chapuli, R., M. Gonzalez-Iriarte, et al. (2002). "Cellular precursors of the coronary arteries." Tex Heart Inst J **29**(4): 243-249.

Mythreye, K. and G. C. Blobe (2009). "The type III TGF-beta receptor regulates epithelial and cancer cell migration through beta-arrestin2-mediated activation of Cdc42." Proc Natl Acad Sci U S A **106**(20): 8221-8226.

Mythreye, K. and G. C. Blobe (2009). "The type III TGF-beta receptor regulates epithelial and cancer cell migration through beta-arrestin2-mediated activation of Cdc42." Proceedings of the National Academy of Sciences of the United States of America **106**(20): 8221-8226.

Nahirney, P. C., T. Mikawa, et al. (2003). "Evidence for an extracellular matrix bridge guiding proepicardial cell migration to the myocardium of chick embryos." Dev Dyn **227**(4): 511-523.

Nakao, A., M. Afrakhte, et al. (1997). "Identification of Smad7, a TGFbeta-inducible antagonist of TGF-beta signalling." Nature **389**(6651): 631-635.

Olivey, H. E., L. A. Compton, et al. (2004). "Coronary vessel development: the epicardium delivers." Trends in cardiovascular medicine **14**(6): 247-251.

Olivey, H. E., L. A. Compton, et al. (2004). "Coronary vessel development: the epicardium delivers." Trends Cardiovasc Med **14**(6): 247-251.

Olivey, H. E., N. A. Mundell, et al. (2006). "Transforming growth factor-beta stimulates epithelial-mesenchymal transformation in the proepicardium." Dev Dyn **235**(1): 50-59.

Olivey, H. E. and E. C. Svensson (2010). "Epicardial-myocardial signaling directing coronary vasculogenesis." Circ Res **106**(5): 818-832.
Oshima, M., H. Oshima, et al. (1996). "TGF-beta receptor type II deficiency results in defects of yolk sac hematopoiesis and vasculogenesis." Dev Biol **179**(1): 297-302.
Overall, C. M., J. L. Wrana, et al. (1989). "Independent regulation of collagenase, 72-kDa progelatinase, and metalloendoproteinase inhibitor expression in human fibroblasts by transforming growth factor-beta." J Biol Chem **264**(3): 1860-1869.
Overall, C. M., J. L. Wrana, et al. (1989). "Transforming growth factor-beta regulation of collagenase, 72 kDa-progelatinase, TIMP and PAI-1 expression in rat bone cell populations and human fibroblasts." Connect Tissue Res **20**(1-4): 289-294.
Ozdamar, B., R. Bose, et al. (2005). "Regulation of the polarity protein Par6 by TGFbeta receptors controls epithelial cell plasticity." Science **307**(5715): 1603-1609.
Pennisi, D. J. and T. Mikawa (2005). "Normal patterning of the coronary capillary plexus is dependent on the correct transmural gradient of FGF expression in the myocardium." Dev Biol **279**(2): 378-390.
Pennisi, D. J. and T. Mikawa (2009). "FGFR-1 is required by epicardium-derived cells for myocardial invasion and correct coronary vascular lineage differentiation." Dev Biol **328**(1): 148-159.
Pennisi, D. J. and T. Mikawa (2009). "FGFR-1 is required by epicardium-derived cells for myocardial invasion and correct coronary vascular lineage differentiation." Developmental Biology **328**(1): 148-159.
Pepper, M. S. (1997). "Transforming growth factor-beta: vasculogenesis, angiogenesis, and vessel wall integrity." Cytokine Growth Factor Rev **8**(1): 21-43.
Perez-Pomares, J. M., A. Phelps, et al. (2002). "Experimental studies on the spatiotemporal expression of WT1 and RALDH2 in the embryonic avian heart: a model for the regulation of myocardial and valvuloseptal development by epicardially derived cells (EPDCs)." Dev Biol **247**(2): 307-326.
Perryn, E. D., A. Czirok, et al. (2008). "Vascular sprout formation entails tissue deformations and VE-cadherin-dependent cell-autonomous motility." Developmental biology **313**(2): 545-555.
Poelmann, R. E., A. C. Gittenberger-de Groot, et al. (1993). "Development of the cardiac coronary vascular endothelium, studied with antiendothelial antibodies, in chicken-quail chimeras." Circ Res **73**(3): 559-568.
Poss, K. D., L. G. Wilson, et al. (2002). "Heart regeneration in zebrafish." Science **298**(5601): 2188-2190.
Quarto, N. and M. T. Longaker (2008). "Differential expression of specific FGF ligands and receptor isoforms during osteogenic differentiation of mouse Adipose-derived Stem Cells (mASCs) recapitulates the in vivo osteogenic pattern." Gene **424**(1-2): 130-140.
Ray, B. N., N. Y. Lee, et al. (2010). "ALK5 phosphorylation of the endoglin cytoplasmic domain regulates Smad1/5/8 signaling and endothelial cell migration." Carcinogenesis **31**(3): 435-441.
Red-Horse, K., H. Ueno, et al. (2010). "Coronary arteries form by developmental reprogramming of venous cells." Nature **464**(7288): 549-553.
Red-Horse, K., H. Ueno, et al. (2010). "Coronary arteries form by developmental reprogramming of venous cells." Nature **464**(7288): 549-553.

Rentschler, S. and J. A. Epstein (2011). "Kicking the Epicardium Up a Notch." Circulation research **108**(1): 6-8.
Rhee, D. Y., X. Q. Zhao, et al. (2009). "Connexin 43 regulates epicardial cell polarity and migration in coronary vascular development." Development **136**(18): 3185-3193.
Rifkin, D. B. (2005). "Latent transforming growth factor-beta (TGF-beta) binding proteins: orchestrators of TGF-beta availability." J Biol Chem **280**(9): 7409-7412.
Rivera-Feliciano, J. and C. J. Tabin (2006). "Bmp2 instructs cardiac progenitors to form the heart-valve-inducing field." Dev Biol **295**(2): 580-588.
Roberts, A. B. (1988). "Transforming growth factor beta: biochemistry and roles in embryogenesis, tissue repair and remodeling, and carcinogenesis." Recent Prog Horm Res **44**: 157-197.
Rodgers, L. S., S. Lalani, et al. (2008). "Differential growth and multicellular villi direct proepicardial translocation to the developing mouse heart." Dev Dyn **237**(1): 145-152.
Runyan, R. B. and R. R. Markwald (1983). "Invasion of mesenchyme into three-dimensional collagen gels: a regional and temporal analysis of interaction in embryonic heart tissue." Developmental biology **95**(1): 108-114.
Rupp, P. A., R. P. Visconti, et al. (2008). "Matrix metalloproteinase 2-integrin alpha(v)beta3 binding is required for mesenchymal cell invasive activity but not epithelial locomotion: a computational time-lapse study." Molecular biology of the cell **19**(12): 5529-5540.
Russell, J. L., S. C. Goetsch, et al. (2011). "A dynamic notch injury response activates epicardium and contributes to fibrosis repair." Circulation research **108**(1): 51-59.
Sanchez, N. S., C. R. Hill, et al. (2011). "The cytoplasmic domain of TGFbetaR3 through its interaction with the scaffolding protein, GIPC, directs epicardial cell behavior." Developmental biology.
Sanford, L. P., I. Ormsby, et al. (1997). "TGFbeta2 knockout mice have multiple developmental defects that are non-overlapping with other TGFbeta knockout phenotypes." Development **124**(13): 2659-2670.
Shi, Y. and J. Massagué (2003). "Mechanisms of TGF-[beta] Signaling from Cell Membrane to the Nucleus." Cell **113**(6): 685-700.
Shikama, N., W. Lutz, et al. (2003). "Essential function of p300 acetyltransferase activity in heart, lung and small intestine formation." EMBO J **22**(19): 5175-5185.
Shull, M. M., I. Ormsby, et al. (1992). "Targeted disruption of the mouse transforming growth factor-beta 1 gene results in multifocal inflammatory disease." Nature **359**(6397): 693-699.
Siegel, P. M. and J. Massague "Cytostatic and apoptotic actions of TGF-[beta] in homeostasis and cancer."
Siegel, P. M. and J. Massague (2003). "Cytostatic and apoptotic actions of TGF-[beta] in homeostasis and cancer." Nature Reviews Cancer(11): 807-821.
Sirard, C., J. L. de la Pompa, et al. (1998). "The tumor suppressor gene Smad4/Dpc4 is required for gastrulation and later for anterior development of the mouse embryo." Genes Dev **12**(1): 107-119.
Smart, N., C. A. Risebro, et al. (2007). "Thymosin beta4 induces adult epicardial progenitor mobilization and neovascularization." Nature **445**(7124): 177-182.

Sridurongrit, S., J. Larsson, et al. (2008). "Signaling via the Tgf-beta type I receptor Alk5 in heart development." Dev Biol **322**(1): 208-218.

Stenvers, K. L., M. L. Tursky, et al. (2003). "Heart and liver defects and reduced transforming growth factor beta2 sensitivity in transforming growth factor beta type III receptor-deficient embryos." Mol Cell Biol **23**(12): 4371-4385.

Svensson, E. C., R. L. Tufts, et al. (1999). "Molecular cloning of FOG-2: a modulator of transcription factor GATA-4 in cardiomyocytes." Proc Natl Acad Sci U S A **96**(3): 956-961.

Takatsu, Y., M. Nakamura, et al. (2000). "TAK1 participates in c-Jun N-terminal kinase signaling during Drosophila development." Mol Cell Biol **20**(9): 3015-3026.

Taylor, M. A., J. G. Parvani, et al. (2010). "The pathophysiology of epithelial-mesenchymal transition induced by transforming growth factor-beta in normal and malignant mammary epithelial cells." J Mammary Gland Biol Neoplasia **15**(2): 169-190.

Tevosian, S. G., A. E. Deconinck, et al. (2000). "FOG-2, a cofactor for GATA transcription factors, is essential for heart morphogenesis and development of coronary vessels from epicardium." Cell **101**(7): 729-739.

Tkachenko, E., A. Elfenbein, et al. (2006). "Syndecan-4 Clustering Induces Cell Migration in a PDZ-Dependent Manner." Circ Res **98**(11): 1398-1404.

Tomanek, R. J. (2005). "Formation of the coronary vasculature during development." Angiogenesis **8**(3): 273-284.

Tomanek, R. J., J. S. Holifield, et al. (2002). "Role of VEGF family members and receptors in coronary vessel formation." Dev Dyn **225**(3): 233-240.

Tomanek, R. J., Y. Ishii, et al. (2006). "VEGF family members regulate myocardial tubulogenesis and coronary artery formation in the embryo." Circ Res **98**(7): 947-953.

Tomanek, R. J., W. Zheng, et al. (2001). "Multiple growth factors regulate coronary embryonic vasculogenesis." Developmental Dynamics **221**(3): 265-273.

Tomanek, R. J., W. Zheng, et al. (2001). "Multiple growth factors regulate coronary embryonic vasculogenesis." Dev Dyn **221**(3): 265-273.

Torlopp, A., J. Schlueter, et al. (2010). "Role of fibroblast growth factor signaling during proepicardium formation in the chick embryo." Developmental dynamics : an official publication of the American Association of Anatomists **239**(9): 2393-2403.

Townsend, T., Robinson, JY How, T, DeLaughter, DM, Blobe, GC, Barnett, JV (2011). "Endocardial cell epithelial-mesenchymal transformation requires Type III TGFβ receptor interaction with GIPC." Cellular Signaling **in press**.

Townsend, T. A., J. Y. Robinson, et al. (2011). "BMP-2 and TGFbeta2 shared pathways regulate endocardial cell transformation." Cells Tissues Organs **194**(1): 1-12.

Townsend, T. A., J. Y. Robinson, et al. (2011). "BMP-2 and TGFbeta2 Shared Pathways Regulate Endocardial Cell Transformation." Cells Tissues Organs.

Townsend, T. A., J. L. Wrana, et al. (2008). "Transforming Growth Factor-{beta}-stimulated Endocardial Cell Transformation Is Dependent on Par6c Regulation of RhoA." J. Biol. Chem. **283**(20): 13834-13841.

Townsend, T. A., J. L. Wrana, et al. (2008). "Transforming growth factor-beta-stimulated endocardial cell transformation is dependent on Par6c regulation of RhoA." J Biol Chem **283**(20): 13834-13841.

Tsukazaki, T., T. A. Chiang, et al. (1998). "SARA, a FYVE domain protein that recruits Smad2 to the TGFbeta receptor." Cell **95**(6): 779-791.

Viloria-Petit, A. M., L. David, et al. (2009). "A role for the TGFbeta-Par6 polarity pathway in breast cancer progression." Proceedings of the National Academy of Sciences of the United States of America **106**(33): 14028-14033.

Viloria-Petit, A. M. and J. L. Wrana (2010). "The TGFbeta-Par6 polarity pathway: linking the Par complex to EMT and breast cancer progression." Cell cycle **9**(4): 623-624.

Viragh, S. and C. E. Challice (1981). "The origin of the epicardium and the embryonic myocardial circulation in the mouse." Anat Rec **201**(1): 157-168.

Waldrip, W. R., E. K. Bikoff, et al. (1998). "Smad2 signaling in extraembryonic tissues determines anterior-posterior polarity of the early mouse embryo." Cell **92**(6): 797-808.

Wang, G. and F. Beier (2005). "Rac1/Cdc42 and RhoA GTPases antagonistically regulate chondrocyte proliferation, hypertrophy, and apoptosis." J Bone Miner Res **20**(6): 1022-1031.

Wang, H. R., A.A. Ogunjimi, Y. Zhang, B. Ozdamar, R. Bose, and J.L. Wrana (2006). "Degradation of RhoA by Smurf1 ubiquitin ligase." Methods Enzymol **406**: 437-447.

Wang, H. R., A. A. Ogunjimi, et al. (2006). "Degradation of RhoA by Smurf1 ubiquitin ligase." Methods Enzymol **406**: 437-447.

Wang, H. R., Y. Zhang, et al. (2003). "Regulation of cell polarity and protrusion formation by targeting RhoA for degradation." Science **302**(5651): 1775-1779.

Wang, J., S. Sridurongrit, et al. (2005). "Atrioventricular cushion transformation is mediated by ALK2 in the developing mouse heart." Dev Biol **286**(1): 299-310.

Wang, L., J. S. Lau, et al. (2010). "RGS-GAIP-interacting protein controls breast cancer progression." Mol Cancer Res **8**(12): 1591-1600.

Wang, X. F., H. Y. Lin, et al. (1991). "Expression cloning and characterization of the TGF-beta type III receptor." Cell **67**(4): 797-805.

Ward, N. L., P. Van Slyke, et al. (2004). "Angiopoietin 1 expression levels in the myocardium direct coronary vessel development." Dev Dyn **229**(3): 500-509.

Ward, S. M., A. P. Gadbut, et al. (2002). "TGFbeta regulates the expression of G alpha(i2) via an effect on the localization of ras." J Mol Cell Cardiol **34**(9): 1217-1226.

Watt, A. J., M. A. Battle, et al. (2004). "GATA4 is essential for formation of the proepicardium and regulates cardiogenesis." Proc Natl Acad Sci U S A **101**(34): 12573-12578.

Watts, J. L., B. Etemad-Moghadam, et al. (1996). "par-6, a gene involved in the establishment of asymmetry in early C. elegans embryos, mediates the asymmetric localization of PAR-3." Development **122**(10): 3133-3140.

Weeke-Klimp, A., N. A. M. Bax, et al. (2010). "Epicardium-derived cells enhance proliferation, cellular maturation and alignment of cardiomyocytes." Journal of molecular and cellular cardiology **49**(4): 606-616.

Weinstein, M., X. Yang, et al. (2000). "Functions of mammalian Smad genes as revealed by targeted gene disruption in mice." Cytokine Growth Factor Rev **11**(1-2): 49-58.

Wiater, E., C. A. Harrison, et al. (2006). "Identification of Distinct Inhibin and Transforming Growth Factor beta-binding Sites on Betaglycan: FUNCTIONAL SEPARATION OF BETAGLYCAN CO-RECEPTOR ACTIONS." J. Biol. Chem. **281**(25): 17011-17022.

Wojciak-Stothard, B., L. Y. Tsang, et al. (2005). "Rac and Rho play opposing roles in the regulation of hypoxia/reoxygenation-induced permeability changes in pulmonary artery endothelial cells." Am J Physiol Lung Cell Mol Physiol **288**(4): L749-760.

Wrana, J. L. (2000). "Crossing Smads." Sci STKE **2000**(23): RE1.

Wrana, J. L. and L. Attisano (2000). "The Smad pathway." Cytokine Growth Factor Rev **11**(1-2): 5-13.

Wrana, J. L., L. Attisano, et al. (1994). "Mechanism of activation of the TGF-beta receptor." Nature **370**(6488): 341-347.

Wu, F., S. Buckley, et al. (1996). "Cell cycle arrest in G0/G1 phase by contact inhibition and TGF-beta 1 in mink Mv1Lu lung epithelial cells." Am J Physiol **270**(5 Pt 1): L879-888.

Wu, H., S. H. Lee, et al. (1999). "Inactivation of erythropoietin leads to defects in cardiac morphogenesis." Development **126**(16): 3597-3605.

Wu, K., D. Gauthier, et al. (1995). "Live cell image segmentation." IEEE transactions on bio-medical engineering **42**(1): 1-12.

Xiong, J. W. (2008). "Molecular and developmental biology of the hemangioblast." Dev Dyn **237**(5): 1218-1231.

Yamaguchi, K., K. Shirakabe, et al. (1995). "Identification of a member of the MAPKKK family as a potential mediator of TGF-beta signal transduction." Science **270**(5244): 2008-2011.

Yang, J. T., H. Rayburn, et al. (1995). "Cell adhesion events mediated by alpha 4 integrins are essential in placental and cardiac development." Development **121**(2): 549-560.

You, H. J., T. How, et al. (2009). "The type III transforming growth factor-{beta} receptor negatively regulates nuclear factor-{kappa}B signaling through its interaction with {beta}-arrestin2." Carcinogenesis: bgp071.

You, H. J., T. How, et al. (2009). "The type III transforming growth factor-{beta} receptor negatively regulates nuclear factor-{kappa}B signaling through its interaction with {beta}-arrestin2." Carcinogenesis.

Yu, L., M. C. Hebert, et al. (2002). "TGF-beta receptor-activated p38 MAP kinase mediates Smad-independent TGF-beta responses." EMBO J **21**(14): 3749-3759.

Yu, W., L.-B. Ruest, et al. (2009). "Regulation of Epithelial-Mesenchymal Transition in Palatal Fusion." Exp. Biol. Med. **234**(5): 483-491.

Zamir, E. A., A. Czirok, et al. (2005). "A digital image-based method for computational tissue fate mapping during early avian morphogenesis." Annals of biomedical engineering **33**(6): 854-865.

Zamora, M., J. Manner, et al. (2007). "Epicardium-derived progenitor cells require beta-catenin for coronary artery formation." Proc Natl Acad Sci U S A **104**(46): 18109-18114.

Zhou, B., Q. Ma, et al. (2008). "Epicardial progenitors contribute to the cardiomyocyte lineage in the developing heart." Nature **454**(7200): 109-113.
Zhu, Y., J. A. Richardson, et al. (1998). "Smad3 mutant mice develop metastatic colorectal cancer." Cell **94**(6): 703-714.